

Naval Surface Warfare Center  
Carderock Division

West Bethesda, MD 20817-5700

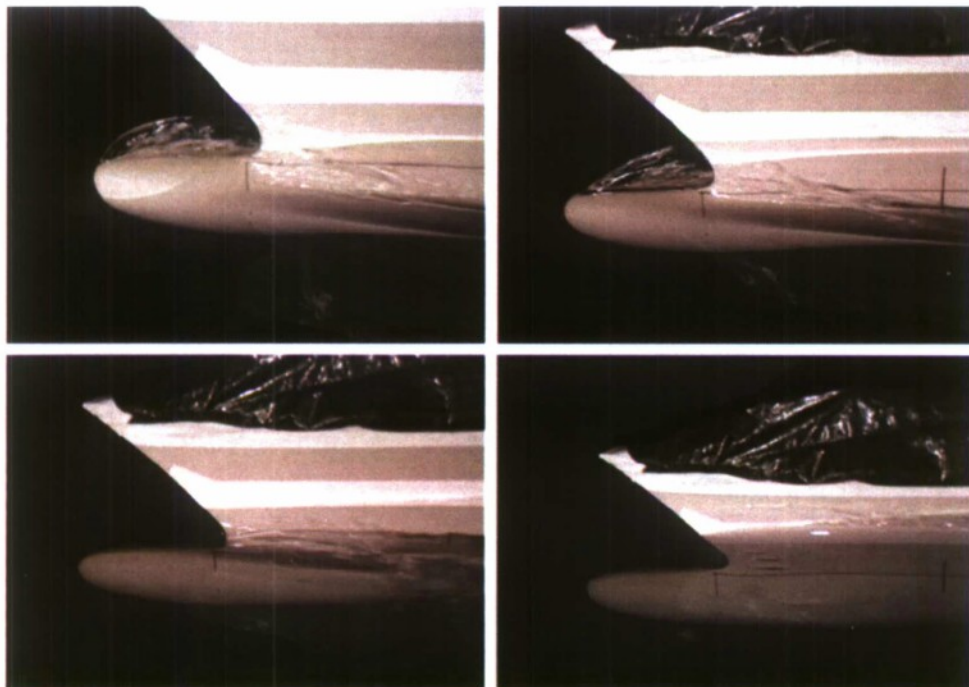


NSWCCD-50-TR-2009/041 April 2009  
Hydromechanics Department Report

**JHSS Baseline Shaft & Strut (BSS) Model 5653-3  
Added Resistance & Powering and Ship Motions,  
Sea State 6 Random Waves and Regular Waves**

By

Dominic S. Cusanelli, Bryson J. Metcalf, and Ann Marie Powers



Approved for public release. Distribution Unlimited.

20090420252

REPORT DOCUMENTATION PAGE				Form Approved OMB No. 0704-0188
<p>Public reporting burden for this collection of information is estimated to average 1 hour per response, including the time for reviewing instructions, searching existing data sources, gathering and maintaining the data needed, and completing and reviewing this collection of information. Send comments regarding this burden estimate or any other aspect of this collection of information, including suggestions for reducing this burden to Department of Defense, Washington Headquarters Services, Directorate for Information Operations and Reports (0704-0188), 1215 Jefferson Davis Highway, Suite 1204, Arlington, VA 22202-4302. Respondents should be aware that notwithstanding any other provision of law, no person shall be subject to any penalty for failing to comply with a collection of information if it does not display a currently valid OMB control number. PLEASE DO NOT RETURN YOUR FORM TO THE ABOVE ADDRESS.</p>				
1. REPORT DATE (DD-MM-YYYY) April 2009	2. REPORT TYPE Final	3. DATES COVERED (From - To) Feb - March 2007		
4. TITLE AND SUBTITLE <b>JHSS Baseline Shaft &amp; Strut (BSS) Model 5653-3 Added Resistance &amp; Powering and Ship Motions, Sea State 6 Random Waves and Regular Waves</b>				
5a. CONTRACT NUMBER				
5b. GRANT NUMBER				
5c. PROGRAM ELEMENT NUMBER				
6. AUTHOR(S) Dominic S. Cusanelli, Bryson J. Metcalf, and Ann Marie Powers				
5d. PROJECT NUMBER				
5e. TASK NUMBER				
5f. WORK UNIT NUMBER 07-1-2125-145				
7. PERFORMING ORGANIZATION NAME(S) AND ADDRESS(ES) AND ADDRESS(ES) Naval Surface Warfare Center Carderock Division 9500 Macarthur Boulevard West Bethesda, MD 20817-5700				
8. PERFORMING ORGANIZATION REPORT NUMBER NSWCCD-TR-2009/041				
9. SPONSORING / MONITORING AGENCY NAME(S) AND ADDRESS(ES) Naval Sea Systems Command 1333 Isaac Hull Ave, SE Washington Navy Yard, DC 20376-5061				
10. SPONSOR/MONITOR'S ACRONYM(S)				
11. SPONSOR/MONITOR'S REPORT NUMBER(S)				
12. DISTRIBUTION / AVAILABILITY STATEMENT Approved for public release. Distribution Unlimited.				
13. SUPPLEMENTARY NOTES				
<b>14. ABSTRACT</b> <p>Resistance and powering tests were conducted on Model 5653-3 in calm water, in sea state 6 (SS6) random waves, and in regular waves. Model 5653-3 is representative of the Joint High Speed Sealift (JHSS) conventional Baseline Shaft &amp; Strut (BSS) hull. The objectives / purposes for resistance and powering in waves experiments and results were twofold; for JHSS indicative hull design support and for US Navy design and evaluation tool validation.</p> <p>Powering tests in waves determined the additional power required by the JHSS indicative hull design to maintain speed in SS6 relative to calm water conditions. SS6 analysis indicates that sizing of the propulsion plant in a sealift-type hull for 39 knots in calm water should assure that sufficient power is available for achieving 36 knots in SS6. The 39-knot speed of interest will not be attainable in SS6 for the indicative JHSS baseline design with the total installed power envisioned.</p> <p>Qualitative observations indicate that the long, slender sealift design, when running in SS6, would likely experience only mild pitching and no occurrences of slamming at the bow or stern regions, despite the heavy sea state. The motions of the model were not significantly influenced by propulsion thrust or the ability to surge longitudinally.</p>				
(continued)				
15. SUBJECT TERMS Joint High Speed Sealift (JHSS), Added Resistance, Random Waves, Regular Waves				
16. SECURITY CLASSIFICATION OF:		17. LIMITATION OF ABSTRACT	18. NO. OF PAGES	19a. RESPONSIBLE PERSON Dominic S. Cusanelli
a. REPORT UNCLASSIFIED	b. ABSTRACT UNCLASSIFIED	c. THIS PAGE UNCLASSIFIED	SAR	19b. TELEPHONE NUMBER 301-227-7008

**14. ABSTRACT (continued)**

The model tests conducted in regular waves conditions were used to determine the critical wavelengths that resulted in the largest increased resistance in regular waves. Subsequent testing at these critical wavelengths provides a large matrix of resistance and powering data for comparisons to various numeric prediction tools

In addition, roll decay tests, with and without bilge keels, were conducted.

CONTENTS	Page
ABSTRACT .....	1
ADMINISTRATIVE INFORMATION .....	1
INTRODUCTION .....	1
MODEL DESCRIPTION .....	2
Model Inspection .....	3
Stock Propeller Series .....	3
Ballasting for Dynamic Response .....	3
Instrumentation and Installation .....	4
FLOW VISUALIZATION .....	5
Bilge Keel Alignment and Installation .....	5
General Flow Observations .....	5
RESISTANCE & POWERING TEST PROCEDURES .....	6
SS6 TEST RESULTS .....	6
Model-Scale Added Resistance & Powering Measurements in SS6 .....	6
JHSS Indicative Baseline Design Powering in SS6 .....	7
REGULAR WAVES TEST RESULTS .....	10
Critical Wavelengths .....	10
Increased Resistance & Powering in Regular Waves .....	10
MODEL MEASUREMENT UNCERTAINTY / VARIABILITY .....	11
SHIP MOTION RESPONSES IN SS6 .....	12
EVALUATION OF POWERING IN WAVES TEST TECHNIQUES .....	12
Glide Rail System .....	12
Fixed-in-Surge versus Free-to-Surge .....	13
CONCLUSIONS .....	14
ACKNOWLEDGMENTS .....	15
REFERENCES .....	17
APPENDIX A: Resistance & Powering Data & Analysis .....	A1
APPENDIX B: Model 5653-3 Motions Data & Analysis .....	B1
APPENDIX C: Measurement Report for Model 5653 .....	C1

**FIGURES**

Page

1. JHSS baseline shaft and struts (BSS) hull with Gooseneck Bulb (GB), Model 5653-3 ....	2
2. JHSS indicative baseline design, added resistance and powering in SS6 random waves and SS6 waves with wind drag included .....	9
3. Glide rail system as installed and tested on Model 5653-3 .....	13

**TABLES**

Page

1. Model-scale added force measurements in SS6 random waves .....	7
2. JHSS indicative baseline design powering in calm water, SS6 random waves, and SS6 waves with wind drag included .....	9
3. Model-scale increased resistance and powering in regular waves .....	11

## ABSTRACT

Resistance and powering tests were conducted on Model 5653-3 in calm water, in sea state 6 (SS6) random waves, and in regular waves. Model 5653-3 is representative of the Joint High Speed Sealift (JHSS) conventional Baseline Shaft & Strut (BSS) hull. The objectives / purposes for resistance and powering in waves experiments and results were twofold; for JHSS indicative hull design support and for US Navy design and evaluation tool validation.

Powering tests in waves determined the additional power required by the JHSS indicative hull design to maintain speed in SS6 relative to calm water conditions. SS6 analysis indicates that sizing of the propulsion plant in a sealift-type hull for 39 knots in calm water should assure that sufficient power is available for achieving 36 knots in SS6. The 39-knot speed of interest will not be attainable in SS6 for the indicative JHSS baseline design with the total installed power envisioned.

Qualitative observations indicate that the long, slender sealift design, when running in SS6, would likely experience only mild pitching and no occurrences of slamming at the bow or stern regions, despite the heavy sea state. The motions of the model were not significantly influenced by propulsion thrust or the ability to surge longitudinally.

The model tests conducted in regular waves conditions were used to determine the critical wavelengths that resulted in the largest increased resistance in regular waves. Subsequent testing at these critical wavelengths provides a large matrix of resistance and powering data for comparisons to various numeric prediction tools.

In addition, roll decay tests, with and without bilge keels, were conducted.

## ADMINISTRATIVE INFORMATION

Project funding was primarily through the JHSS Project Office, NAVSEA 05D1. The High Speed Sealift Hydro Working Group (HWG), with representatives from NAVSEA, NSWCCD, ONR and CSC, coordinates all hydrodynamic, propulsion, hull form and structural loads R&D for this program. Tests were conducted at the David Taylor Model Basin, Naval Surface Warfare Center, Carderock Division Headquarters (NSWCCD), by the Resistance & Propulsion Division (Code 5800), under work unit number 07-1-2125-145.

## INTRODUCTION

The Joint High Speed Sealift (JHSS) was a potential FY12 ship acquisition sponsored by OPNAV N42. Originally designated the Rapid Strategic Lift Ship (RSLS) and outlined in "Rapid Strategic Lift Ship Feasibility Study Report" [Ref. 1], the ship's capability was then broadened as the "Joint High Speed Sealift (JHSS)" [Ref. 2]. Under the auspices of several sealift research programs, numerous hullforms, bulbous bows, and propulsion system configurations were designed and evaluated on the JHSS parent hull platform [Ref. 3].

The extensive model testing under the sealift programs, which extends well over a year in duration, will be documented in several reports of reduced scope. The present report documents the model-scale resistance and powering experiments in sea state 6 (SS6) random waves and in regular waves, conducted on JHSS baseline shaft and strut (BSS) Model 5653-3, as outlined in Appendix A, Table A1. The objectives / purposes for the present model experiment in waves were twofold:

### (1) JHSS Indicative Design Support

- Appendage alignment (flow visualization)
- Resistance and powering characteristics determined in random SS6 waves
- Time history and peak motions responses and accelerations determined in random SS6 waves
- Roll decay, with and without bilge keels

## (2) US Navy Design and Evaluation Tool Validation

- Resistance response operators determined for a large matrix of regular waves conditions
- Speed-dependant critical wavelengths determined for maximum value response operators
- Resistance and powering characteristics determined for a range of wave heights tested at critical wavelengths
- Model test results are to be compared with various numeric prediction tools

There is little model-scale or full-scale experience in the assessment of power increase and/or speed loss in waves for large sealift-type hulls similar to the envisioned JHSS. Analysis of the Model 5653-3 experiments in random sea state 6 (SS6) waves, presented in Appendix A, when compared to calm water experiments, will determine the added resistance and powering characteristics of this type of hullform with conventional open propellers. In addition, increased resistance and powering characteristics will also be determined in regular waves, for a range of wave heights tested at hull critical wavelengths. Results such as these can be used to develop and validate numerical tools for the prediction of ship motions in waves.

The results of time histories and peak motions responses and accelerations, determined in random SS6 waves, as presented in Appendix B, will assist with safety and habitability evaluations of the indicative JHSS and future sealift designs.

## MODEL DESCRIPTION

Current tests were conducted on Model 5653-3, representative of the JHSS baseline shaft and struts (BSS) hullform with Gooseneck Bulb (GB). Model 5653-3 was built at NSWCCD of fiberglass to a linear scale ratio  $\lambda = 34.121$ , and LBP = 27.86 ft (8.5 m). The suffix -3 affixed to the model number denotes the installation of the Gooseneck Bulb (GB), selected for the BSS during the alternate bow evaluations and selection phase of testing [Ref. 4]. A detailed description of Model 5653, and photographs while under construction, are presented in Ref. 4. Photographs of Model 5653-3, while in the Carriage 2 dry dock, are presented in Figure 1, and in Appendix A, Figure A1.

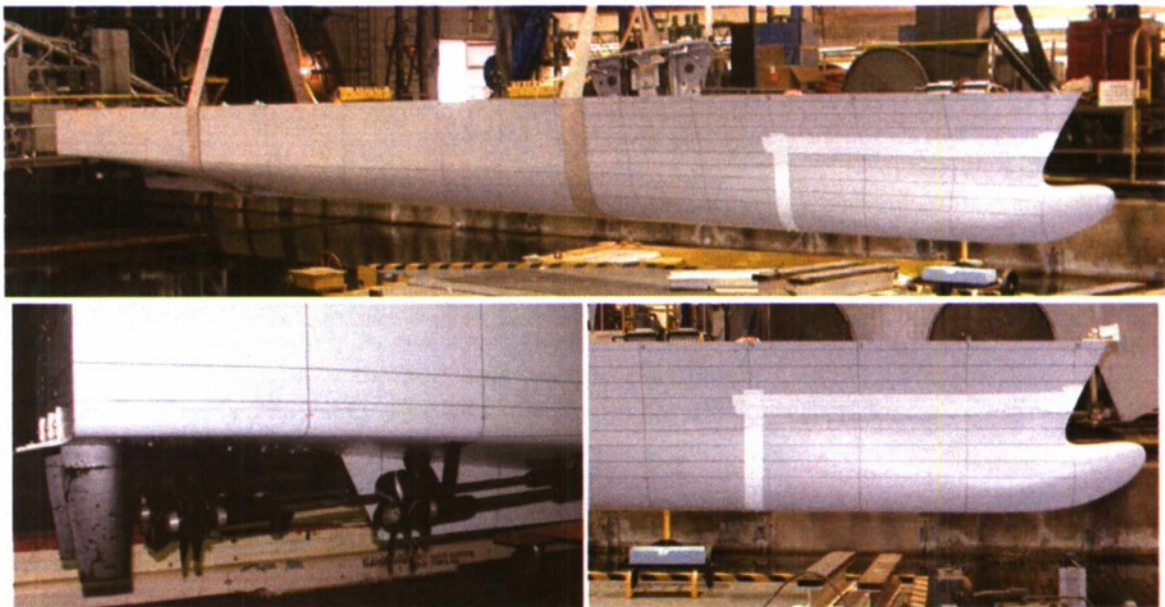


Fig. 1. JHSS baseline shaft and struts (BSS) hull with Gooseneck Bulb (GB), Model 5653-3

During the tests in waves, the selected stern flap was installed on Model 5663-3. The selected stern flap has full-scale dimensions of chord length 12.8 ft (3.9 m) equivalent to 1.35%

LWL, span 52.9 ft (16 m), and angle of 10° trailing edge down relative to the transom centerline buttock slope. This stern flap was selected during stock propeller powering tests [Ref. 5].

To promote turbulent flow along the model, turbulence stimulator studs of 1/8 inch diameter by 1/10 inch height, spaced 1 inch apart, were affixed to the model approximately 2 inches aft of the stem, and continuing down to and around the bulbs approximately 2 inches aft of the FP.

### **Model Inspection**

Prior to the current test series, an inspection of Model 5653-3 was conducted with a laser tracker.<sup>1</sup> The complete model measurement report is reproduced in Appendix C. The measured model points were compared to a numeric representation (CAD file) of the hull surface. The measured points and the CAD file were aligned with the greatest emphasis placed on the surfaces below the design water line (DWL). Approximately 96.5% of the measured points on Model 5653-3, below the DWL, fall within the  $\pm 2\text{mm}$  ( $\pm 0.079$  inch) tolerance specified by the Code 5800 project (model test) engineer. Model 5653-3 exceeds the minimum standard (75% of the measured points within tolerance) set forth for model acceptance by NSWCCD for resistance and propulsion model manufacture.

### **Stock Propeller Series**

The model scale ratio was based on the availability of 7.5 inch (19.05 cm) diameter model propellers selected for the JHSS BSS stock propeller powering tests [Ref. 5], and subsequently utilized during the current powering tests in waves. The stock propeller series is 5233A, 5234, 5234A, and 5235, a matching set of (2 each) left-handed (LH) and right-handed (RH) propellers. These stock propellers are representative of full-scale 6-bladed propellers with a diameter of 21.33 ft (6.5 m) and a pitch-to-diameter ratio (P/D) of 1.449 at the 0.7 radius. The existing open water performance characteristics for stock propeller series 5233-5, as presented in Ref. 5, were used during the powering data reduction.

### **Ballasting for Dynamic Response**

All Model 5653-3 experiments contained herein were conducted at the full-scale design displacement (DES) of 36,490 tons, even keel. DES was determined to be representative of a likely loading scenario for the indicative JHSS baseline hull.

Generally, ballasting a model for a calm water resistance test requires that the model displacement and longitudinal center of gravity (LCG) correspond to the full-scale ship values. Ballasting a model for the correct dynamic response in head seas, however, requires that the pitch radius of gyration, the displacement, the vertical center of gravity (VCG), and longitudinal center of gravity (LCG), also correspond to the values for the design at full-scale as presented in Appendix A, Table A2. Due to the freedom to heave and pitch in a dynamic fashion in waves, it is necessary to have the physical properties affecting these dynamic motions scaled and modeled appropriately. Pitch radius of gyration and the vertical and longitudinal center of gravity are the primary properties affecting these motions.

The ballast properties were determined by measuring the properties of the model using an inertial "A" frame [Ref. 6]. Drive system, model attachment, and force measurement equipment and instrumentation, etc, are installed in Model 5653-3 prior to this measurement. The model was suspended from a ballast beam that translated lift points to multiple bulkheads on the model, and hung in 'pendulum' fashion from an inertial pivot bracket through a single pivot point, refer to Appendix A, Figure A1. The pivot point was located near the anticipated ship LCG and above the anticipated VCG. First the ballast beam, and then the beam with model attached, were

---

<sup>1</sup> Model 5653-3 laser inspection was conducted by R. Lerner and A. M. Powers (Code 6530), February 2007.

inclined to determine VCG and swung in pitch to determine inertia. The determined model values were used as initial start values for the dynamic ballasting of the model. The final desired conditions were obtained through precise placement of the remaining necessary ballast weights.

### Instrumentation and Installation

The Model 5653-3 installation on Carriage 2, for all testing contained herein, was such that all testing techniques (calm water, and in random and regular waves, both fixed and free-to-surge) could be accommodated by a single model set-up and instrumentation. Photographs of Model 5653-3, instrumentation, and installation are presented in Appendix A, Figure A1.

Linear bearing, floating platform "Cusanelli" tow posts [Ref. 7], were utilized for both the forward and aft attachment points of the model to the carriage towing girder. To accommodate wave generation in Basin #2, it is required that the nominal water level be lowered by 30 inches. This necessitated that the model tow posts be attached to the Carriage 2 floating girder through 'box' extension brackets. The linear rails of the tow posts, which were kept well lubricated during testing, allowed for the vertical movement of the model required during the tests in waves. Vertical forces and inertia due to the weight of the linear bearings and instrumentation of the tow posts was accounted for in the dynamic ballasting of the model. Mechanical connection between the tow posts' instrumentation and the model was made through double-axis gimbal assemblies. The gimbal assemblies were mounted on two linear glide rails attached to the model, fore and aft. These glide rails were locked in a single longitudinal position during the fixed-in-surge resistance and powering tests, and allowed to move freely fore-and-aft during the free-to-surge powering tests. The installation in this fashion allowed for the model to be restrained in yaw, but free to pitch, heave, and roll, whether restrained in surge or free-to-surge.

Model primary resistance (drag) measurement was collected using a DTMB 4-inch block gauge of 200-lbf. capacity. The primary drag force measurement was made at the forward tow post, with block gage measurement point located at position, when fixed-in-surge,  $x = 129.77$  inches aft of FP (station 7.76),  $y = 0$ ,  $z = 20.98$  inches above BL. A secondary drag force measurement was made at the aft tow post, location  $x = 285.14$  inches (station 17.06),  $y = 0$ ,  $z = 20.98$  inches. During testing, this drag gage was allowed to 'float' so as to impart minimal forces on the model. The drag forces measured at this point, were, however, incorporated into the overall drag measurement.

Model side force measurement was collected at the forward post with DTMB 4-inch block gauge of 50-lbf. capacity. Side force, using sign convention positive (+) force to Port and negative (-) force to Starboard, was monitored to maintain an essentially zero value to insure zero model yaw angle.

Dynamic sinkage, defined as positive (+) downward, was measured by wire potentiometers located at the intersection of the deck line at Station 2 forward and Station 16 aft.

The thrust and torque on the four propeller shafts were measured with Kempf and Remmer's (K&R) model R31 dynamometers, of 22-lbf. thrust (T) / 35-in-lbf. torque (Q) capacity. To insure equivalent shaft rotational speed (RPM), all four shafts were driven through 1:1 drive ratio 'T' gearboxes and mechanically coupled so that all four shafts were powered by a single 19 hP constant-torque electric drive motor. Shaft rotation for all four propellers was outboard-over-the-top. A single electronic pulse counter system was used to measure shaft RPM.

Wave height measurements were made with a SENIX ultrasonic probe, mounted from an "A" frame projecting off the west end of the carriage, at a location precisely 14.0 ft forward of the model forward perpendicular (FP), approximately on the centerline of the towing basin.

Calibration of all aforementioned instrumentation was performed prior to the tests in the NSWCCD Code 5800 calibration lab by D. Mullinix (CSC contractor).

Motions sensors consisted of the following. Pitch and roll, both angle and rate, were measured with a single 2-axis Crossbow solid state vertical gyro model VG400CC-100, with the center axis of measurement located at the ship/model center of gravity (CG), station 10.02. Accelerations along three axes, longitudinal, vertical, and transverse, were measured by three Columbia Research model SA-307HPTX 3-Axis Accelerometers, with centers of measurement located forward at station 0.76, mid-ship at the LCG, and aft at station 19.92.

Calibration of motions sensors was performed prior to the tests by H. Vo (Code 5300).

### FLOW VISUALIZATION

A flow visualization experiment was conducted on Model 5653-3 prior to the resistance and powering test series. Flow observations can aid in the proper placement and orientation of appendages to avoid adverse flow conditions, and can help determine if there are regions where the flow might adversely impact the ship's performance. During the flow visualization experiments on Model 5653-3, general observations were made of the flow patterns over the starboard hull afterbody, propulsion appendages, rudders, and stern flap, with specific flow observations made in way of the starboard bilge keel for alignment purposes. Flow visualization streamlines were produced on Model 5653-3 by an oil paint flow technique, at a ship speed 36 knots, and are presented in Appendix A, Figure A2.

### **Bilge Keel Alignment and Installation**

In support of the JHSS indicative design effort, 36-knot flow visualization streamlines around the bilge radius of Model 5653-3 were used to align and install the port and starboard bilge keels, a requirement for both the ship's roll stability and for accurate motion responses in waves. This empirical data will be used in support of appendage design and resistance prediction Tool Validation.

The bilge keel anchoring point was set equivalent to the bilge keel pre-test location at station 10. A flexible temporary medium was carefully placed on the model hull at the anchoring point, and shaped to best represent the most appropriate compromise between the indicated streamlines spanning the approximate length of the bilge keels, ship stations of 7.5 to 13.5. A recommended bilge keel alignment was thus determined, and is presented in Appendix A, Figure A3.

The model-scale port and starboard bilge keels were then installed on Model 5653-3 at the recommended alignment position. The bilge keels were manufactured from a highly flexible PVC material, and as so, were able to conform closely to the desired alignment. After being fastened in place, a fillet of silicone sealant was used to fill any small gaps between the hull surface and the base of the bilge keels.

A resistance test was subsequently conducted at the two speeds of interest, 25 and 36 knots, and model-scale added resistance for the bilge keels was determined, Appendix A, Table A3. Model-scale increase in total resistance,  $R_T$ , was 2.56% and 2.50%, for ship speeds of 25 and 36 knots, respectively. The increase in total ship wetted surface due to the bilge keels is 2.52%.

### **General Flow Observations**

The general flow over the Model 5653-3 starboard afterbody appears to be mostly along the buttock lines of the hull, with a small outward flow tendency aft of station 19. No areas of separated or reversed flow were observed on the afterbody. There does exist small localized areas of highly angular flow surrounding the through-hull shaft bossings, and at the leading edge of the rudders.

Flow on the rudder mid-section indicated strict chord-wise flow, however, at the rudder tip a strong wrapped-around upward flow was exhibited. Across the rudder shoe, the strong downward curvature indicated over the trailing third of the chord length should be considered

ineonclusive. It may possibly indicate an influence of the stern flap on the flow streamlines, however, it may be due to the laek of sufficient oil placed on the root of the rudder shoe.

Flow patterns on the main and intermediate strut barrels indicated the expected cross flow due to the influence of the slope (run) of the hull in these regions.

### **RESISTANCE & POWERING TEST PROCEDURES**

Tests were conducted on Model 5653-3 in the NSWCCD Deepwater Towing Basin #2 using Carriage 2. The Test Agenda is presented as Appendix A, Table A1. The cross-sectional area of the tank provided sufficient area to eliminate the need for blockage correction, even with the water level lowered to accommodate wave making. Resistance and stock propeller powering experiments were conducted and analyzed according to standard NSWCCD practice [Ref. 8]. For all of the tests herein, only two speeds of interest were evaluated, equivalent to 25 and 36 knots full-scale.

Ship-model correlation allowance of  $C_A = 0.0$  was recommended by NSWCCD Code 5800 based on the NAVSEA guidance as modified by more recent correlation allowance experience, and was accepted by the HWG. Predictions are made for the full-scale JHSS operating in smooth, deep, salt water, with a uniform standard temperature of 59°F.

The varying test procedures, data collections methods, and analysis techniques employed, for the model-scale tests in the three different waves environments, calm water, random (irregular) sea state 6, and regular waves, are described in detail in Appendix A.

Long crested random and regular waves were generated using the Basin #2 pneumatic wave-maker. Definitions and criteria, for annual random (irregular) sea state occurrences in the open ocean for the northern hemisphere, are presented in Appendix A, Table A4. For the experimental representation of random waves, Bretschneider formulated wave spectrum are utilized. Once the input functions were satisfactorily adjusted, resulting in the desired SS6 output spectra, the wave-maker representative output wave spectra was measured and compared to the Bretschneider formulated SS6 wave spectra, Appendix A, Figure A5. For the experiments in regular waves, the wave-maker output was measured in terms of wavelength,  $\lambda$ , generally expressed as a function of ship length overall,  $\lambda/LOA$ , and wave height,  $\zeta$ , and characterized by wave slope,  $\zeta/\lambda$ . The range of wavelengths tested was  $0.744 \leq \lambda/LOA \leq 1.237$ , and the range of wave slopes tested was  $1/150 \leq \zeta/\lambda \leq 1/60$ . Pneumatic wavemaker output regular waves characteristics, for specified valve frequency and blower RPM conditions, are depicted in Appendix A, Figure A6.

### **SS6 TEST RESULTS**

In support of JHSS indicative design, resistance and powering experiments were conducted on Model 5663-3 in random sea state 6 (SS6) waves system. SS6 is characterized as a heavy sea state, with large waves of 13 to 20 feet significant wave height. This sea state was approximated by a Bretschneider spectrum. Qualitative observations of Model 5653-3 throughout the testing, indicated that the long, slender scallop design, when running in SS6, would likely experience only mild pitching and no occurrences of slamming at the bow or stern regions, despite the heavy sea state.

#### **Model-Scale Added Resistance & Powering Measurements in SS6**

Cumulative data measurement time interval greater than one hour full-scale operation in SS6 waves was collected for each of the two test speeds, 25 and 36 knots, for all resistance and powering test conditions.

Added resistance experiments in SS6 were conducted with Model 5653-3 fixed-in-surge. Added resistance in waves,  $R_w$ , was determined by difference in the measured average resistance in SS6 waves (from the summation of data equivalent to one hour full-scale in waves),  $RT_w$ , and the comparable value in calm water,  $R_T$ , presented in Appendix A, Table A5 and Figure A7. Model 5653-3 exhibited an  $R_w$  in SS6, expressed as a percentage of the calm water resistance,  $R_T$ , equivalent to 13.17% and 6.80% for ship speeds of 25 and 36 knots, respectively.

Calm water powering and added powering in SS6 experiments were conducted with Model 5653-3 first in the fixed-in-surge configuration (conducted at the ship propulsion point), presented in Appendix A, Tables A6 and A7, and then in the free-to-surge configuration (conducted at the model self-propulsion point), presented in Tables A8 and A9. The 'added' force values (thrust, torque, RPM, etc. on each of four shaftlines), for powering in SS6 random waves, was determined by difference in the measured total force value in waves and the comparable value in calm water; see Appendix A for details.

A summary of the model-scale force measurements in calm water and SS6 random waves are presented in Appendix A, Table A10. Model-scale added force measurements in SS6 random waves are presented in Figure A7, and are presented in brief, expressed as a percentage of the calm water force values, in Table 1.

Table 1. Model-scale added force measurements in SS6 random waves

Sea Condition	Model Attachment	Added % in Waves, 25 knots				Added % in Waves, 36 knots			
		$R_w$ (%)	$T_w$ (%)	$Q_w$ (%)	$RPM_w$ (%)	$R_w$ (%)	$T_w$ (%)	$Q_w$ (%)	$RPM_w$ (%)
SS6	Fixed	13.2	22.1	15.2	2.4	6.8	8.6	6.6	0.8
	Free to Surge	N/A	18.9	13.0	1.9	N/A	7.8	6.2	0.6
	Combined	13.2	20.5	14.1	2.1	6.8	8.2	6.4	0.7

Because the two methods, fixed-in-surge versus free-to-surge, produced such similar results, the authors have chosen to utilize the 'Combined' (averaged) added force measurements for the continued evaluation of the JHSS indicative baseline design in SS6 random waves. A comparison of the two testing techniques will be discussed in greater detail in a subsequent section of this report.

### JHSS Indicative Baseline Design Powering in SS6

An extensive series of calm water resistance and stock propeller powering experiments were conducted on Model 5653-3 in support of the JHSS baseline shaft & strut (BSS) design, Ref. 5. The calm water effective power prediction, Appendix A, Table A11, for the BSS at design displacement (DES) with stern flap installed, was used as the foundation resistance experiment for the current JHSS indicative baseline design performance in waves evaluation.

The model-scale added resistance measured for the bilge keels was added to the calm water resistance, resulting in the effective power presented Table A12. Full-scale increase in effective power due to the bilge keels was 2.66% and 2.61%, for ship speeds of 25 and 36 knots, respectively. As stated, the increase in total ship wetted surface due to the bilge keels is 2.52%.

The effective power prediction for the JHSS indicative baseline design in SS6 random waves, Table A13, was then determined from model-scale added resistance measurements in waves,  $R_w$ , applied to the calm water resistance with stern flap and bilge keels. Full-scale increase in effective power due to SS6 random waves was 21.6% and 10.9%, for ship speeds of 25 and 36 knots, respectively. These values represent relatively modest increases in resistance for such a large sea state.

The calm water powering prediction, Table A14 and Figure A8, for the BSS at design displacement (DES) with stern flap installed, was used as the foundation powering experiment for the current performance in waves evaluation. The calm water propeller-hull interaction

coefficients were then applied to the effective power prediction with bilge keel installed, resulting in the delivered power presented in Table A15. Full-scale increase in delivered power due to the bilge keels was 2.35% and 2.21%, for ship speeds of 25 and 36 knots, respectively.

Using the JHSS effective power prediction in SS6 random waves (Table A13) with stern flap and bilge keels, and the calm water propeller-hull interaction coefficients (Table A15), an estimate was first made of the JHSS indicative baseline design powering in SS6. This would have been the only means of estimating the powering in SS6 if no model-scale powering tests in SS6 had been conducted. Full-scale increase in delivered power due to SS6 random waves, estimated from the effective power prediction in SS6 and calm water interaction coefficients, was 19.3% and 9.7%, for ship speeds of 25 and 36 knots, respectively. This estimated powering is presented for comparison purposes only, and should not be utilized as the powering prediction for the JHSS indicative BSS in SS6.

The JHSS indicative baseline design delivered power prediction in SS6 random waves, Table A17 and Figure A9, was determined from the model-scale added force measurements in SS6 random waves and the effective power prediction in SS6 (Table A13), with stern flap and bilge keels installed. Full-scale increase in delivered power due to SS6 random waves was 17.5% and 7.5%, for ship speeds of 25 and 36 knots, respectively. At both model test speeds, the increase in propulsive power due to SS6 random waves, as measured on Model 5653-3 during the powering in waves testing, was less than the comparable powering estimated by using the calm water propeller-hull interactions.

Wind drag in SS6 was calculated, Table A18, using the ship forward speed,  $V_s$ , and assuming that in a head seas condition, as tested, the ship would be sailing directly into a head wind equivalent to the SS6 mean sustained wind speed as reported,  $Wind_{SS6} = 37.5$  knots. Frontal reference area,  $AV = 8269 \text{ ft}^2$  was estimated as  $0.75 * Bx^2$ , where  $Bx = \text{ship maximum beam, ft.}$

The effective power for the JHSS indicative baseline design in SS6 random waves with estimated wind drag included is presented in Table A19. Full-scale increase in effective power due to SS6 estimated wind drag, relative to the effective power in SS6 waves alone, was 15.7% and 11.4%, for ship speeds of 25 and 36 knots, respectively. The increase in effective power due to the estimated wind drag in SS6 was of the same magnitude as the increase in effective power due to the SS6 random waves.

The JHSS indicative baseline design powering in SS6 random waves with estimated wind drag included is presented in Table A20 and Figure A10. This powering analysis was computed using the effective power in SS6 random waves with estimated wind drag included (Table A19), and the propeller-hull interaction coefficients from the model powering test in SS6 random waves (Table A17). Full-scale increase in delivered power due to SS6 random waves and estimated wind drag, relative to the calm water effective power, was 35.0% and 18.7%, for ship speeds of 25 and 36 knots, respectively.

For the JHSS indicative baseline design, effective and delivered power in calm water and SS6 random waves (with and without wind drag included) are summarized and compared in Tables A21-23, and summarized in brief, in Table 2. The added resistance and powering in SS6 random waves with/without wind drag included are presented as a percentage increase relative to the calm water values, and are also presented in Figure 2. It should be noted that the presented results for powering in SS6 random waves with/without wind drag do not include assessments of possible propeller cavitation or cavitation thrust breakdown.

Table 2. JHSS indicative baseline design powering in calm water, SS6 random waves, and SS6 waves with wind drag included

	25 knots			36 knots		
	PE (hP)	PD (hP)	RPM	PE (hP)	PD (hP)	RPM
Calm	32837	51611	89.6	98864	153007	127.2
SS6 Waves	39923	60664	91.5	109655	164467	128.1
	21.6%	17.5%	2.2%	10.9%	7.5%	0.7%
	[% increases due to Waves, relative to calm water]					
SS6 Waves & Wind	46194	69692	93.7	122144	181587	130.2
	40.7%	35.0%	4.6%	23.5%	18.7%	2.4%
	[% increases due to Waves & Wind, relative to calm water]					

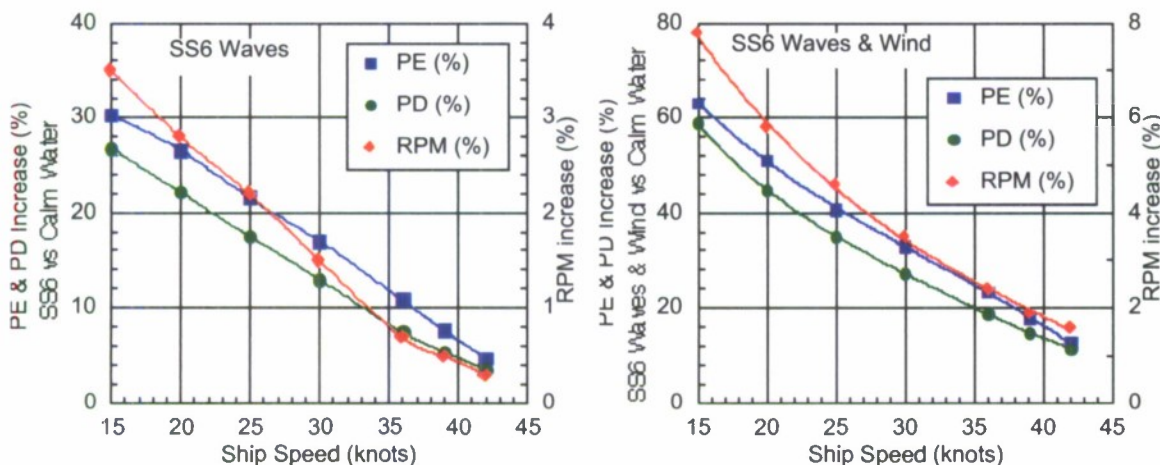


Fig. 2. JHSS indicative baseline design, added resistance and powering in SS6 random waves (left) and SS6 waves with wind drag included (right)

Results of powering analysis in SS6 random waves, with the addition of associated wind drag, indicate that a sea margins of approximately 40% at 25 knots or 20% at 36 knots would be adequate for the assessment of power increase and/or speed loss in SS6 for the JHSS indicative baseline design and for future sealift-type hull designs.

The results of the JHSS indicative baseline design powering in SS6 random waves with estimated wind drag included, indicates that 36 knots would be attainable in SS6 with approximately 182,000 hP. 39 knots would not be attainable in SS6 for this sealift design, envisioned to have a total installed power of 240,000 hP.

Even though the SS6 power increase at low speed appears high when expressed as a percentage of calm water values (approximately 60% for 15 knots), sizing of the propulsion plant for the required power at 39 knots in calm water, would exceed the power requirements at low speeds, or even at 36 knots, in SS6.

## **REGULAR WAVES TEST RESULTS**

The Model 5653-3 test results in regular waves will be used for comparisons and validations with various numeric prediction tools, for both increased resistance in waves, and for possible future motions simulations.

### **Critical Wavelengths**

Critical wavelengths were determined for Model 5653-3 operating in regular waves, at ship speeds of 25 and 36 knots. Critical wavelength at each speed was defined as that which produces the largest increased resistance, as evaluated by the added resistance operator (ARO), Equ. [1].

$$\text{Equ. [1]: } \text{ARO} = R_{\text{AW}} / (\rho * g * A_w^2 * B_x^2 / L)$$

Where:  $R_{\text{AW}}$  = added resistance in regular waves;  $\rho$  = water density;  $g$  = gravity;  $A_w$  = wave amplitude;  $B_x$  = maximum beam;  $L$  = length

ARO was formulated to evaluate the model-scale resultant increased resistance in regular waves, with varying wavelength,  $\lambda$ , expressed as a function of wave height,  $\zeta$ . A critical wavelength, at each speed, was determined by the largest value of ARO produced in regular waves, evaluated over a range of wavelengths at a single selected wave slope,  $\zeta/\lambda = 1/75$ .

The sensitivity of the wave-maker valve frequency control ( $\sim 0.01$  Hz) dictated the minimum variability in the range of wavelengths tested, and iterations on wave-maker blower RPM allowed for the generation of wave heights required for the 1/75 wave slope. The data from all of the variations in wavelength and wave heights tested in regular waves, targeting desired wave slope of 1/75, and calculation of ARO, are presented in Appendix A, Table A22. The selected data in regular waves over variations in wavelength, at the desired wave slope of 1/75, utilized for the determination of critical wavelengths, are presented in Table A23 and Figure A11.

For a ship speed of 25 knots, the critical wavelength, expressed as a function of ship length overall,  $\lambda/LOA$ , was determined to be 0.882. Similarly, the critical wavelength for a ship speed of 36 knots was 0.966. The remainder of the model-scale resistance and powering tests in regular waves were conducted at these two respective critical wavelengths.

Prior to the experiments, values of the added resistance operator (ARO), for each of the two test speeds, were calculated by using the SWAN1 numeric prediction tool. SWAN1 is a linear potential flow code using Rankin source method (Ref. 9). As a preliminary comparison with a numeric prediction tool<sup>2</sup>, the model-scale resultant ARO values were compared to the values predicted by SWAN1, which are included in Figure A11.

### **Increased Resistance & Powering in Regular Waves**

Resistance and powering experiments were conducted in regular waves at a critical wavelengths of  $\lambda/LOA = 0.882$  for the 25 knots test speed and  $\lambda/LOA = 0.966$  for the 36 knots test speed for a variety of wave slopes,  $\zeta/\lambda$ , in the range of  $1/150 \leq \zeta/\lambda \leq 1/60$ .

Model-scale resistance test data in regular waves at critical wavelengths, for variations in wave slope, are presented as increased resistance relative to calm water values, and as calculated added resistance operator (ARO), in Appendix A, Tables A24-A26 and in Figure A12. Similarly, increased model-scale force values from the powering tests in regular waves, fixed-in surge and free-to-surge, are presented in Tables A27-A28 and in Figures A13-14. As expected, at fixed wavelength, increases in all force values in regular waves, for resistance and powering, become greater with increasing wave slope. Model-scale resistance and powering measured forces in calm water and regular waves (at critical wavelengths), and force value increases in

<sup>2</sup> Model 5653-3 resultant data comparisons and validations with various numeric prediction tools will be documented in a separate report.

regular waves, are presented in Appendix A, Table A29. Model-scale increased resistance and powering in regular waves, expressed as a percent of calm water values averaged from the fixed-in-surge and free-to-surge configurations, are summarized in brief, in Table 3.

Table 3. Model-scale increased resistance and powering in regular waves

Slope $\zeta\lambda$	Increased % in Waves, 25 kts Critical Wavelength $\lambda/LOA = 0.882$			Increased % in Waves, 36 kts Critical Wavelength $\lambda/LOA = 0.966$		
	Rw (%)	PDw (%)	RPMw (%)	Rw (%)	PDw (%)	RPMw (%)
1/150	10.4	10.5	1.5	6.4	9.0	0.9
1/120	13.1	17.0	2.3	10.7	12.3	1.2
1/100	16.3	22.3	2.9	15.7	15.8	1.7
1/75	28.1	39.9	5.2	23.4	31.0	3.7
1/60	42.0	61.0	7.7	28.3	-	-

### **MODEL MEASUREMENT UNCERTAINTY / VARIABILITY**

Model 5653-3 calm water measurement uncertainties were determined for the model quantities of speed and resistance, and for combined inboard and outboard shafts quantities of thrust, torque, and rotational speed (RPM). The values for torque and RPM were then used to determine the uncertainty in the calculation of delivered power. Model-scale calm water uncertainties were derived by combining bias and precision errors using the root-sum-square (RSS) method for a 95% confidence level.

As per standard practice, calm water precision errors were determined by conducting singular speed passes (minimum of two passes) down the length of the test basin, during which as many (10 sec @ 20 Hz) data spots as time permits are collected. The precision error limit values are determined directly from the total number of repeated individual data spots (minimum of 12-15). Model 5653-3 calm water measurement uncertainties were determined at full-scale speeds of 25 and 36 knots, and are presented in Appendix A, Table A30. In calm water, Model 5653-3 resistance measurement uncertainties were  $\pm 1.78\%$  and  $\pm 0.62\%$  of the measured nominal mean values, for 25 and 36 knots, respectively. Likewise, the delivered power measurement uncertainties were  $\pm 1.70\%$  and  $\pm 0.76\%$ . The stated uncertainties for measured model delivered power reflect the combined measurement uncertainties of eight model quantities, shaft torque and RPM, for each of four shafts.

The collection of capricious (unsteady) model-scale measurements, during the non-steady state testing in SS6 random waves, renders the standard determination of measurement uncertainties invalid. A determination of the variability in the unsteady force measurements reflects more accurately the model test repeatability. Model-scale variability in the measurements during tests in SS6 waves were derived by combining bias and precision errors using the root-sum-square (RSS) method for a 95% confidence level. With the use of identical equipment and instrumentation, the bias error, characterized as a fixed or systematic error, is assumed equivalent when testing in either calm water or waves. The precision error (random or repeatability error) is a function of the unsteadiness of the phenomenon being measured and the stability of test equipment. Since the model response and all force measurements during SS6 testing are inherently unsteady, the precision error for tests in SS6 waves will be significantly higher than that for tests in calm water.

Data for a single spot, when testing in SS6, was collected continuously throughout an entire pass down the length of the basin. Therefore, it was determined that the precision error analysis should reflect this procedure. The precision error limit values, for each test speed in SS6, were determined from the end-of-pass averaged values regarded as individual data points. The small number of samples (5-9) required that a large Student T value be applied to the standard deviations. The force measurement variabilities were not always consistent, due both to the

limited number of sample points and the unsteadiness of the measurements. For Model 5653-3 operating in SS6 random waves, the variability in the model-scale measurements were determined at full-scale speeds of 25 and 36 knots, and are presented in Appendix A, Table A30. In SS6 random waves, the resistance measurement variabilities (fixed-in-surge), for Model 5653-3, at 25 and 36 knots, were determined to be  $\pm 4.99\%$  and  $\pm 3.63\%$  of the measured nominal mean values, respectively. The delivered power measurement variabilities, for the fixed-in-surge condition in SS6, were  $\pm 6.68\%$  and  $\pm 1.71\%$ , and in the free-to-surge condition in SS6 were  $\pm 3.73\%$  and  $\pm 3.24\%$ .

### **SHIP MOTION RESPONSES IN SS6**

The model was ballasted and instrumented to acquire properly scaled motions and accelerations due to advancement in waves from ahead. The resulting data was processed and presented to highlight the influence of test procedures with regards to the use of an un-propelled or a self-propelled model and the model freedom-to-surge.

The data was processed find the basic statistics of the data; maximums, minimums, means, and standard deviations. Significant single amplitude responses (SSA) are also computed for the identification of seakeeping motion characteristics. All ship motions data and analysis is presented in Appendix B.

For a model that is fixed-in-surge, the comparison between an unpropelled and propelled conditions indicated that there is no appreciable influence by the addition of propulsion thrust.

For a propelled model, the free-to-surge condition as compared to the fixed-in-surge condition, again indicated that the motions were not appreciably affected. The pitch rate did, however, increase in the 36 knot condition when the model is free-to-surge even though the wave height was slightly lower.

Unfortunately, due to the influence of broad-range noise from the electric propulsion motors, it was not possible to make valid conclusions about the accelerations during any propulsion tests.

### **EVALUATION OF POWERING IN WAVES TEST TECHNIQUES**

A new testing technique, using glide rails, for conducting powering in waves experiments with the model either fixed-in-surge or free-to-surge was evaluated. Comparisons were made of the added powering results and ship motions and accelerations responses for the model fixed and free-to-surge, operating at both ship propulsion and model self-propulsion conditions.

#### **Glide Rail System**

Code 5800 test engineers devised an innovative glide rail system for the attachment of the model to the tow post / towing carriage. The standard tow post and instrumentation was mounted on two linear glide rails attached to the model, fore and aft, as depicted in Figure 3. These glide rails were locked in a single longitudinal position during the fixed-in-surge resistance and powering tests, and allowed to move freely fore and aft during the free-to-surge powering tests. This system allowed for the model to freely surge fore and aft as necessary, while eliminating the constant rudder angle adjustments normally required for course corrections on either a tethered or free-running model. The glide rail system installed and tested on Model 5653-3 proved to be a valid method by which to conduct 'back-to-back' free-to-surge and fixed-in-surge experimentation in waves.



Fig. 3. Glide rail system as installed and tested on Model 5653-3

There were two possible disadvantages identified for the glide rail system during free-to-surge experiments. (1) Constant surging / movement of the model fore and aft could result in unaccounted residual friction in the glide bearings. Glide bearing frictional forces, measured with block gages at the fore and aft model attachment points, were determined to be inconsequential. (2) Due to the inclusion of the weight of the tow post's floating components and instrumentation in the dynamic ballasting of the model, any significant movement fore or aft could render the ballasting imprecise, and result in misleading model dynamic pitch and incorrect resistance and powering measurements. To minimize these inaccuracies, the model test engineers attempted to limit the fore and aft movement of the model during any single powering run to  $\pm 6$  inches of the initial ballasting (centered) position. This required constant adjustments to the model drive system shaft speed (RPM). These adjustments, however, were of no greater magnitude than is generally necessary during free-to-surge powering experiments in waves.

#### Fixed-in-Surge versus Free-to-Surge

A comparison of the model-scale added force measurements in SS6 random waves, from the fixed-in-surge versus free-to-surge powering test techniques, revealed that the two methods produced very similar results. This was somewhat unexpected, as there was a significant difference in the force levels measured, fixed-in-surge tests being conducted at ship propulsion point while free-to-surge tests are conducted at model self-propulsion. However, the 'added' force values (thrust, torque, RPM, etc.), for powering in SS6 random waves, determined by difference in the measured total force value in waves and the comparable value in calm water, did not show an appreciable difference between the two methods. Differences between the added force value measurements were within experimental accuracy. For the evaluation of the JHSS indicative baseline design in SS6 random waves, presented herein, the averaged added force measurements from the two test techniques were utilized.

## CONCLUSIONS

Resistance and powering tests were conducted on Model 5653-3 in calm water, in sea state 6 random waves, and in regular waves. Model 5653-3 is representative of the Joint High Speed Sealift (JHSS) conventional Baseline Shaft & Strut (BSS) hull.

In order to assist in the indicative JHSS baseline hull design, resistance and powering experiments were conducted on Model 5653-3 in a large SS6 random waves system. The presented results for powering in SS6 random waves do not include assessments of possible propeller cavitation or cavitation thrust breakdown. The following is a summary of the results:

- Sizing of the propulsion plant in a sealift-type hull for 39 knots in calm water should assure that sufficient power is available for achieving 36 knots in Sea State 6.
- Full-scale increase in delivered power due to SS6 random waves was 17.5% and 7.5%, for ship speeds of 25 and 36 knots, respectively.
- Powering in SS6 random waves with associated wind drag indicates a full-scale increase in power of 35.0% and 18.7%, for ship speeds of 25 and 36 knots, respectively.
- The increase in power due to the wind drag associated with SS6 was of approximately the same magnitude as the increase in power due to the SS6 random waves.
- The 39-knot speed of interest will not be attainable in SS6 for the indicative JHSS baseline design with the total installed power envisioned.
- Qualitative observations indicate that the long, slender sealift design, when running in SS6, would likely experience only mild pitching and no occurrences of slamming at the bow or stern regions, despite the heavy sea state.
- The motions of the model were not significantly influenced by propulsion thrust or the ability to surge longitudinally. Even though the current data reveals that the motions are not appreciably affected, it is expected that the acceleration data would be influenced, most noticeably in the longitudinal accelerations.

Additionally, it should be noted that:

- The test results in regular waves will be used for comparisons and validations with various numeric prediction tools, for both increased resistance in waves, and for motions simulations.
- The critical wavelength, defined as that which produces the largest increased resistance in regular waves, was determined at each tested ship speed, 25 and 36 knots.
- Subsequent testing at these critical wavelengths, for variations in wave slope, provides a large matrix of resistance and powering data for comparisons to various numeric prediction tools.

### ACKNOWLEDGEMENTS

Project funding was primarily through the JHSS Project Office, NAVSEA 05D1.

NSWWCD points of contact for the topics contained within this document are: Dominie S Cusanelli (Code 5800) for the resistance, powering, and flow visualization; Bryson Metcalf (5800) for the ship motions analysis, and Anne Marie Powers (6530) for the model laser measurements.

Current members of the High Speed Sealift Hydro Working Group (HWG) include the following individuals. From NSWCCD: Robert Anderson, HWG chairman (Code 2410); Stuart Jessup (503); Gabor Karafath, Dominie S. Cusanelli, Rae Hurwitz, Scott Blaek, Michael Wilson and Thad Michael (5800); Andy Silver (5500); Siu Fung, Colen Kennell, and George Lamb (2420); and Edward Devine (6540). Additional HWG members are: Jack Offutt (consultant); Christopher Dicks (FORNATL-UK); and Jeff Bohn, Steve Morris, and John Slager (CSC).

The authors would also like to acknowledge the following personnel for their contributions towards this model test series: Hong Vo (Code 5300); Daniel Lyons and Stephanie Basha (Code 5800); Ray Lerner (6530); and Dennis Mullinx (CSC).

This page intentionally left blank.

## REFERENCES

1. "Rapid Strategic Lift Ship Feasibility Study Report", Ser 05D/097, NAVSEA 05D, (29 Sept. 2004).
2. Wynn, Steven, "Joint High Speed Sealift (JHSS)", NAVSEA Presentation, (March 8, 2006).
3. Fung, S.C., G. Karafiath, D.S. Cusanelli, and D. McCallum, "JHSS (Joint High-Speed Sealift Ship) Hull Form Development, Test and Evaluation", Ninth International Conference on Fast Sea Transportation, FAST2007, Shanghai, China (Sept 2007)
4. Cusanelli, D.S., "Joint High Speed Sealift (JHSS) Baseline Shaft & Strut (Model 5653) Series 1: Bare Hull Resistance, Appended Resistance, and Alternative Bow Evaluations" 50-TR-2007/066 (Aug 2007)
5. Cusanelli, D.S., and C.J. Chesnakas, "Joint High Speed Sealift (JHSS) Baseline Shaft & Strut (BSS) Model 5653-3: Series 2, Propeller Disk LDV Wake Survey; and Series 3, Stock Propeller Powering and Stern Flap Evaluation Experiments", NSWCCD-50-TR-2007/007, (March 2007)
6. Stahl, R.G., "Ship Model Size Selection, Facilities, and Notes on Experimental Techniques", CRDKNSWC/HD-1448-01, (May 1995)
7. Cusanelli, D.S., and J. Bradel, "Floating Platform Tow Post" United States Patent No. 5,343,742 (Sept. 6, 1994)
8. Grant, J.W. and C.J. Wilson, "Design Practices for Powering Predictions", Ship Performance Department, Departmental Report SPD-693-01, (Oct, 1976).
9. SWAN1 2001, Ship Flow Simulation in Calm Water and in Waves, User Manual, M.I.T.

This page intentionally left blank.

**APPENDIX A**

**RESISTANCE & POWERING DATA & ANALYSIS**

Model 5653-3 in SS6 Random Waves and Regular Waves

	<u>APPENDIX A</u>	Page
TEST PROCEDURES .....		A5
Calm Water .....		A5
Random (Irregular) Sea State 6 .....		A5
Regular Waves .....		A6

	<u>FIGURES OF APPENDIX A</u>	Page
A1. Model 5653-3 photographs: Equipment and installation .....		A7
A2. Model 5653-3 test photographs: Flow visualization .....		A11
A3. JHSS BSS recommended bilge keel alignment, 36 knots .....		A18
A4. Model 5653-3 test photographs: Underway in waves .....		A19
A5. Basin 2 pneumatic wavemaker representative output wave spectra for sea state 6 (SS6).....		A22
A6. Basin 2 pneumatic wavemaker output regular waves characteristics for specified valve frequency and blower RPM conditions .....		A22
A7. Model 5653-3, comparison of added resistance, thrust, torque and RPM, in SS6 random waves .....		A23
A8. JHSS BSS effective and delivered power in calm water .....		A24
A9. JHSS BSS effective and delivered power in SS6 random waves, with a comparison to calm water values .....		A25
A10. JHSS BSS effective and delivered power in SS6 random waves with wind drag included, with a comparison to calm water values .....		A26
A11. Model 5653-3 added resistance operator (ARO) in regular waves, variations in wavelength, selected data at desired wave slope of 1/75 for determination of critical wavelengths .....		A27
A12. Model 5653-3 added resistance operator (ARO) for variations of wave slope at determined critical wavelengths for 25 and 36 knots .....		A28
A13. Model 5653-3, comparison of added resistance, thrust, torque and RPM, 25 knots in regular waves at critical wavelength $\lambda/LOA = 0.882$ .....		A29
A14. Model 5653-3, comparison of added resistance, thrust, torque and RPM, 36 knots in regular waves at critical wavelength $\lambda/LOA = 0.966$ .....		A30

	<u>TABLES OF APPENDIX A</u>	Page
A1. Test Agenda: JHSS BSS Model 5653-3 added resistance and powering in random and regular waves .....		A31
A2. JHSS BSS specified inertial criteria for model 5653-3 ballasting .....		A32
A3. Model 5653-3, bilge keel added resistance, 25 and 36 knots .....		A33

**TABLES OF APPENDIX A (continued)**

Page

A4. Definitions and criteria, annual random (irregular) sea state occurrences in the open ocean for the northern hemisphere .....	A33
A5. Model 5653-3 Exp 56, added resistance in SS6 random waves, locked in surge, 25 and 36 knots .....	A34
A6. Model 5653-3 Exp 54, calm water powering, locked in surge (ship propulsion point), 25 and 36 knots .....	A34
A7. Model 5653-3 Exp 57, added powering in SS6 random waves, locked in surge (ship propulsion point), 25 and 36 knots .....	A34
A8. Model 5653-3 Exp 55, calm water powering, free to surge (model self-propulsion), 25 and 36 knots .....	A35
A9. Model 5653-3 Exp 58, added powering in SS6 random waves, free to surge (model self-propulsion), 25 and 36 knots .....	A35
A10. Model 5653-3, summary of added resistance and powering in SS6 random waves .....	A36
A11. JHSS BSS, calm water effective power at DES with stern flap .....	A37
A12. JHSS BSS, calm water effective power at DES with stern flap and bilge keels .....	A37
A13. JHSS BSS effective power in SS6 random waves, determined from model-scale added resistance measurements .....	A38
A14. JHSS BSS calm water powering at DES with stern flap .....	A39
A15. JHSS BSS calm water powering at DES with stern flap and bilge keels .....	A40
A16. JHSS BSS powering estimate in SS6 random waves, determined from effective power prediction in SS6 and calm water interaction coefficients .....	A41
A17. JHSS BSS powering in SS6 random waves, determined from model-scale added powering measurements .....	A42
A18. Wind drag estimates, for JHSS BSS in sea state 6 with associated mean sustained wind speed .....	A43
A19. JHSS BSS effective power in SS6 random waves with estimated wind drag included .....	A44
A20. JHSS BSS powering in SS6 random waves with estimated wind drag included .....	A45
A21. JHSS BSS with bilge keels, summary and comparison of effective and delivered powers in calm water .....	A46
A22. JHSS BSS, summary and comparison of effective and delivered powers in SS6 random waves .....	A47
A23. JHSS BSS, summary and comparison of effective and delivered powers in SS6 random waves and associated wind .....	A48
A24. Model 5653-3 Exp 59, regular waves, variations in wavelength and wave height targeting desired wave slope of 1/75, and calculation of added resistance operator (ARO) .....	A49
A25. Model 5653-3 Exp 59, regular waves, determination of critical wavelengths (maximum ARO) at 25 and 36 knots, selected data at desired wave slope of 1/75 .....	A50
A26. Model 5653-3 Exp 60, added resistance operator (ARO) at 25 knots, for variations of wave slope at critical wavelength $\lambda/LOA = 0.882$ .....	A51

**TABLES OF APPENDIX A (continued)**

Page

A27. Model 5653-3 Exp 60, added resistance operator (ARO) at 36 knots, for variations of wave slope at critical wavelength $\lambda/LOA = 0.966$ .....	A52
A28. Model 5653-3 Exp 60, resistance increase in regular waves, locked in surge, variations of wave slope at critical wavelengths, 25 and 36 knots .....	A53
A29. Model 5653-3 Exp 62, powering increase in regular waves, locked in surge (ship propulsion point), variations of wave slope at critical wavelengths, 25 and 36 knots .....	A54
A30. Model 5653-3 Exp 61, powering increase in regular waves, free to surge (model self-propulsion), variations of wave slope at critical wavelengths, 25 and 36 knots .....	A55
A31. Model 5653-3, summary of resistance and powering increases in regular waves .....	A56
A32. Model 5653-3, model measurement uncertainty, calm water .....	A57
A33. Model 5653-3, model measurement variability, SS6 random waves .....	A58

## RESISTANCE & POWERING TEST PROCEDURES

Tests were conducted on Model 5653-3 in the NSWCCD Deepwater Towing Basin using Carriage 2. The Test Agenda is presented as Appendix A, Table A1.

### **Calm Water**

Data collection time interval, for any individual data 'spot' of the calm water resistance experiment, was set to the standard of 10 seconds. Contained within each data spot was the collection of measurement data from each of the 28 channels monitored for this test series. Data sampling rate was set to 20 hertz (Hz), in order to be equivalent to the intended sampling rate when testing in waves, rather than the standard calm water sampling rate of 100 Hz. In general, three data spots for each of the two test speeds were collected during each single pass down the basin. A data spot for each force measurement was determined by the average value for each 10-second collection interval. A minimum of 12 data points was initially collected for each calm water test speed, which required multiple passes. Calm water data collection was repeated throughout the test series to insure consistency, as judged necessary by the Project Engineer. The final reported force value in calm water, for example total resistance,  $R_T$ , was then determined by a straight average of the entire number of collected individual data spots.

A wave suppression beach is installed at the east end of Basin #2, however, due to the reduction in the water level, the wave-damping equipment along the length (edge) of the basin was not able to be utilized. Approximately a 40-minute time interval between successive passes down the basin was determined to be necessary to insure that the water surface was calm. (Standard time interval is 15 minutes.) The basin water surface was judged to be calm by observing the residual waves heights as registered on the ultrasonic probe.

### **Random (Irregular) Sea State 6**

The Model 5653-3 experiments in support of JHSS indicative design for added resistance and powering in random (irregular) waves were conducted in a simulated waves condition representative of sea state 6 (SS6), head seas. Definitions and criteria for annual sea state occurrences in the open ocean for the northern hemisphere, as recognized by the U.S. Navy, are presented in Table A3. For the experimental representation of irregular waves, Bretschneider formulated wave spectrum are utilized, defined by two parameters, significant wave height ( $H_s$ ) and modal wave period ( $T_w$ ). Model-scale values utilized for the SS6 spectra are as follows:  $H_s = 4.6 - 6.9$  ineh (mean 5.77 ineh) and  $T_w = 1.54 - 2.91$  sec (most probable 2.05 sec).

Long crested random waves were generated using the Basin #2 pneumatic wave-maker. Pneumatic wave-makers require many input function iterations, and adjustments to blower speed (RPM), to obtain the desired output wave height and spectra, particularly during the generation of irregular (random) waves. SS6 random waves were generated continuously throughout a morning or afternoon testing session. A 10-12 minute waiting period was observed after commencement of wavemaking or after each wavemaker adjustment. Wave heights and spectra were then sampled at the approximate center of Basin #2, over a period of 12 minutes duration. Once the input functions were satisfactorily adjusted, resulting in the desired SS6 output spectra, the wave-maker representative output wave spectra was measured and compared to the Bretschneider formulated SS6 wave spectra, Figure A5.

The output significant wave height was monitored constantly by the Code 5800 test engineers, and the pneumatic wave-maker blower RPM was adjusted during the test, if required. Twice daily, the wave output was collected for a 12-minute interval, the output wave spectra was determined, and adjustments made to the pneumatic wave-maker, if required.

Model data collection in SS6 random waves commenced when the model speed reached steady state and was collected continuously for a single test speed throughout an entire pass down Basin #2. Again, each data spot contained the collection of measurement data from each of the 28 channels at a data sampling rate of 20 Hz. A data spot for each force measurement was determined by the average value for the entire pass duration. Additional passes were completed until a cumulative data measurement time equivalent to one hour full-scale operation in SS6 waves was collected for each of the two test speeds. SS6 random waves were generated continuously throughout a morning or afternoon testing session. A 30-minute time interval between successive passes down the basin was used during the testing in SS6.

The reported force value in SS6 random waves, for example total resistance in waves,  $RT_w$ , was then determined by an average of the summation of data measurements (equivalent to one hour full-scale) for each speed. The "added" force value in SS6 random waves, for example added resistance in waves,  $R_w$ , was then determined by difference in the measured total resistance in waves,  $RT_w$ , and the comparable value in calm water,  $R_T$ .

### Regular Waves

Long crested regular waves were generated using the Basin #2 pneumatic wave-maker by setting its two primary inputs, the valve frequency (Hz), to obtain variations in the output wavelength,  $\lambda$ , and the blower speed (RPM), to obtain the desired output wave height,  $\zeta$ , at the resultant output wavelength. Desired and resultant output wavelength was generally expressed as a function of ship length overall,  $\lambda/LOA$ , and characterized with a wave slope of wave height over wavelength,  $\zeta/\lambda$ . The sensitivity of the wave-maker valve frequency control is +/- 0.01 Hz. This frequency sensitivity resulted in a minimum adjustability of  $\lambda = 1.02$  ft at the shortest wavelengths tested varying up to  $\lambda = 1.73$  ft at the longer wavelengths tested. The range of wavelengths tested was  $0.744 \leq \lambda/LOA \leq 1.237$ , and the range of wave slopes tested was  $1/150 \leq \zeta/\lambda \leq 1/60$ . Desired output wave slopes could be estimated by the linear relationships between output wave height resulting from adjustments in pneumatic wave-maker blower RPM, at a set valve frequency, depicted in Figure A6.

It was recommended that the data collection time interval in regular waves encompass, at a minimum, twenty wave encounters. During runs where both test speeds were measured, the basin length allowed for data collection time intervals of 40-50 seconds for each speed, corresponding to 35-45 wave encounters. When a single speed was run down the entire basin length, the data collection time interval for each of two spots, on average, was 68 seconds (corresponding to 50 wave encounters) at 25 knots, and was 46 seconds (corresponding to 37 wave encounters) at 36 knots. Again, each data spot contained the collection of measurement data from each of the 28 channels at a data sampling rate of 20 Hz.

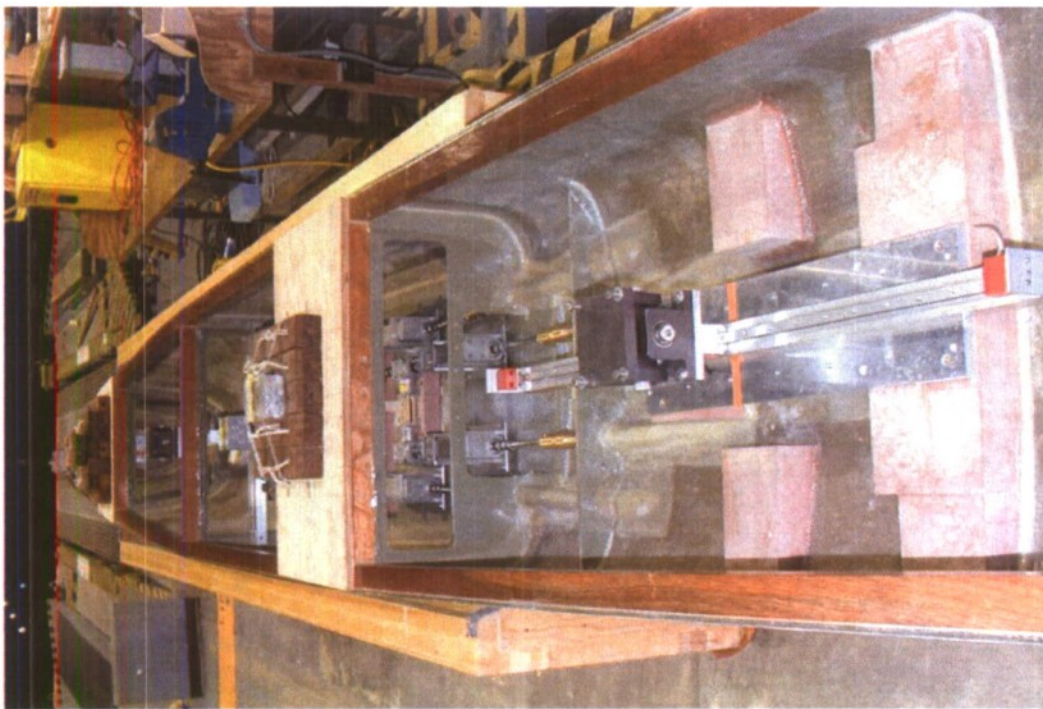
The reported force value in regular waves, for example total resistance in waves,  $RT_w$ , was determined by the single spot data measurement (minimum wave encounters greater than 20 recommended) for each speed. The "increased" force value in regular waves, for example increased resistance in waves,  $R_w$ , was then determined by difference in the measured total resistance in waves,  $RT_w$ , and the comparable value in calm water,  $R_T$ .



*Stern flap, rudders, stock propellers*

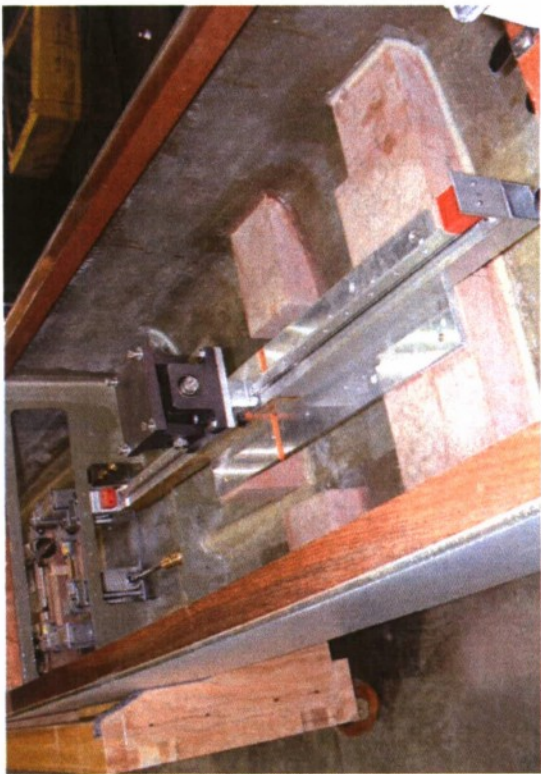


LCG Motions Sensors (2-axis Pitch & Roll, 3-axis Acceleration)

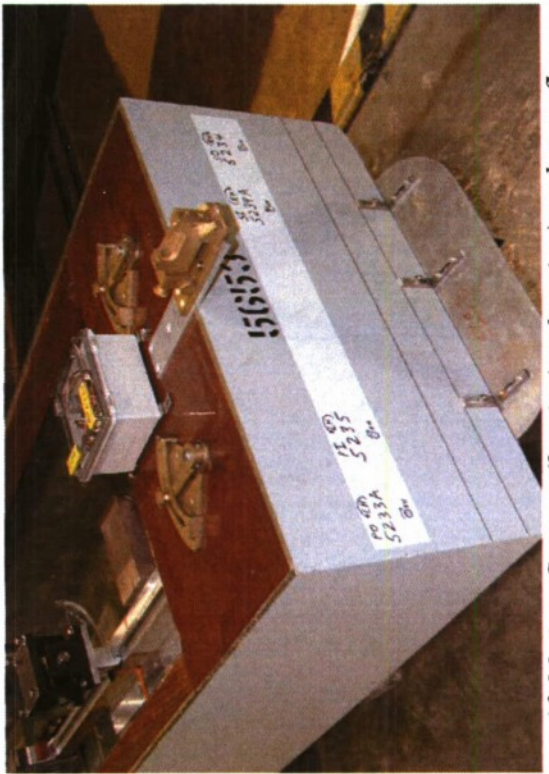


*All equipment installed and dynamically ballasted*

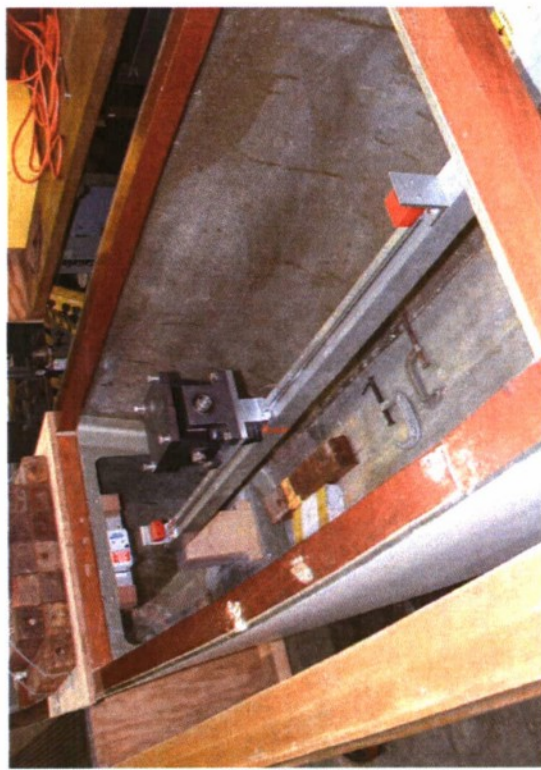
Fig. A1. Model 5653-3 photographs: Equipment and installation



*Aft 'Free-to-Surge' Glide Rail*



*Aft Motions Sensors (3-axis Acceleration) and stern flap*



*Forward 'Free-to-Surge' Glide Rail*



*Forward Motions Sensors (3-axis Acceleration)*

Fig. A1. Model 5653-3 photographs: Equipment and installation - continued



*Installed beneath inertial "A" frame*

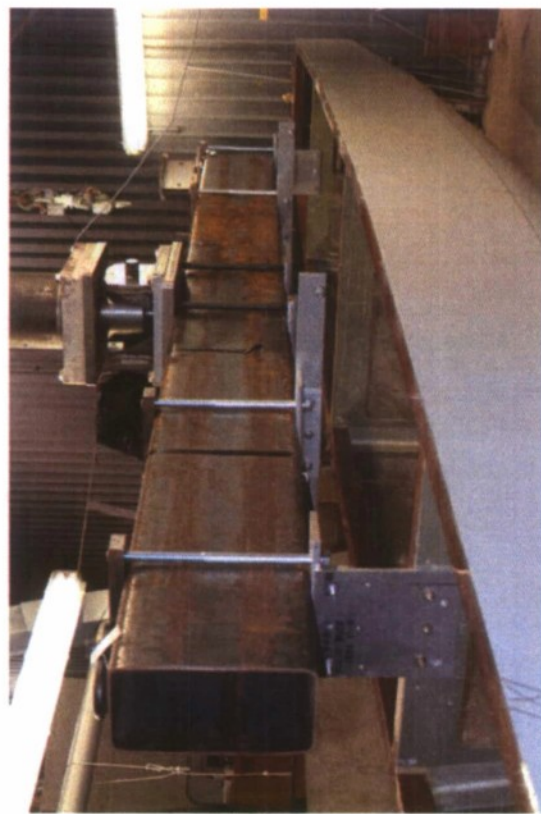
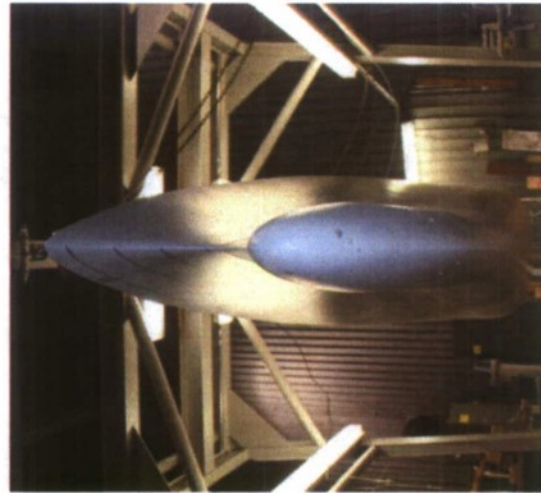
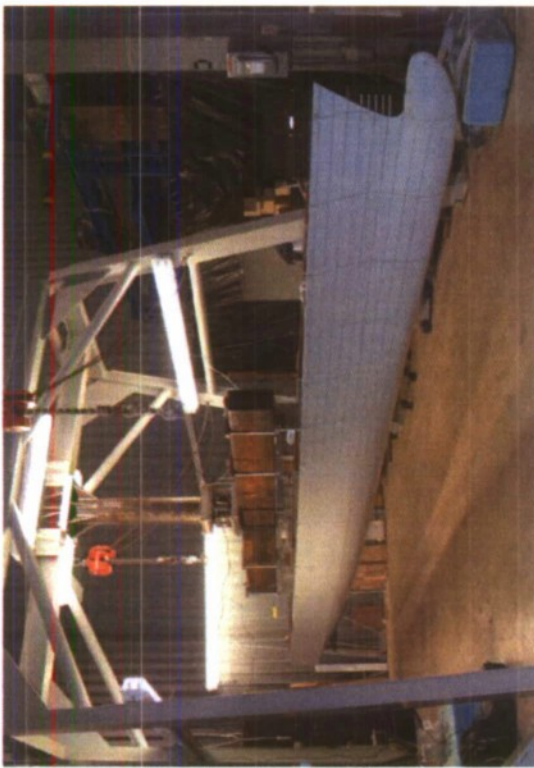
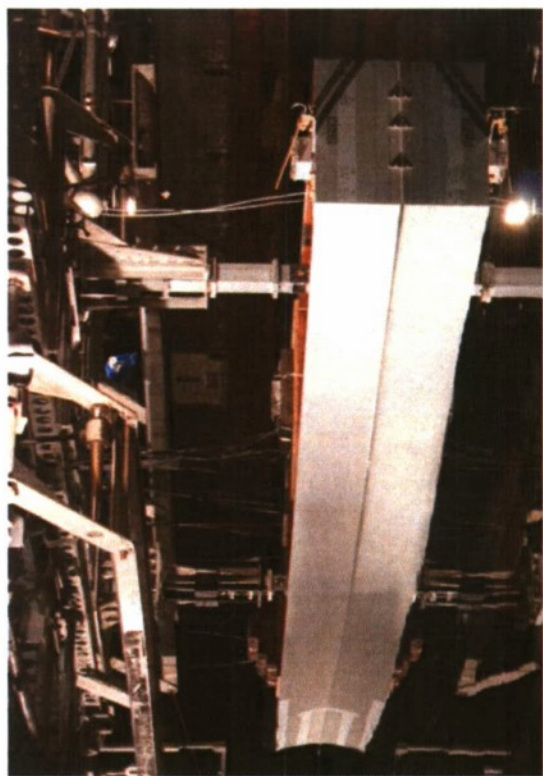
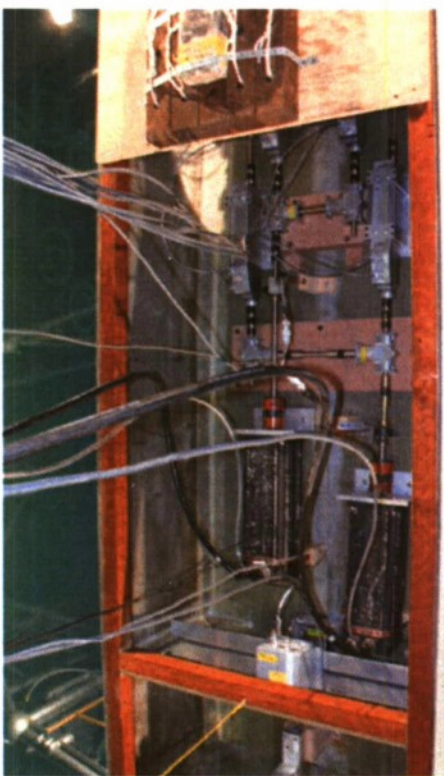


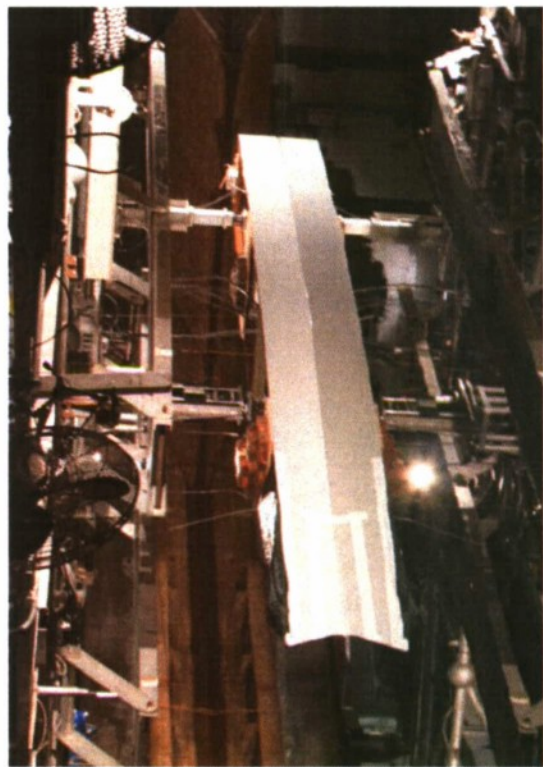
Fig. A1. Model 5653-3 photographs: Equipment and installation - continued



*Installed beneath Carriage 2, stern quartering view*



*Drive system and shaftline instrumentation*

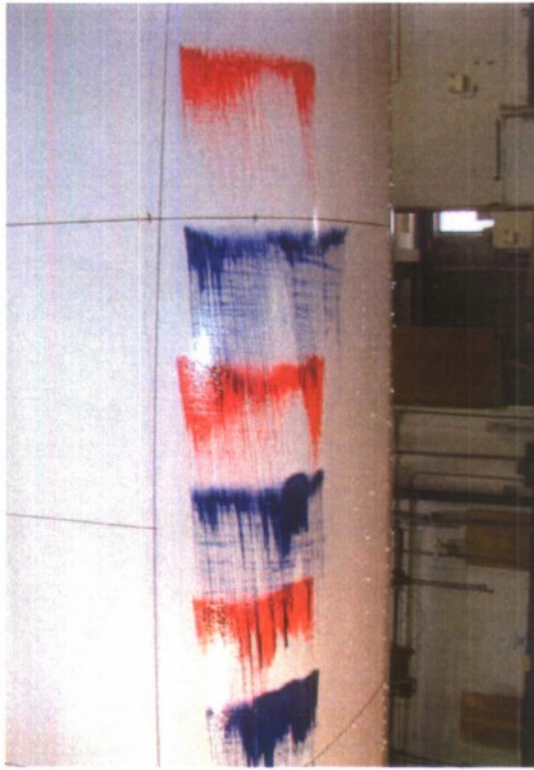


*Installed beneath Carriage 2, bow quartering view*

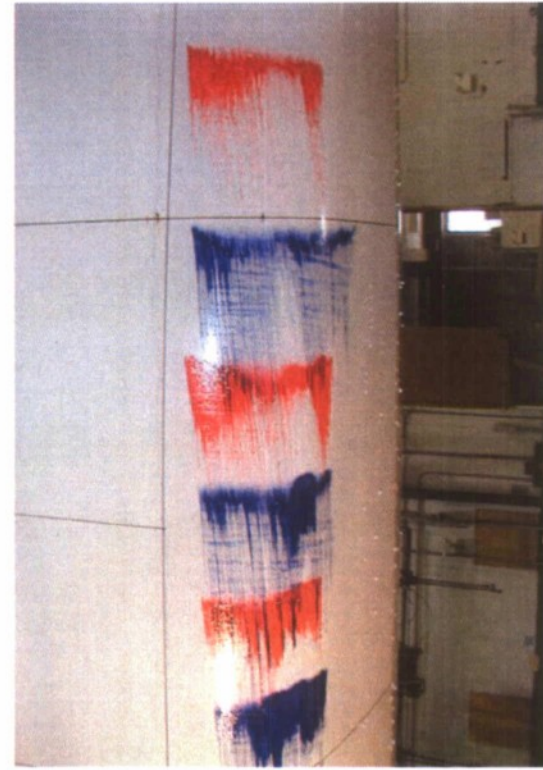


*Forward tow post and instrumentation installed on glide rail*

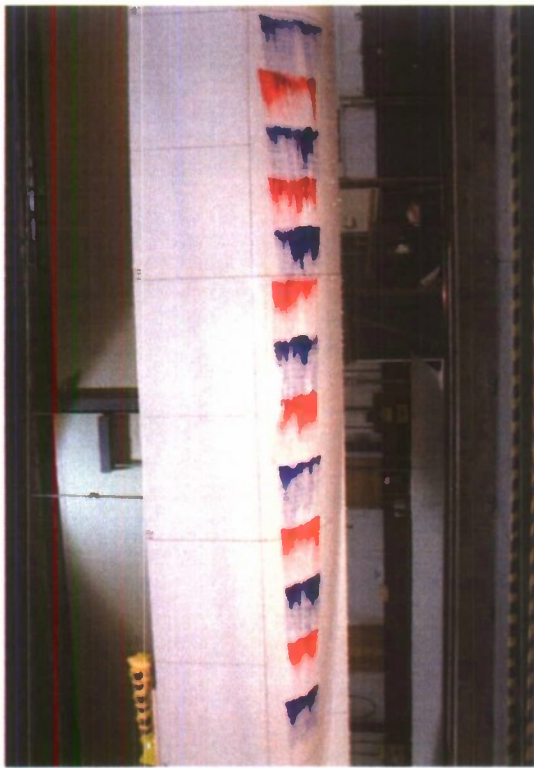
Fig. A1. Model 5653-3 photographs: Equipment and installation - continued



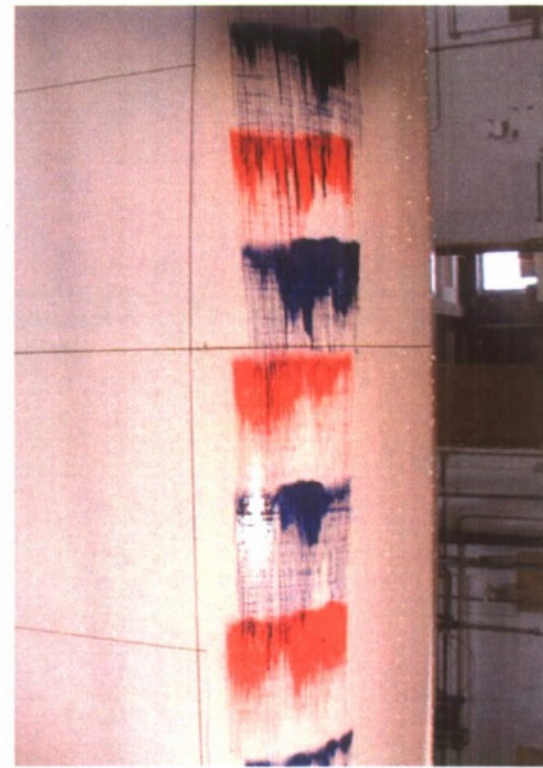
Starboard bilge keel trace, forward



Starboard bilge keel trace, aft

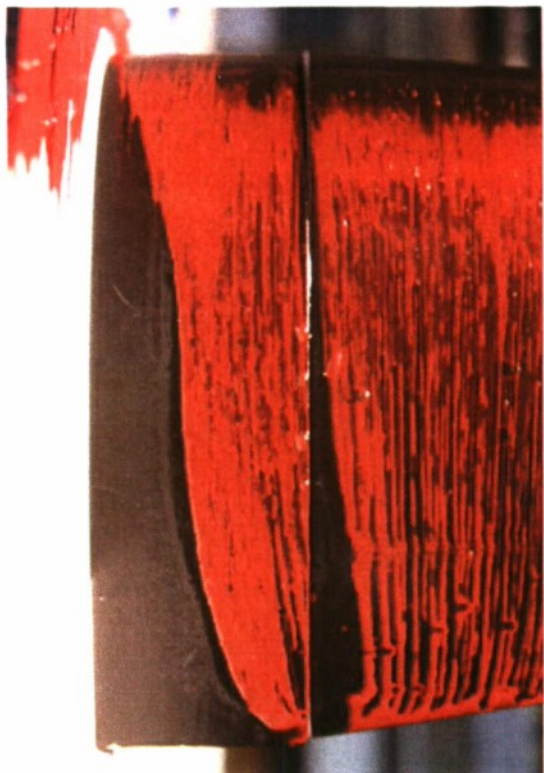


Starboard bilge keel trace, mid

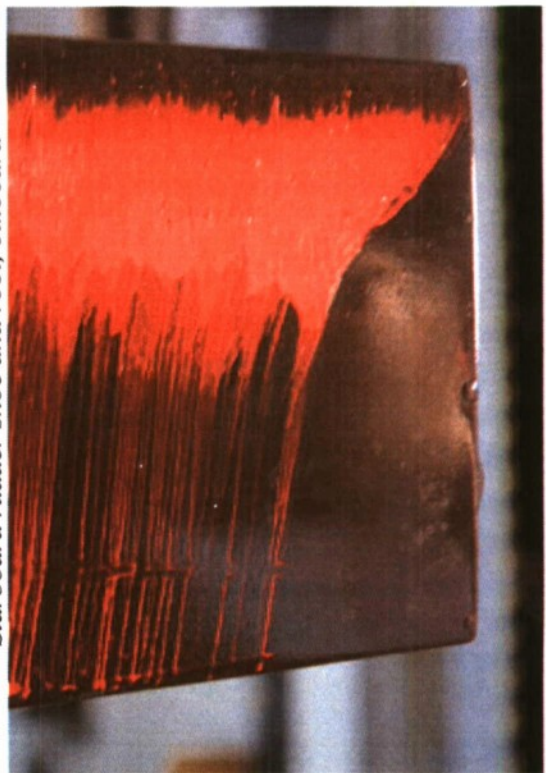


Starboard bilge keel trace, mid

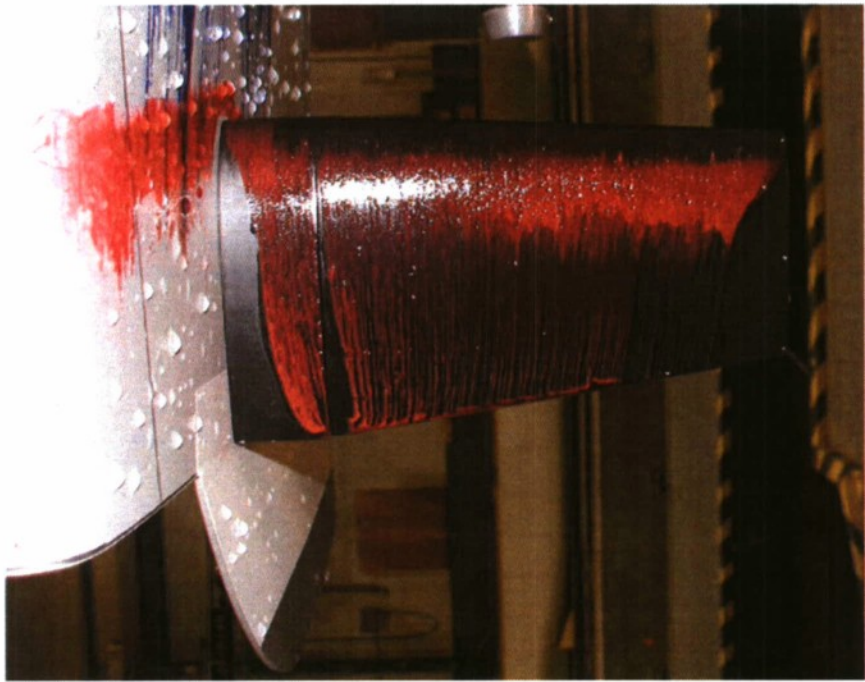
Fig. A2. Model 5653-3 test photographs: Flow visualization



Starboard rudder shoe and root, outboard

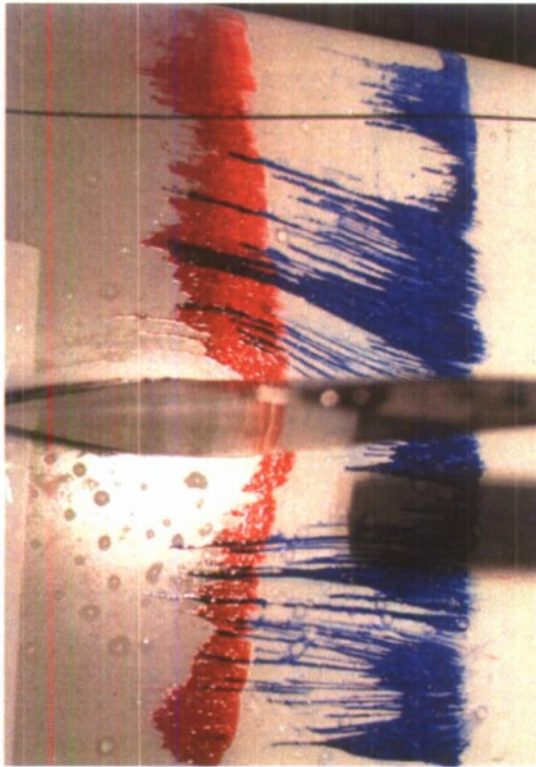


Starboard rudder tip, outboard

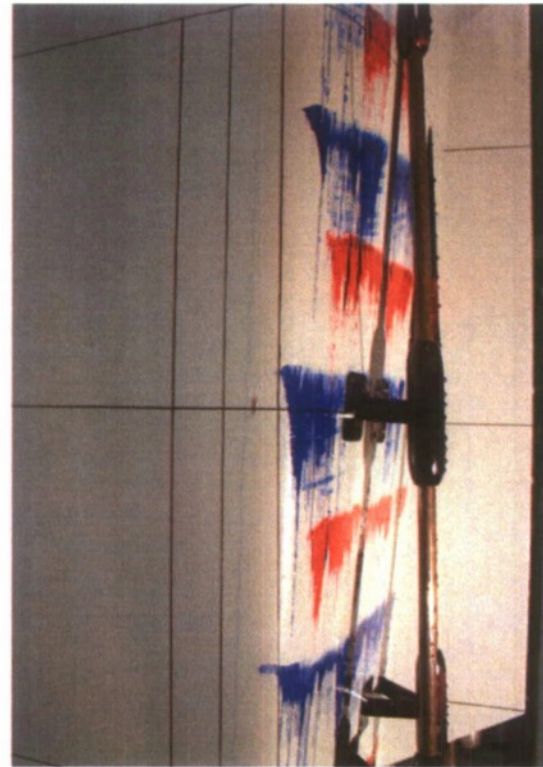


Starboard rudder, outboard

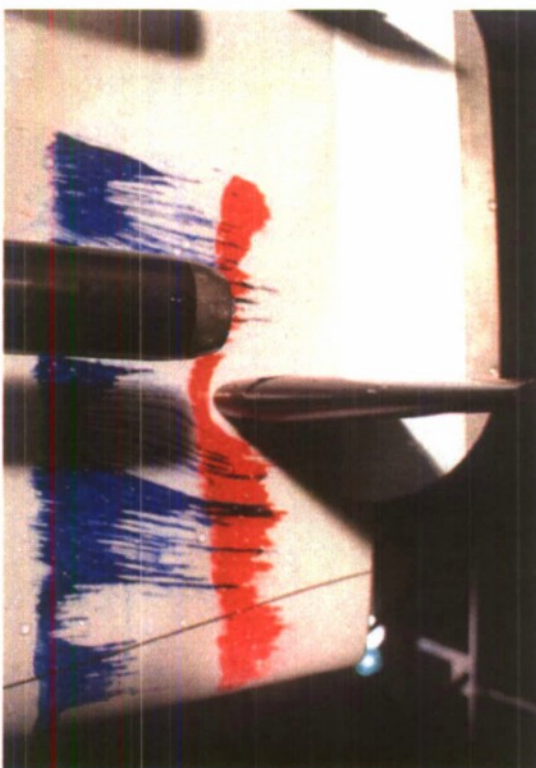
Fig. A2. Model 5653-3 test photographs: Flow visualization - continued



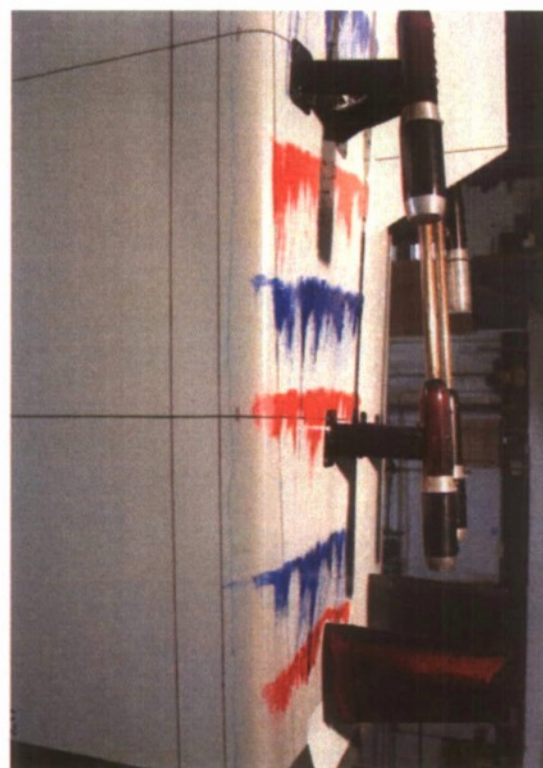
Starboard rudder, view from aft-underneath



Starboard side, outboard, stations 18-19

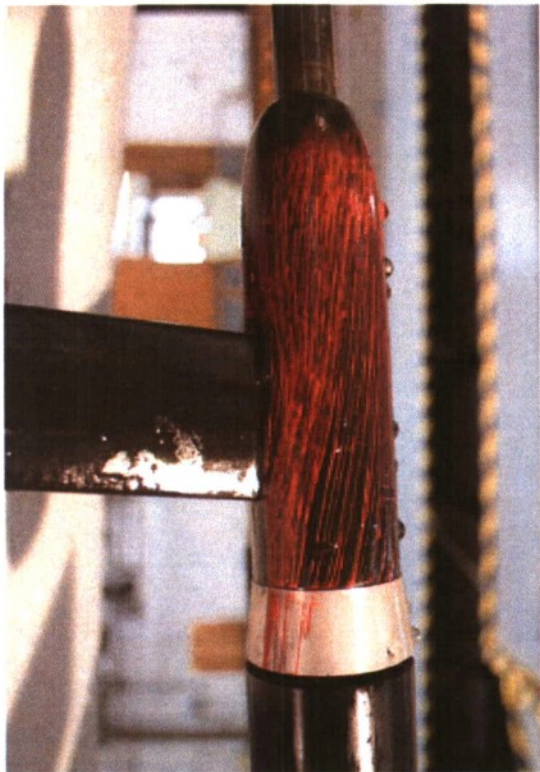


Starboard rudder, view from forward-underneath

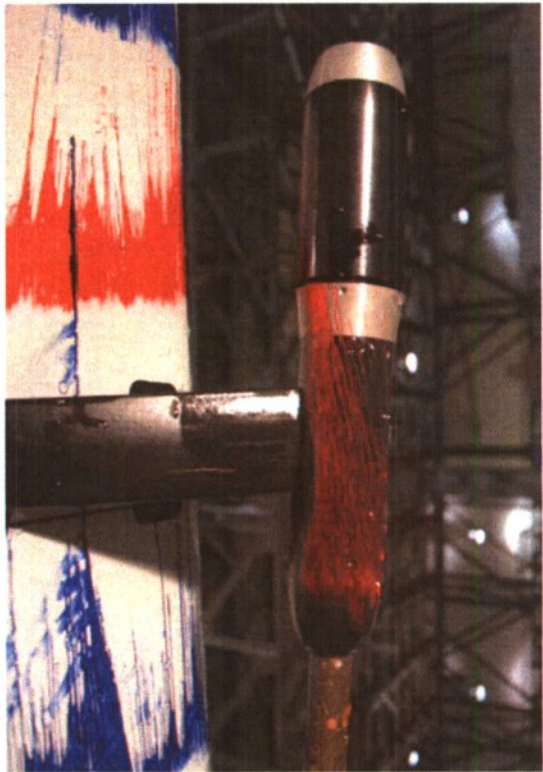


Starboard side, outboard, stations 19-20

Fig. A2. Model 5653-3 test photographs: Flow visualization - continued



*Main strut barrel 4, outward*



*Main strut barrel 4, inward*



*Main strut barrel 4 and Intermediate strut barrel 3, outward*

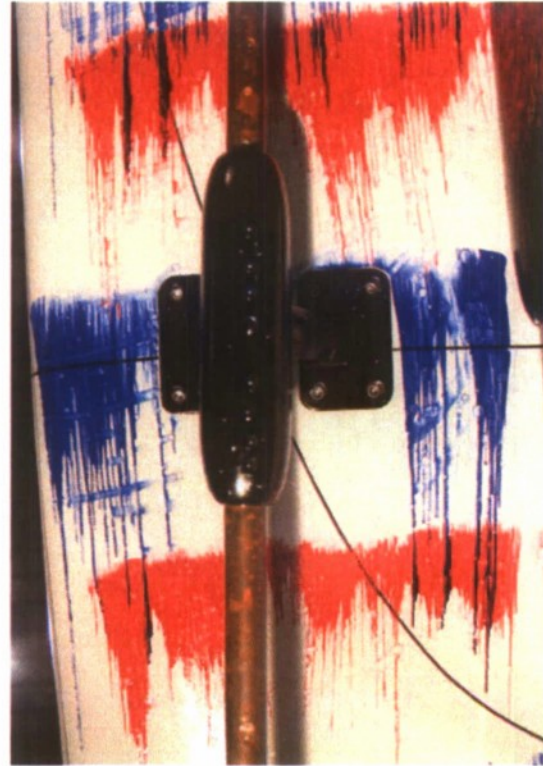


*Main strut barrel 4, underside*

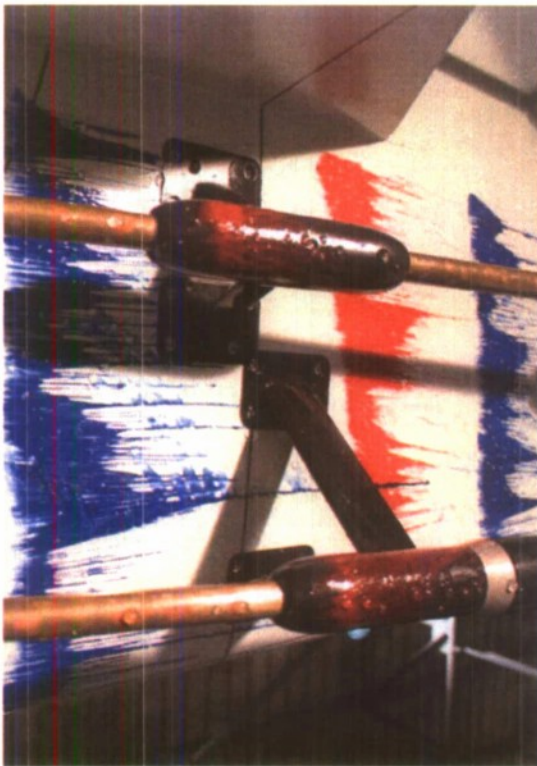
Fig. A2. Model 5653-3 test photographs: Flow visualization - continued



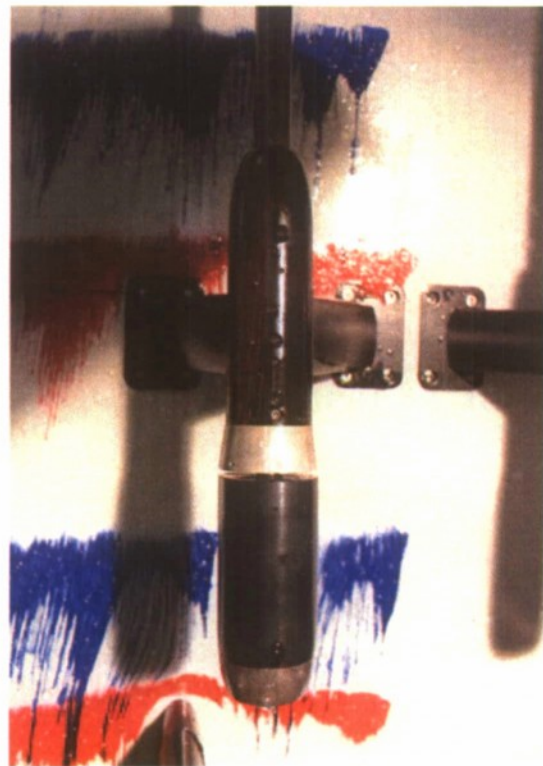
Intermediate barrel 3 (left) and Main strut barrel 4 (right)



Intermediate barrel 4, underside



Main strut barrel 3 (left) and Intermediate barrel 3 (right)

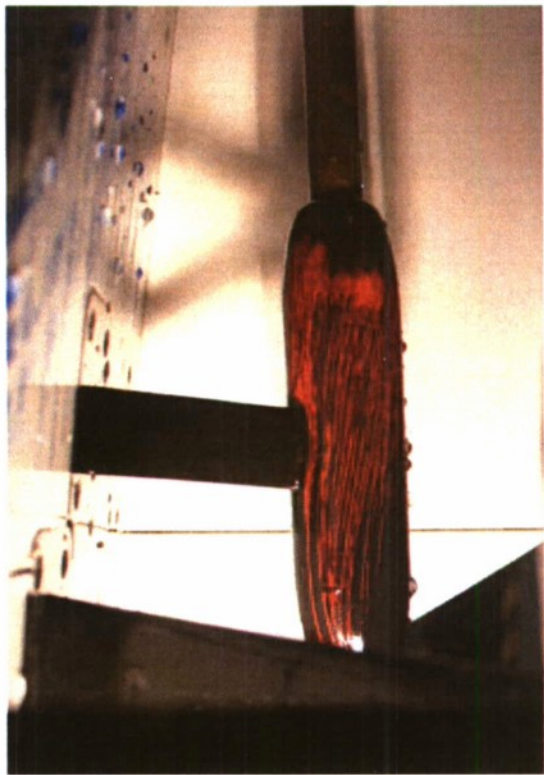


Main strut barrel 3, underside

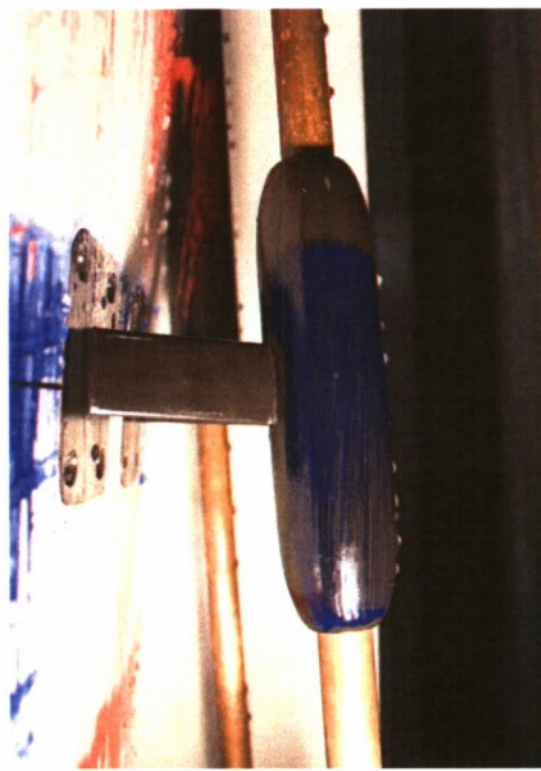
Fig. A2. Model 5653-3 test photographs: Flow visualization - continued



Intermediate barrel 4, inboard



Intermediate barrel 3, outboard

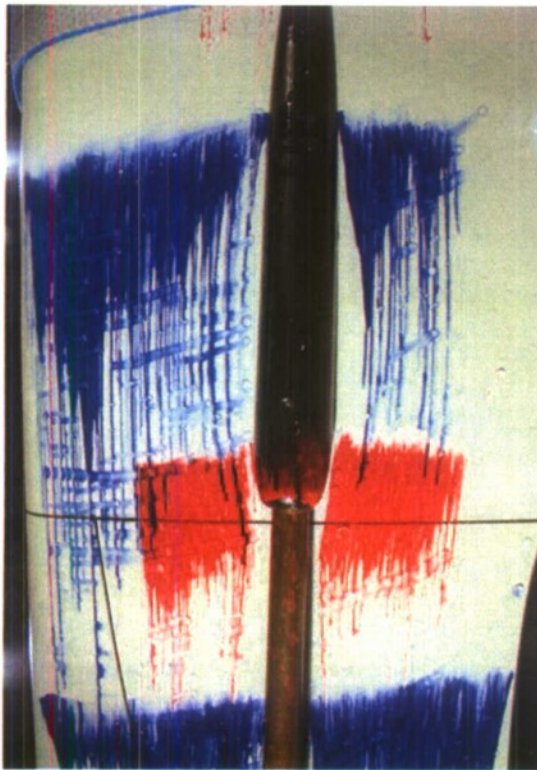


Intermediate barrel 4, outboard

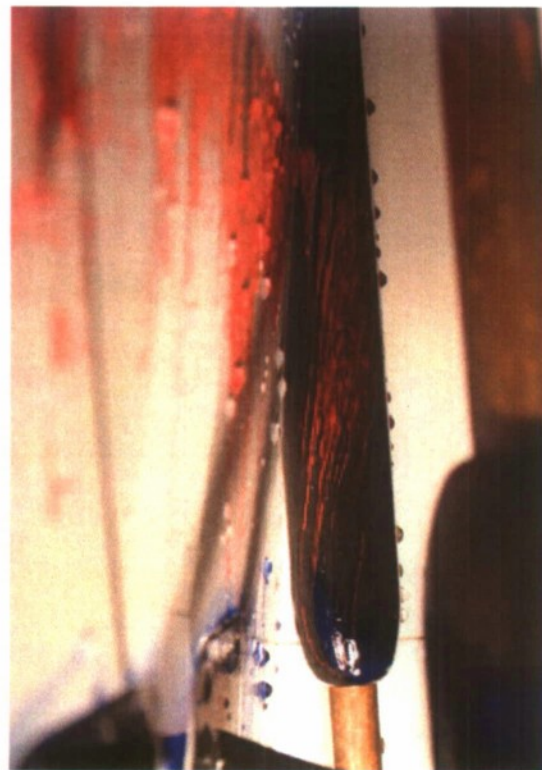


Intermediate barrel 3 'V' struts

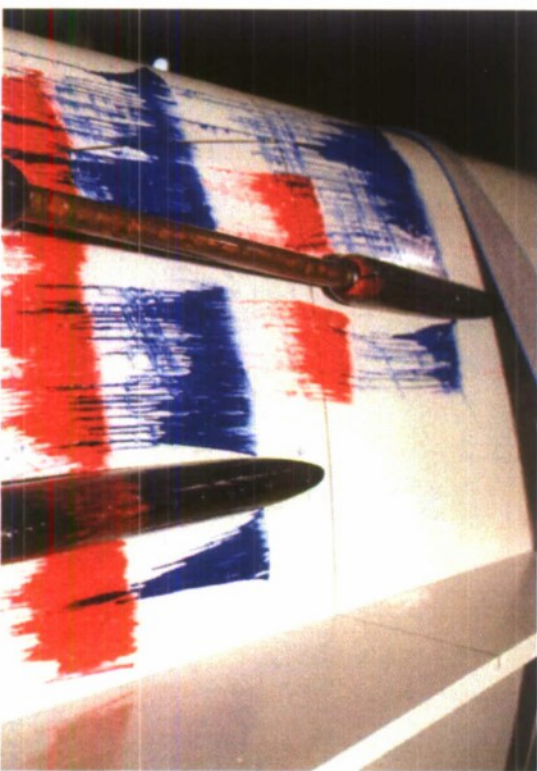
Fig. A2. Model 5653-3 test photographs: Flow visualization - continued



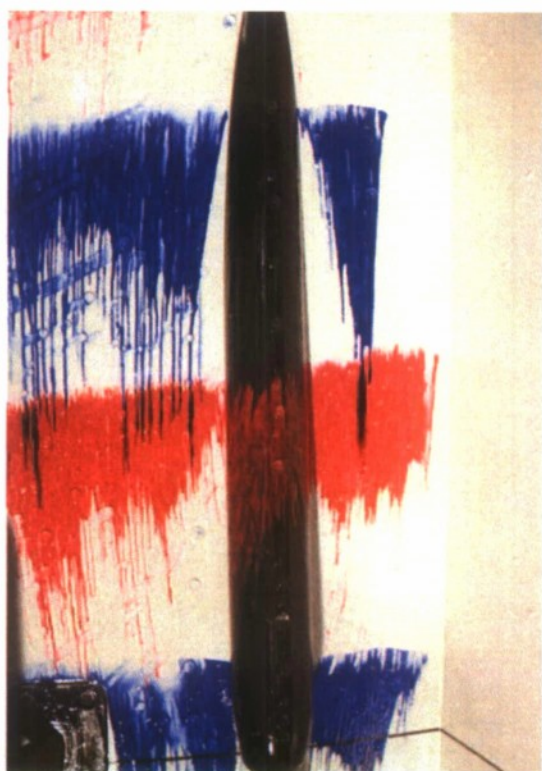
*Forward bossing 4, underside*



*Forward bossing 3, outboard*

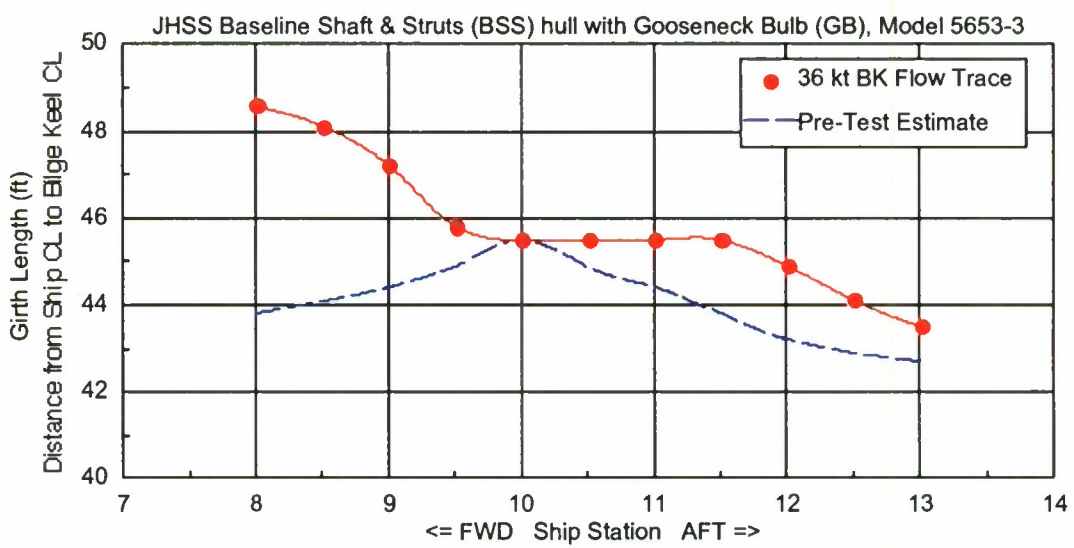
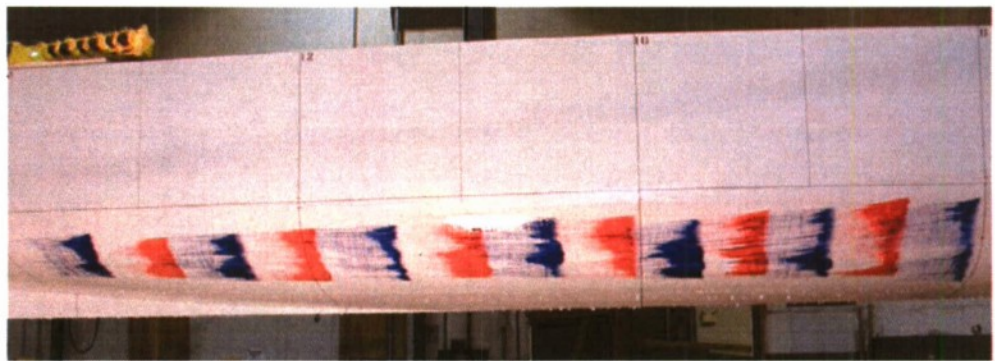


*Forward bossing 3 (left) and Forward bossing 4 (right)*



*Forward bossing 3, underside*

Fig. A2. Model 5653-3 test photographs: Flow visualization - continued



Full-Scale			
	Pre-Test Estimate	36 knot Flow Trace	
Station	Girth Length (ft)	Girth Length (ft)	$\Delta$ (ft)
8	43.8	48.6	4.8
8.5	44.1	48.1	4.0
9	44.4	47.2	2.8
9.5	44.9	45.8	0.9
10	45.5	45.5	0.0
10.5	44.9	45.5	0.6
11	44.4	45.5	1.1
11.5	43.8	45.5	1.7
12	43.2	44.9	1.7
12.5	42.9	44.1	1.1
13	42.7	43.5	0.9

Girth Length is the distance from Model or Ship CL to Bilge Keel CL

Fig. A3. JHSS BSS recommended bilge keel alignment, 36 knots

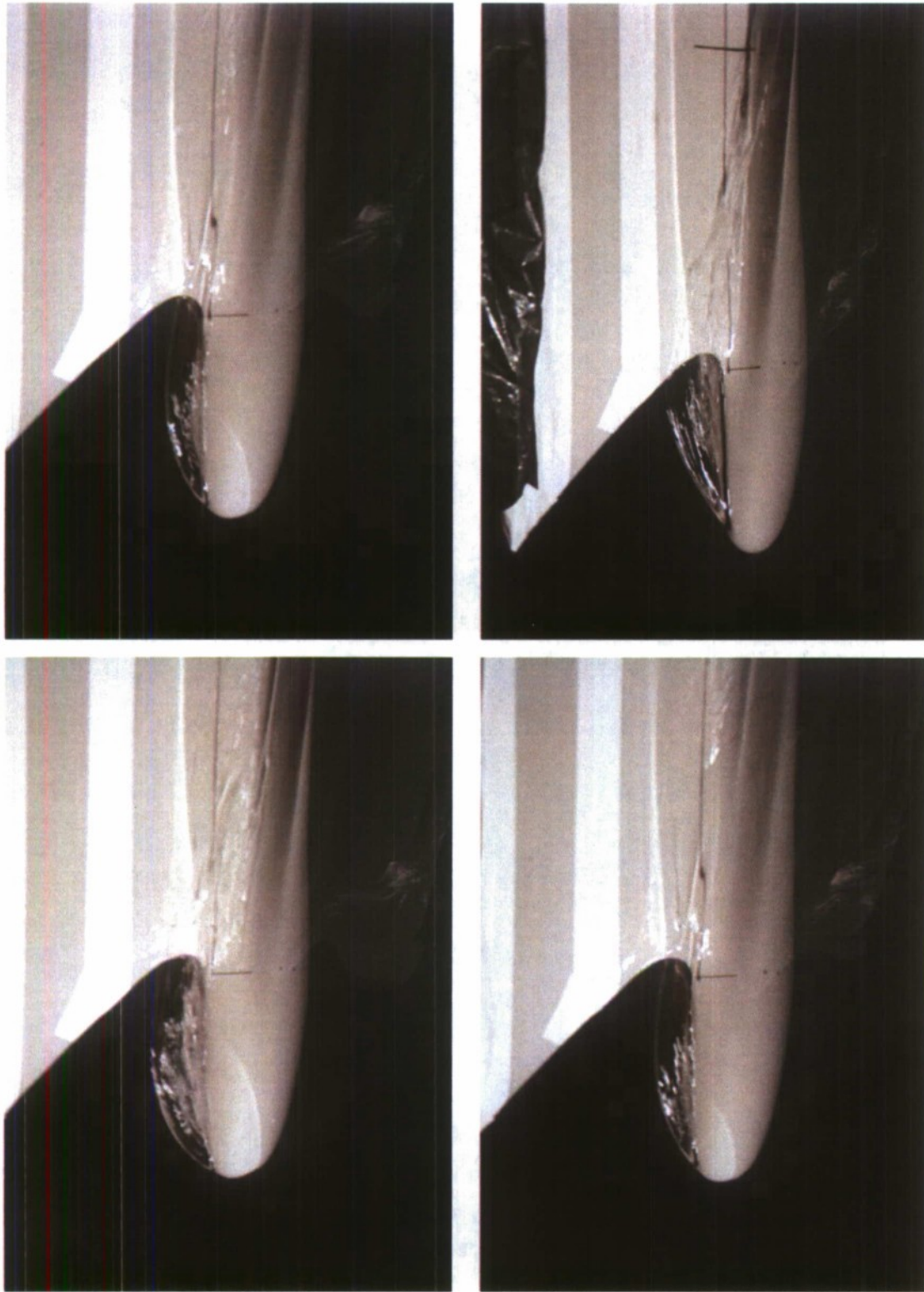


Fig. A4. Model 5653-3 test photographs: Underway in waves

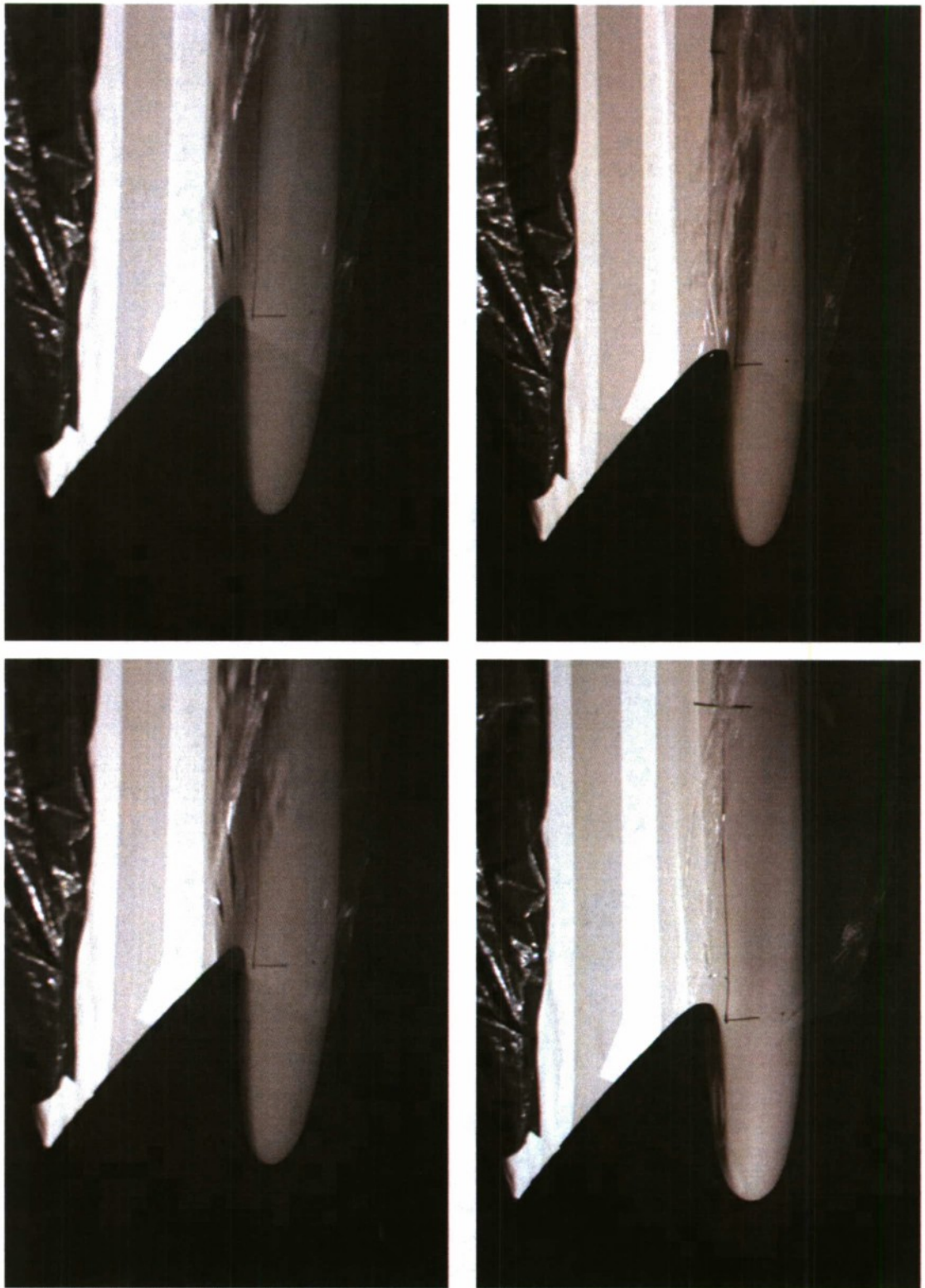


Fig. A4. Model 5653-3 test photographs: Underway in waves - continued

A 20

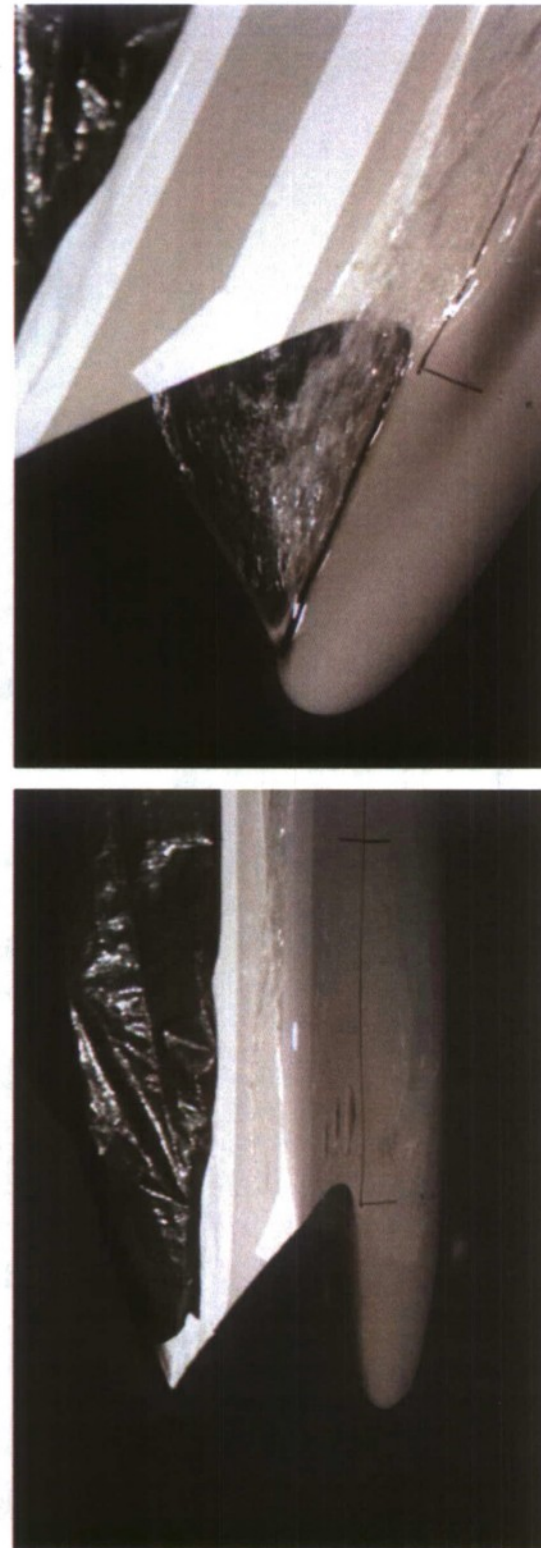
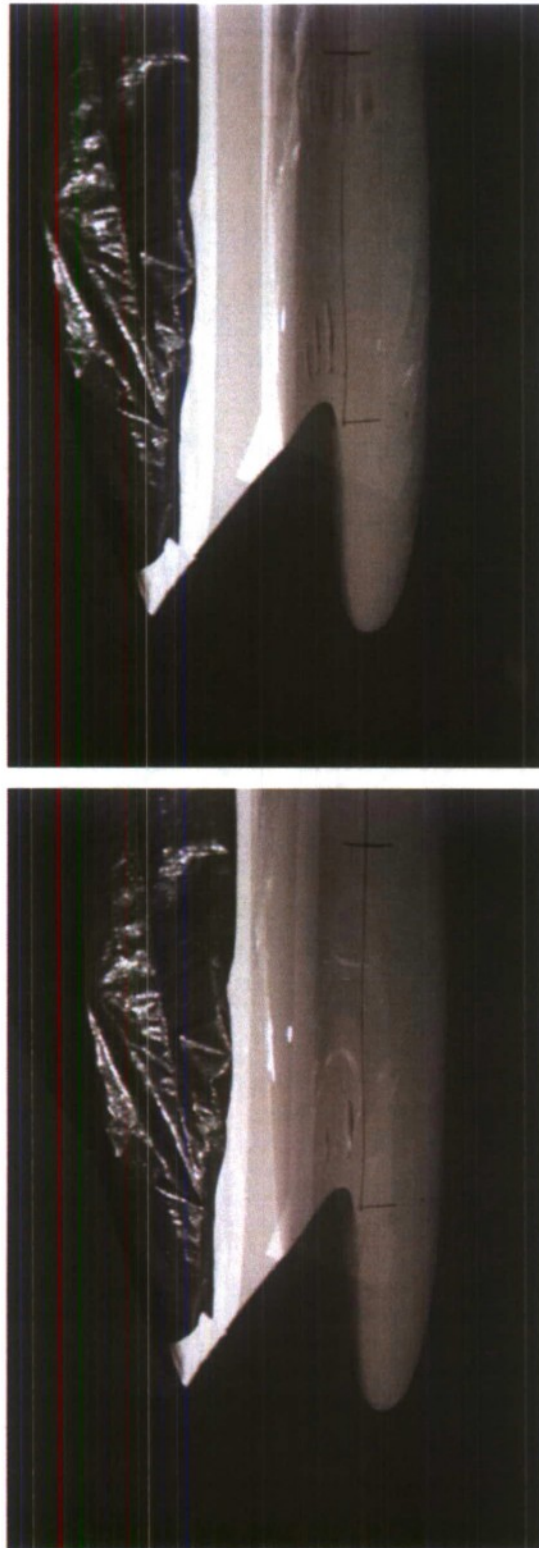


Fig. A4. Model 5653-3 test photographs: Underway in waves - continued

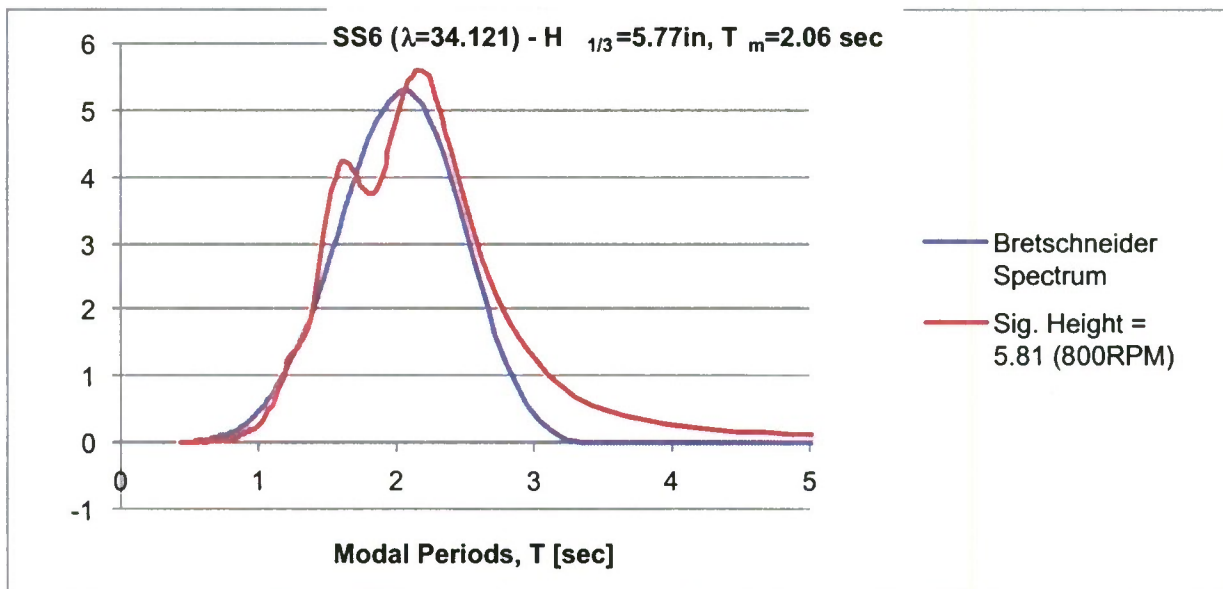


Fig. A5. Basin 2 pneumatic wavemaker representative output wave spectra for sea state 6 (SS6)

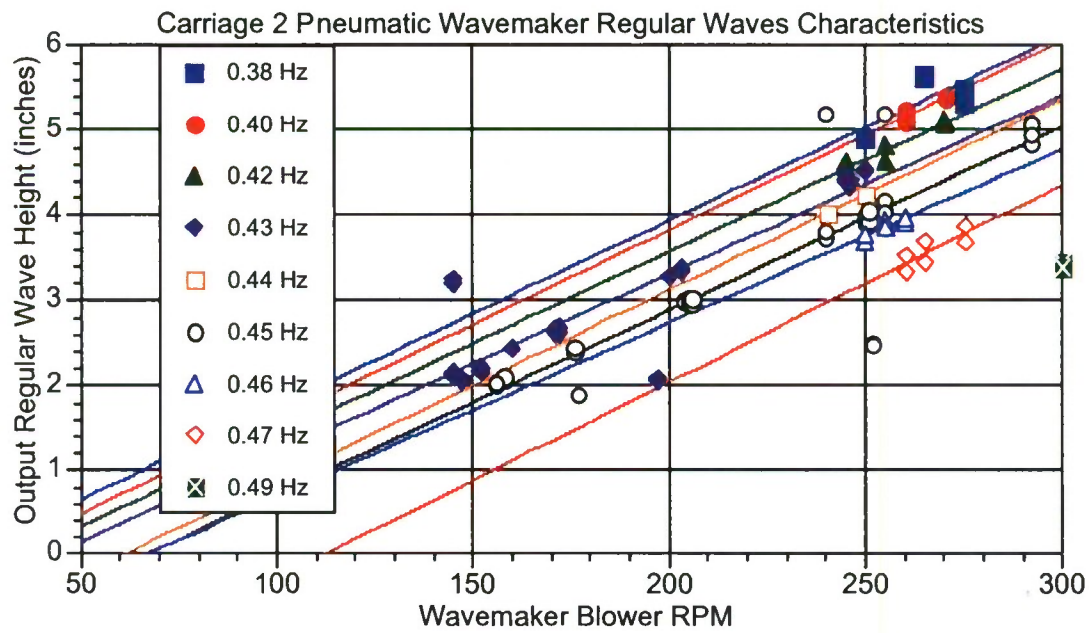


Fig. A6. Basin 2 pneumatic wavemaker output regular waves characteristics for specified valve frequency and blower RPM conditions

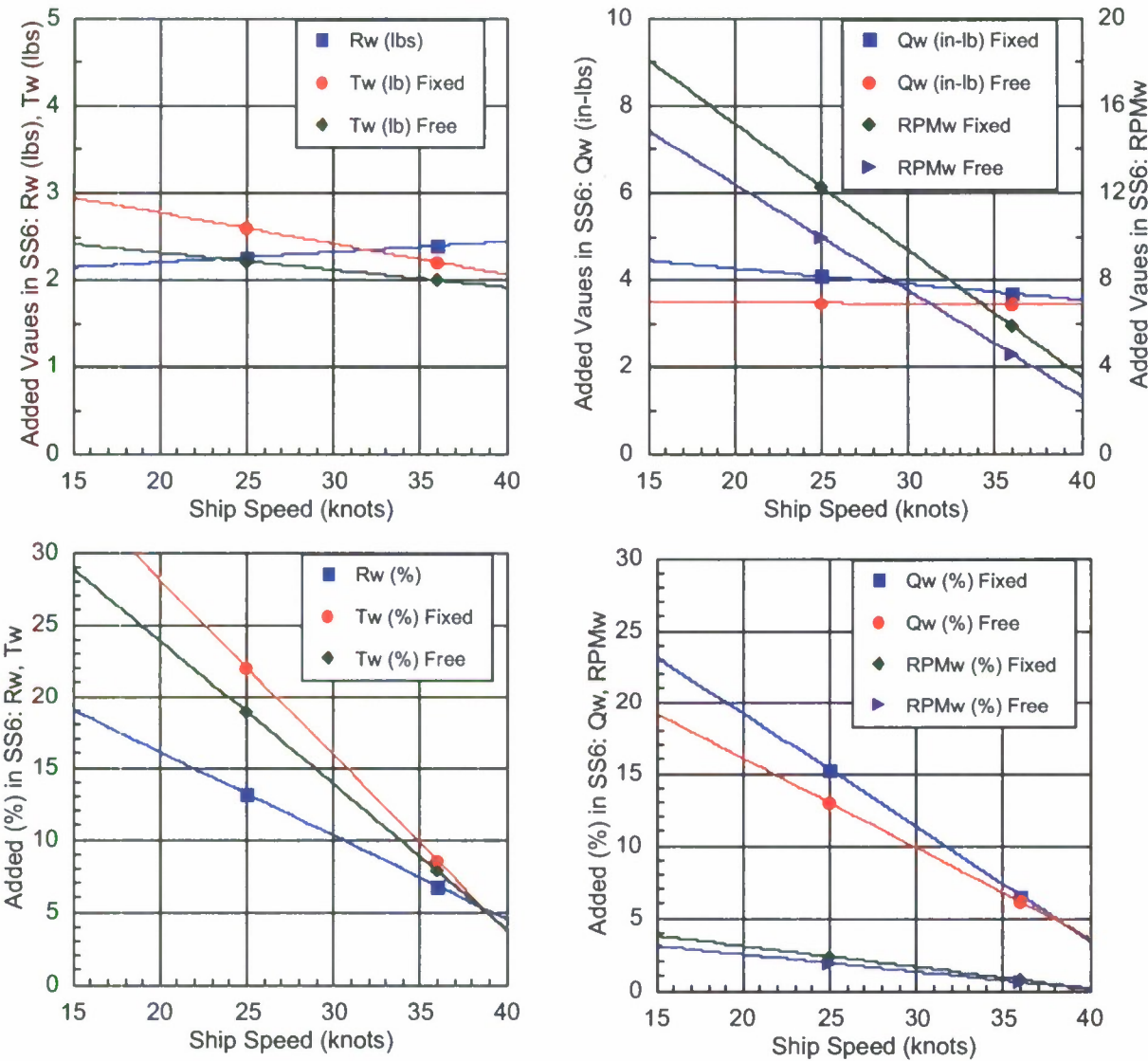


Fig. A7. Model 5653-3, comparison of added resistance, thrust, torque and RPM, in SS6 random waves

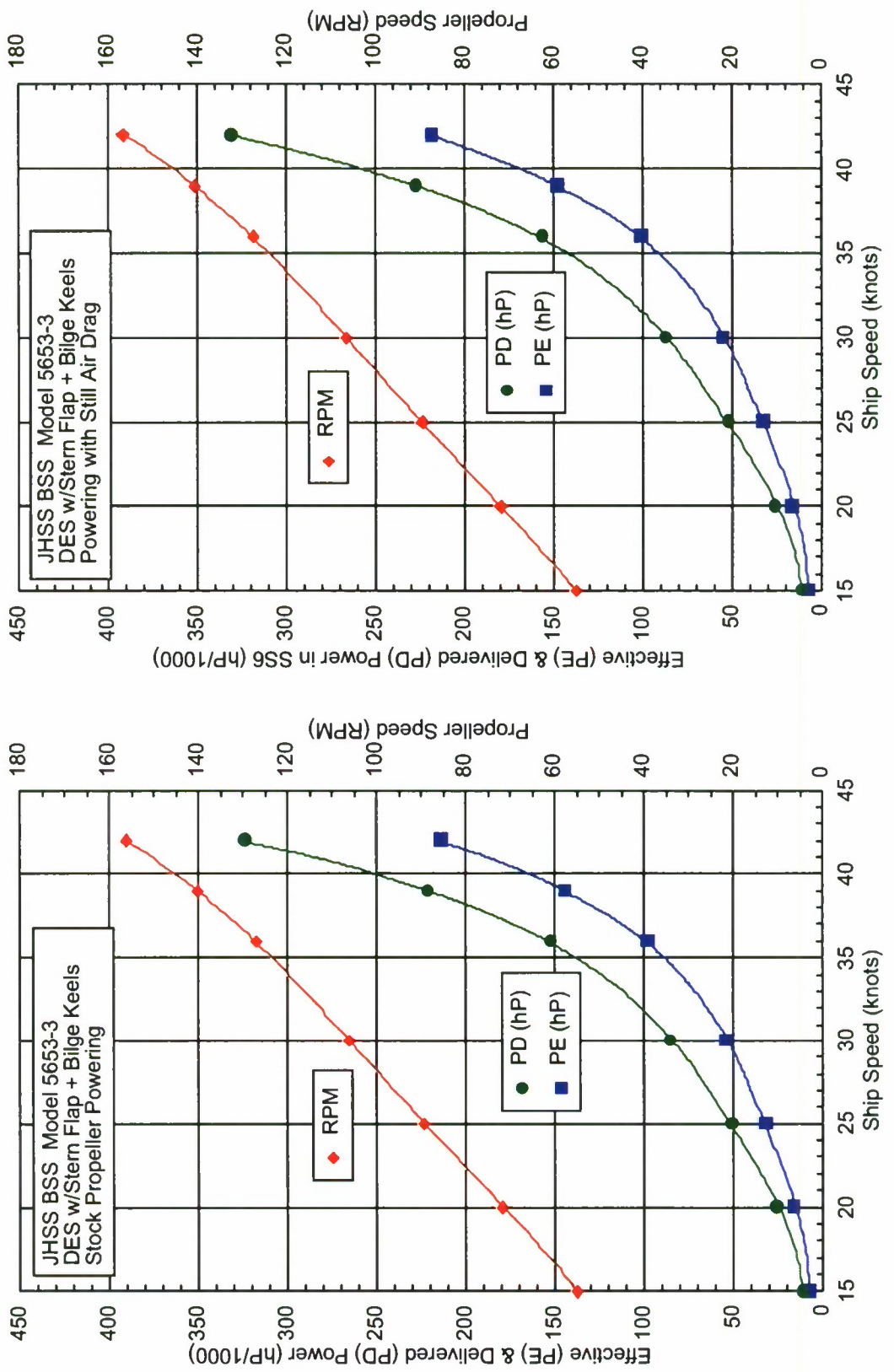


Fig. A8. JHSS BSS effective and delivered power in calm water

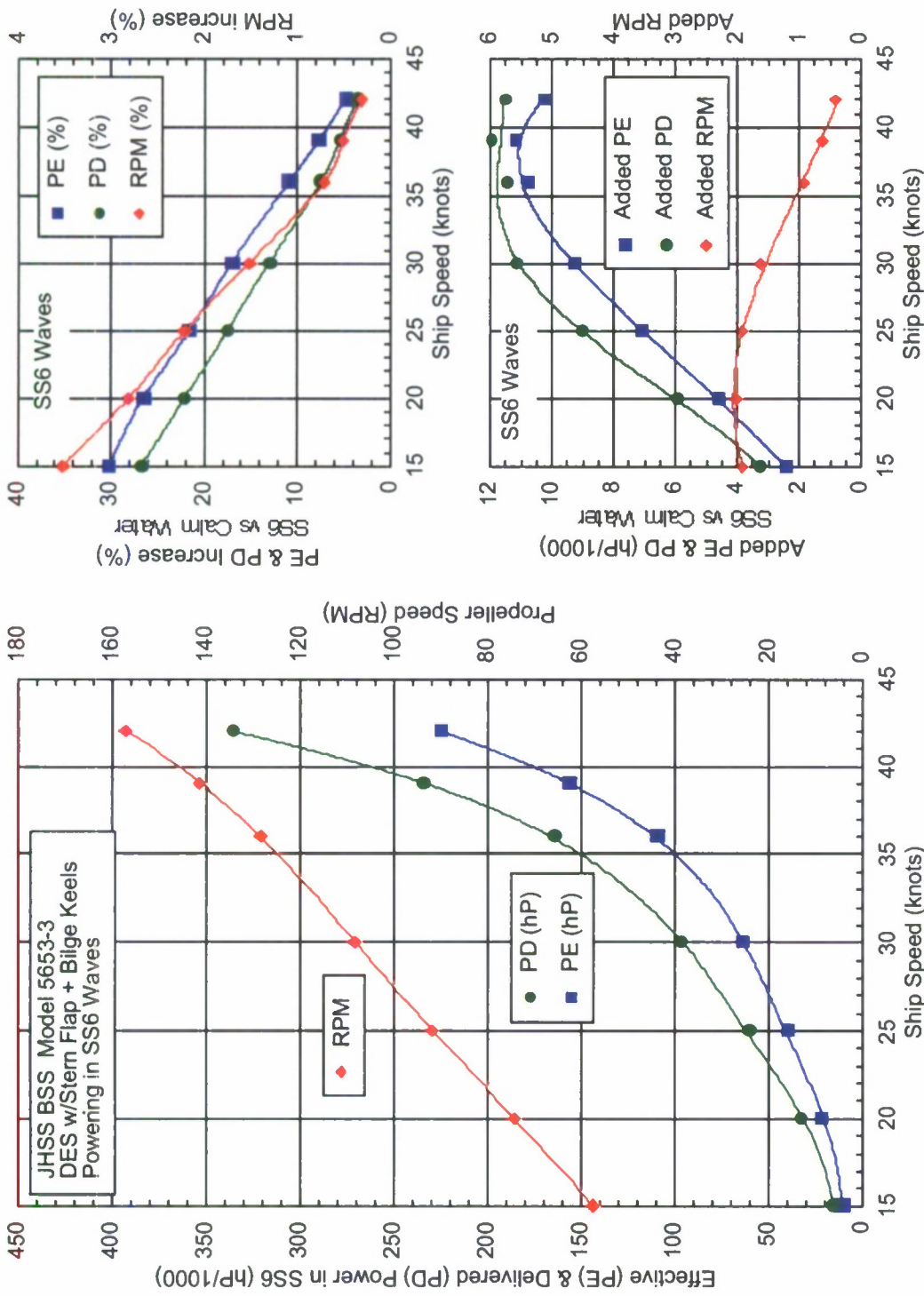


Fig. A9. JHSS BSS effective and delivered power in SS6 random waves, with a comparison to calm water values

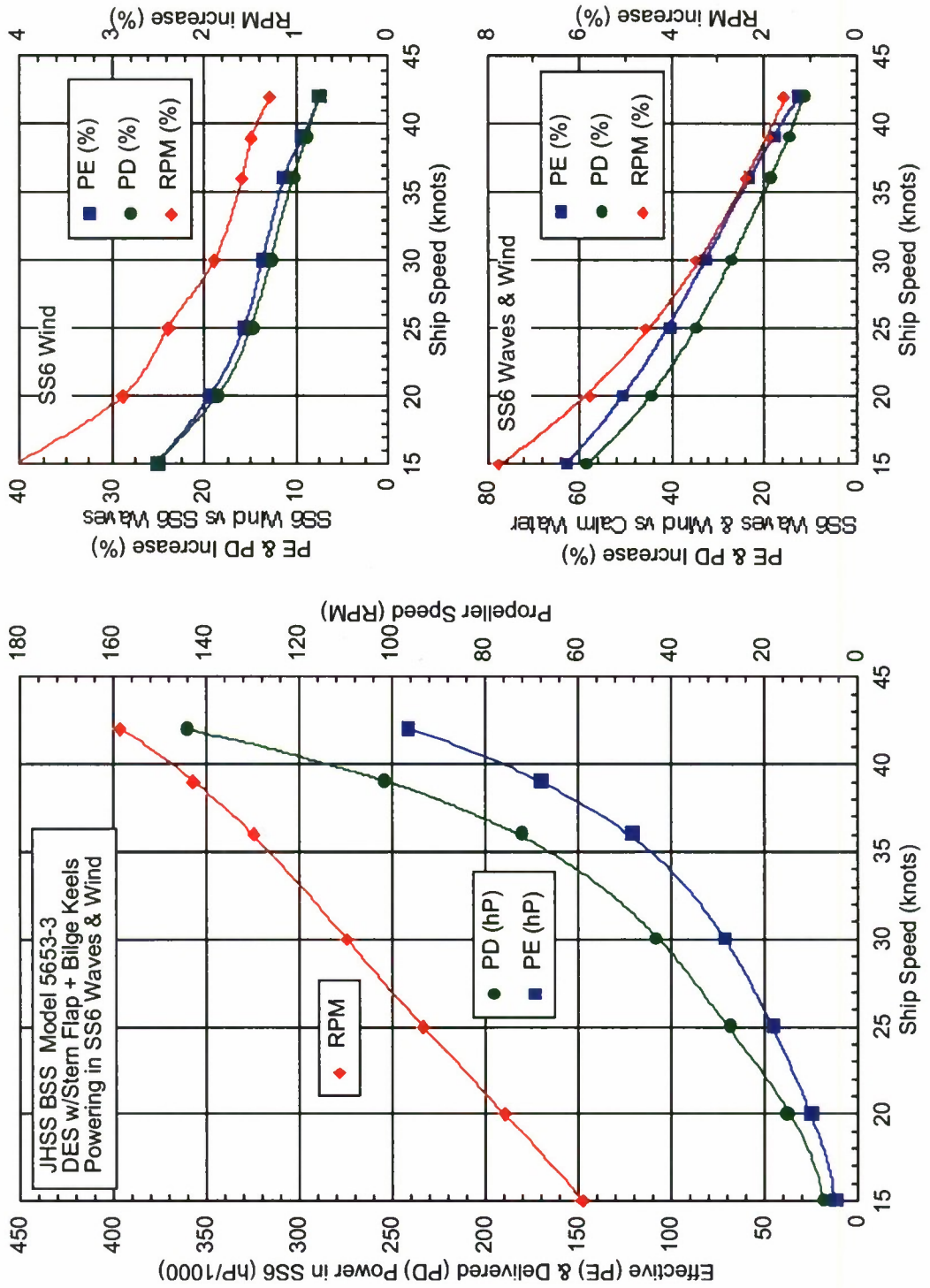


Fig. A10. JHSS BSS effective and delivered power in SS6 random waves with wind drag included, with a comparison to calm water values

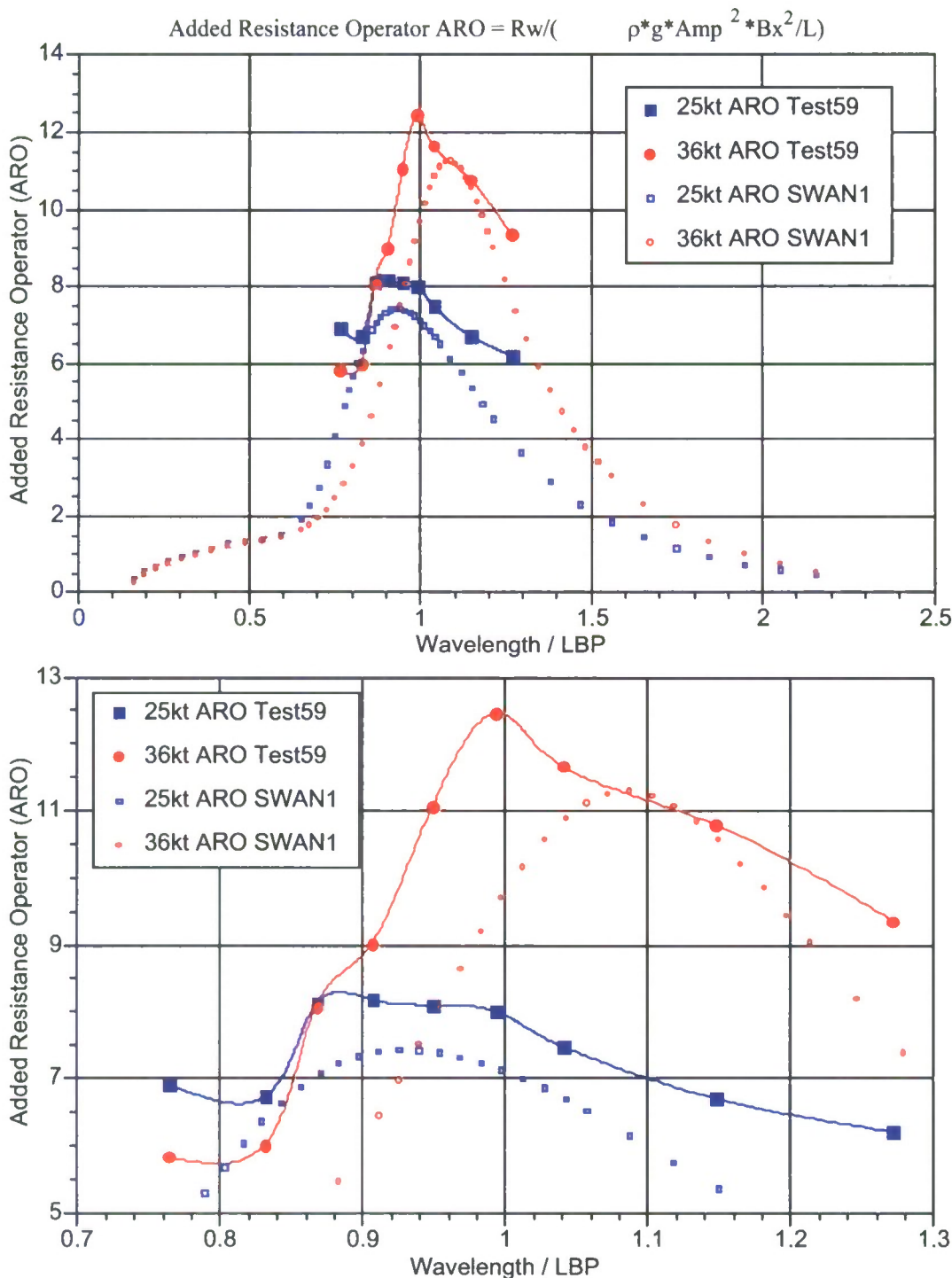


Fig. A11. Model 5653-3 added resistance operator (ARO) in regular waves, variations in wavelength, selected data at desired wave slope of 1/75 for determination of critical wavelengths

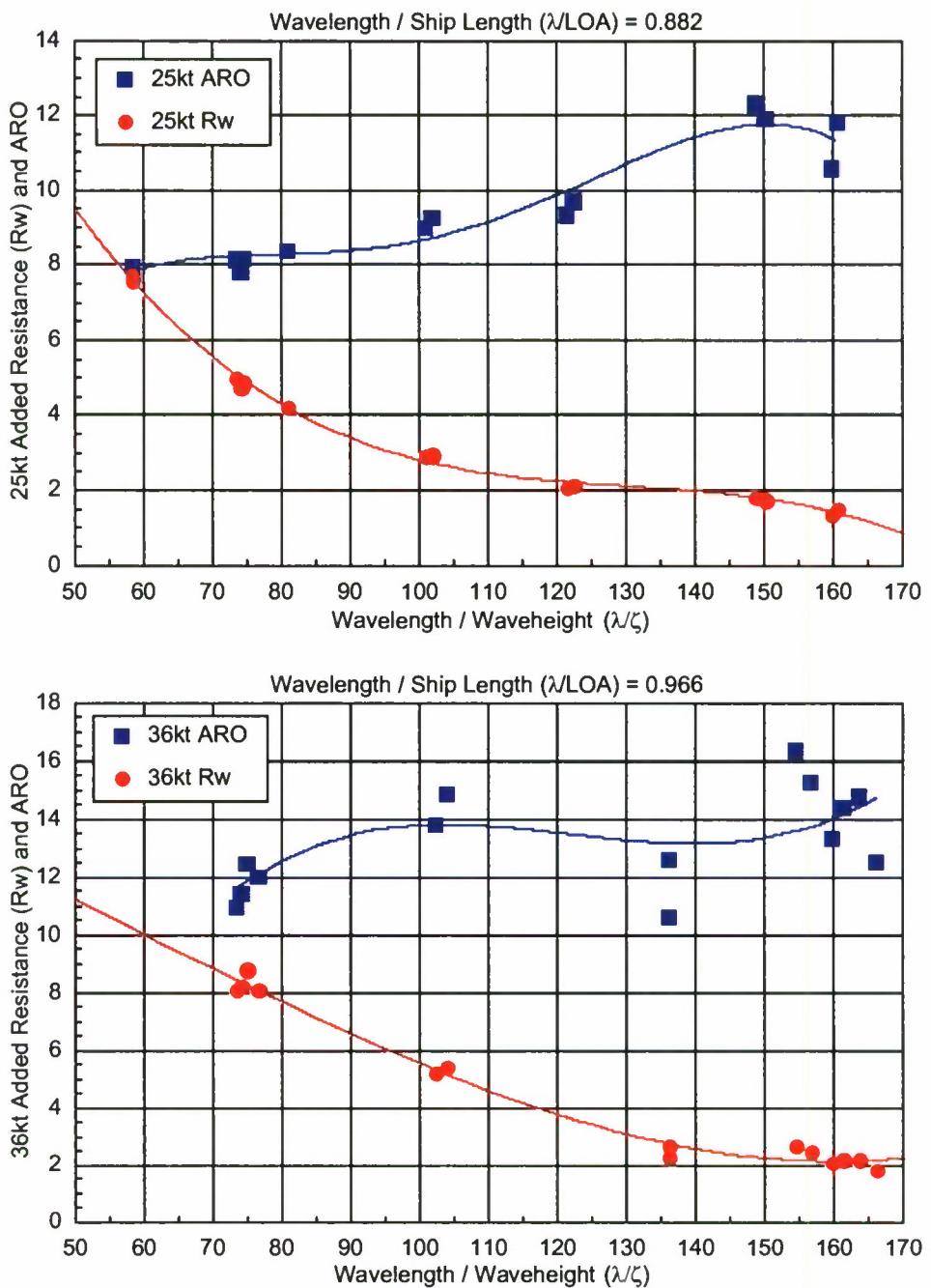


Fig. A12. Model 5653-3 added resistance operator (ARO) for variations of wave slope at determined critical wavelengths for 25 and 36 knots

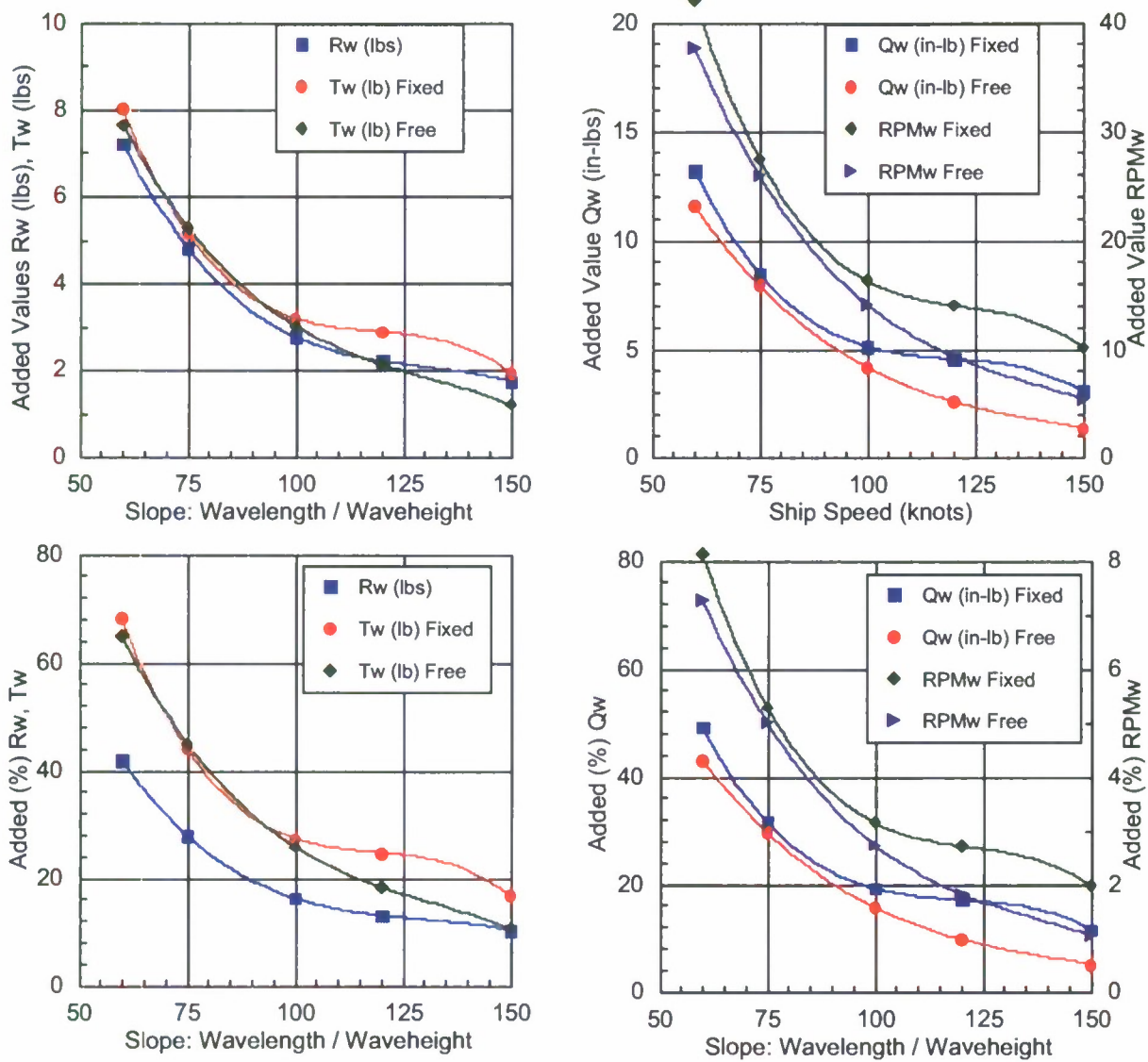


Fig. A13. Model 5653-3, comparison of added resistance, thrust, torque and RPM, 25 knots in regular waves at critical wavelength  $\lambda/LOA = 0.882$

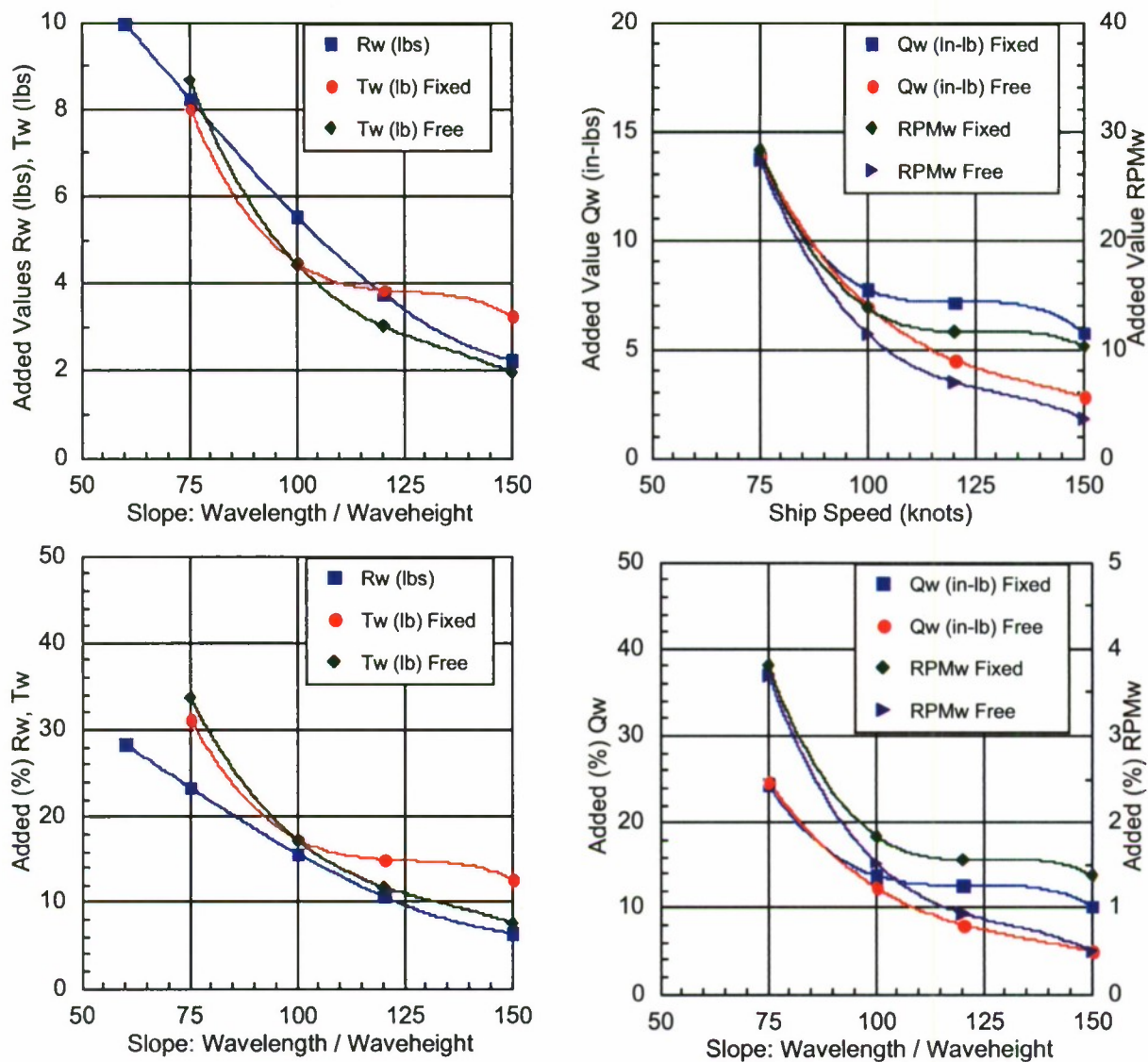


Fig. A14. Model 5653-3, comparison of added resistance, thrust, torque and RPM, 36 knots in regular waves at critical wavelength  $\lambda/LOA = 0.966$

Table A1. Test Agenda: JHSS BSS Model 5653-3 added resistance and powering in random and regular waves

DATE	TEST	TYPE	GLIDE	WAVES	$\lambda/LOA$	$\zeta/\lambda$	VS (knots)	DAYS	Hrs	Wave Length, $\lambda$ (ft)	Wave Height, $\zeta$ (inches)
5-6-Mar	-	Completion of Model Rigging. Model Ballasting. Model Hardware and Instrument & Electronics Installation on Carriage.						2.0			
7-Mar	(5)1	Roll Decay, No Bilge Keels	Not Attached	None	N/A	0	0.2	2.0		N/A	N/A
	-	Model and attachment hardware installed. Model then removed from carriage. Flow Viz Oil & Pigment applied. Model Re-Installed.					0.6	7.0			
	-	Bilge Keel Trac & Flow-Viz	Locked	None	N/A	36	0.1	1.0			
		Model Removed from Carriage. Photographed. Bilge Keels Aligned to Flow Streamlines.					0.2	2.0			
8-Mar	-	Installation of bilge keels. Wavemaker Controls Troubleshooting.					1.0				
9-Mar	(5)2	Continued Wavemaker Troubleshooting. Initial Wavemaker Calibrations (Random SS6)					1.0				
12-Mar	-	Install Weave Probe on Boom. Re-install Model. Model Instrumentation Verification.					0.5	6.0		N/A	N/A
13-Mar	(5)2	Complete Random SS6 Wavemaker Calibrations. Conduct Regular Waves Wavemaker Calibrations					0.8			N/A	N/A
	53	Calm Water Resistance	Locked	None	N/A	25, 36	0.2	2.0			
	54	Calm Water Power, Ship Propulsion Point, w/over power Df=0				25, 36	0.3	3.0			
	55	Calm Water Power, Model Self-Propulsion	Free to Surge			25, 36	0.3	3.0			
14-Mar	56	ADDED Resistance (included additional wave sampling)	Locked	RANDOM	SS6	25, 36	0.7	8.5		12.17 - 43.41 (Most Prob 21.63)	4.6 - 6.9 (Most Prob 5.77)
	57	ADDED Power, Ship Propulsion Point				25		3.5			
15-Mar	58	ADDED Power, Model Self-Propulsion	Free to Surge			36	0.7	4.5			
16-Mar	59	INCREASED Resistance. Determination of Wavelengths for maximum added resistance operator (ARO) at 25 and 36 knots	Locked	REGULAR	0.809	1/75				23.18	3.71
19-Mar					0.882	1/75				25.27	4.04
					1.013	1/75				29.02	4.64
					0.923	1/75				26.44	4.23
					0.844	1/75				24.18	3.87
					1.116	1/75				31.97	5.12
					0.966	1/75				27.67	4.43
					1.237	1/75				35.44	5.67
					0.744	1/75				21.31	3.41
					1/150					2.02	
					1/100					3.03	
					1/75					4.04	
					1/60					5.05	
					1/125					2.43	
					1/150					2.21	
					1/100					3.32	
					1/75					4.43	
					1/125					2.66	
					1/150					2.02	
					1/100					3.03	
					1/75					4.04	
					1/60					5.05	
					1/125					2.43	
					1/150					2.21	
					1/100					3.32	
					1/75					4.43	
					1/125					2.66	
					1/150					2.02	
					1/100					3.03	
					1/75					4.04	
					1/60					5.05	
					1/125					2.43	
					1/150					2.21	
					1/100					3.32	
					1/75					4.43	
					1/125					2.66	
22-Mar	62	INCREASED Power, Ship Propulsion Point 25 knots. Max ARO Wavelength.	Locked	REGULAR	0.882	1/75	25	1.0	12.0	25.27	4.04
		INCREASED Power, Model Self-Propulsion 36 knots. Max ARO Wavelength.			0.966	1/75	36				
		INCREASED Power, Ship Propulsion Point 36 knots. Max ARO Wavelength.			0.966	1/75	36				
		Model Detached from Carriage.									
	63	Roll Decay with Bilge Keels Installed	Not Attached	None	N/A	0	0.1	1.0		N/A	N/A
23-Mar	-	DERIG: Model and Carriage						0.7	8		
26-Mar	-						0.3	4			

Table A2. JHSS BSS specified inertial criteria for model 5653-3 ballasting

JHSS Resistance Ship LCG for Zero Trim				Shell = 10% VCG m				47.11 ft			
Weight Station tonnes	Weight from Amidships	Weight LCG from Amidships	Moment from Amidships	Moment from Amidships	Moment of Inertia from Amidships	WL Half- breadth	Moment of Inertia from Centerline	Y	Y	Y	Moment of Inertia from VCG
-14.50											
0.00	834.89	153.88	128473	19769498		1.08	316				55953
14.50	694.98	139.38	96867	13501299		2.02	922				46577
29.00	663.99	124.88	82920	10355000		3.11	2087				44500
43.50	696.46	110.38	76875	8485463		4.83	5280				46675
58.00	741.35	95.88	71081	6815234		6.64	10623				49684
72.50	935.31	81.38	76116	6194305		8.50	21962				62683
87.00	1654.35	66.88	110643	7399781		10.33	57373				110871
101.50	2518.02	52.38	131894	6908589		12.12	120212				168753
116.00	2994.78	37.88	113442	4297187		13.83	186162				200704
130.50	3162.66	23.38	73943	1728785		15.21	237790				211955
145.00	3181.88	8.88	28255	250905		15.90	261433				213243
159.50	2988.86	-5.62	-16797	94401		15.98	248052				200308
174.00	2618.11	-20.12	-52676	1059849		15.99	217555				175461
188.50	2529.03	-34.62	-87555	3031150		15.98	209889				169491
203.00	2621.22	-49.12	-128754	6324418		15.91	215639				175669
217.50	2446.41	-63.62	-155641	9901862		15.48	190526				163954
232.00	2018.68	-78.12	-157700	12319488		14.88	145264				135288
246.50	1597.15	-92.62	-147928	13701070		14.25	105404				107038
261.00	1105.66	-107.12	-118438	12687102		13.60	66463				74099
275.50	718.87	-121.62	-87429	10633160		12.92	39000				48178
290.00	299.98	-136.12	-40833	5558248		12.10	14274				20104
304.50	51.57	-150.62	-7767	1169930		12.10	2454				3456
37074.21	-0.297		-11012	162186727	Avg	11.49	2358682				2484644
			-0.97								
VCG				Pitch Gyradius				70.85	Roll Gyradius		12.31
16.57 Model inches				$I_0 = 13\%$				0.244	$I_0 = 16\%$		0.385
LCG				Yaw Gyradius				70.82	0.244		
-0.34 Model inches				$I_0 = 13\%$							

Table A3. Model 5653-3, bilge keel added resistance, 25 and 36 knots

Calm Water Exp 53, Bilge Keel Added Resistance		BSS	BSS	Bilge Keel Added Resistance	
VS	DES	DES	DES	Bilge Keel Added Resistance	
(kts)	FA+Flap	w/BK	Δ Rt	Resistance (%)	
25	16.77	17.20	0.43	2.56	
36	34.38	35.24	0.86	2.50	

\*BK wetted surface increase = 2.52%

Table A4. Definitions and criteria, annual random (irregular) sea state occurrences in the open ocean for the northern hemisphere

Full Scale Random (Irregular) Sea Conditions for Northern Hemisphere		Model Wave Period (sec)				Sustained Wind Speed (knots)						
Sea State Number	Probability of Sea State (%)	Significant Wave Height (ft)		Range	Mean	Range	Mean	Most Probable	Min	Range	Max	Mean
0-1	0	0	0.3	0.2	-	-	-	-	0	6	3.0	
2	5.7	0.3	1.6	1.0	3	15	7	7	7	11	8.5	
3	19.7	1.6	4.1	2.9	5	15.5	8	12	12	16	13.5	
4	28.3	4.1	8.2	6.2	6	16	9	17	17	21	19.0	
5	19.5	8.2	13.1	10.7	7	16.5	10	22	22	27	24.5	
6	17.5	13.1	19.7	16.4	9	17	12	28	28	47	37.5	
7	7.6	19.7	29.5	24.6	10	18	14	48	48	55	51.5	
8	1.7	29.5	45.9	37.7	13	19	17	56	56	63	59.5	

Model Scale Values

Model Scale Ratio		Model Wave Period (sec)				Sustained Wind Speed (knots)						
Sea State Number	Probability of Sea State (%)	Significant Wave Height (in)		Range	Mean	Range	Mean	Most Probable	Min	Range	Max	Mean
0-1	0	0	0.1	0.06	-	-	-	-	0	1.0	0.5	
2	5.7	0.1	0.6	0.34	0.51	2.57	1.20	1.2	1.2	1.9	1.5	
3	19.7	0.6	1.4	1.02	0.86	2.65	1.37	2.1	2.1	2.7	2.3	
4	28.3	1.4	2.9	2.17	1.03	2.74	1.54	2.9	2.9	3.6	3.3	
5	19.5	2.9	4.6	3.75	1.20	2.82	1.71	3.8	3.8	4.6	4.2	
6	17.5	4.6	6.9	5.77	1.54	2.91	2.05	4.8	4.8	8.0	6.4	
7	7.6	6.9	10.4	8.66	1.71	3.08	2.40	8.2	8.2	9.4	8.8	
8	1.7	10.4	16.1	13.27	2.23	3.25	2.91	9.6	9.6	10.8	10.2	

Table A5. Model 5653-3 Exp 56, added resistance in SS6 random waves, locked in surge, 25 and 36 knots

Table A5. Random SS6 Exp 56, Locked in Surge (Fixed), Added Resistance						
VS	Exp53		SS6		Avg Wave Height (in)	
(kts)	Calm Water	Rt (lbs)	RTw (lbs)	Rw (lbs)	Added Resistance (%)	No. Runs
25	17.20	19.46	2.27	13.17	5.62	5
36	35.24	37.63	2.40	6.80	5.77	7
						Total Sampling Time (min)
						714
						636
						61.9

Table A6. Model 5653-3 Exp 54, calm water powering, locked in surge (ship propulsion point), 25 and 36 knots

Table A6. Calm Water Exp54, Locked in Surge (Fixed), Model Scale Measurements at Ship Propulsion Point						
VS	RPM	INBD	Total Thrust	RPM	OUTBD	Total Torque
(kts)		INBD	INBD	OUTBD	OUTBD	INBD
25	517.78	15.14	6.91	518.12	11.68	4.86
36	742.40	31.10	14.59	742.67	25.11	11.08
						Total Power (hP)
						0.05
						0.22
						517.9
						Total Power (hP)
						0.15
						0.66
						742.5
						Total Thrust (lbf)
						11.77
						25.67

Table A7. Model 5653-3 Exp 57, added powering in SS6 random waves, locked in surge (ship propulsion point), 25 and 36 knots

Table A7. Random SS6 Exp57, Locked in Surge (Fixed), Model Scale Measurements at Ship Propulsion Point						
VS	RPM	INBD	Total Thrust	RPM	OUTBD	Total Torque
(kts)		INBD	INBD	OUTBD	OUTBD	INBD
25	529.90	16.77	8.06	530.55	14.14	6.31
36	748.50	32.55	15.47	748.33	27.35	12.41
						Total Power (hP)
						0.07
						0.06
						530.22
						748.41
						Total Thrust (lbf)
						14.36
						27.88
SS6			Total Sampling Time			* PCT relative to measured model values at ship propulsion point
VS	Avg $\zeta$ (in)	No. Runs	Model	Full-Scale	Added Power, SS6	Avg RPM Increase
(kts)	(in)	(sec)	(min)	(hP)	(%)*	Added Thrust, SS6
25	5.68	4	538	52.4	0.04	12.27
36	5.69	5	462	45.0	0.05	5.88
						2.60
						22.06
						2.21
						8.60

Table A8. Model 5653-3 Exp 55, calm water powering, free to surge (model self-propulsion), 25 and 36 knots

Table A8. Calm Water Exp55, Free to Surge, Model Scale Measurements at Model Self-Propulsion												
VS (kts)	RPM INBD	Total Torque		Total Thrust		Total Torque		Total Thrust		Total Power (hp)	Avg RPM	Total Thrust (lbf)
		INBD (in-lbf)	INBD (lbf)	INBD (in-lbf)	INBD (lbf)	OUTBD (in-lbf)	OUTBD (lbf)	OUTBD (in-lbf)	OUTBD (lbf)			
25	559.99	21.58	561.46	17.57	8.44	0.10	0.08	0.35	560.7	19.12	39.86	
36	800.69	43.11	801.43	36.71	18.03	0.23	0.27	0.23	1.01	801.1	39.86	

Table A9. Model 5653-3 Exp 58, added powering in SS6 random waves, free to surge (model self-propulsion), 25 and 36 knots

Table A9. Random SS6 Exp58, Free to Surge, Model Scale Measurements at Model Self-Propulsion												
VS (kts)	RPM INBD	Total Torque		Total Thrust		Total Torque		Total Thrust		Total Power (hp)	Avg RPM	Total Thrust (lbf)
		INBD (in-lbf)	INBD (lbf)	INBD (in-lbf)	INBD (lbf)	OUTBD (in-lbf)	OUTBD (lbf)	OUTBD (in-lbf)	OUTBD (lbf)			
25	569.00	22.71	572.39	19.92	9.80	0.10	0.09	0.25	0.39	570.7	21.34	21.34
36	806.02	44.56	805.31	38.72	19.18	0.28	0.28	0.25	1.06	805.7	41.86	41.86
SS6										*PCT relative to measured model values at ship propulsion point		
VS	Avg $\zeta$ (in)	No. Runs	Model	Full-Scale	Free to Surge	Added Power, SS6	RPM Increase	Free to Surge			Added Thrust, SS6	
(kts)	(in)			(sec)	(min)	(hp)	(%)	(lbf)			(%)*	
25	5.70	4		538	52.4	0.038	17.10	2.22			18.86	
36	5.62	6		413	40.2	0.050	7.58	4.6			7.81	

Table A10. Model 5653-3, summary of added resistance and powering in SS6 random waves

Summary of Model 5653-3 Tests in SS6 Random Waves									
Sea Condition	Model	Attachment	Model-Scale Measurements, 25 kts				Model-Scale Measurements, 36 kts		
			RT (lbs)	T (lb)	Q (in-lbs)	RPM	RT (hp)	T (lb)	Q (in-lbs)
Calm	Fixed	17.20	11.77	26.82	517.9	0.22	35.24	25.67	56.21
	Free to Surge	N/A	19.12	39.15	560.7	0.35	N/A	39.86	79.82
SS6	Fixed	19.46	14.36	30.91	530.2	0.26	37.63	27.88	59.90
	Free to Surge	N/A	21.34	42.63	570.7	0.39	N/A	41.86	83.28
Sea Condition									
Sea Condition	Model	Added Values in Waves, 25 kts				Added Values in Waves, 36 kts			
		Rw (lbs)	Tw (lb)	Qw (in-lbs)	RPMw	PDw (hp)	Rw (lbs)	Tw (lb)	Qw (in-lbs)
SS6	Fixed	2.27	2.60	4.09	12.27	0.04	2.40	2.21	3.69
	Free to Surge	N/A	2.22	3.48	9.97	0.04	N/A	2.00	3.46
	Combined	2.27	2.41	3.78	11.12	0.04	2.40	2.11	3.57
Sea Condition									
Sea Condition	Model	Added Percentage* in Waves, 25 kts				Added Percentage* in Waves, 36 kts			
		Rw (%)	Tw (%)	Qw (%)	RPMw (%)	PDw (%)	Rw (%)	Tw (%)	Qw (%)
SS6	Fixed	13.2	22.1	15.2	2.4	18.0	6.8	8.6	6.6
	Free to Surge	N/A	18.9	13.0	1.9	17.1	N/A	7.8	6.2
	Combined	13.2	20.5	14.1	2.1	17.5	6.8	8.2	6.4

\*Percent relative to measured model values at ship propulsion point

Table A11. JHSS BSS, calm water effective power at DES with stern flap

JHSS Exp40: DES Flap (PE from Rt input)							
LAMBDA	SHIP		MODEL		FN	V-L	1000CR
	LWL	ft	34.121	ft			
S	106845	ft <sup>2</sup>	91.772	ft <sup>2</sup>			
WT	36491	LT	2000.6	lbs			
RHO	1.9905	(lbf*sec <sup>2</sup> )/ft <sup>4</sup>	1.9365	(lbf*sec <sup>2</sup> )/ft <sup>4</sup>			
NU	1.2817E-05	ft <sup>2</sup> /sec	1.0692E-05	ft <sup>2</sup> /sec			
Ca			0.0000				
Vs knots	EFFECTIVE POWER (PE)		FRICTIONAL POWER		FN	V-L	1000CR
	HP	KW	HP	KW			
15.0	7867	5867	4433	3305	0.143	0.480	1.095
20.0	16866	12577	10155	7573	0.190	0.640	0.902
25.0	31986	23852	19326	14412	0.238	0.799	0.872
30.0	53156	39638	32702	24386	0.285	0.959	0.815
36.0	96351	71849	55348	41273	0.343	1.151	0.945
39.0	141664	105639	69736	52002	0.371	1.247	1.304
42.0	209630	156321	86376	64410	0.400	1.343	1.790

Table A12. JHSS BSS, calm water effective power at DES with stern flap and bilge keels

JHSS Exp40+BK: DES Flap+BK (PE from Rt input)							
LAMBDA	SHIP		MODEL		BK Wetted Surface	delta (%)	
	LWL	ft	34.121	ft			
S	109537	ft <sup>2</sup>	94.084	ft <sup>2</sup>			
WT	36491	LT	2000.6	lbs			
RHO	1.9905	(lbf*sec <sup>2</sup> )/ft <sup>4</sup>	1.9365	(lbf*sec <sup>2</sup> )/ft <sup>4</sup>			
NU	1.2817E-05	ft <sup>2</sup> /sec	1.0692E-05	ft <sup>2</sup> /sec			
Ca			0.0000				
Vs knots	EFFECTIVE POWER (PE)		FRICTIONAL POWER		FN	V-L	1000CR
	HP	KW	HP	KW			
15.0	8077	6023	4544	3389	0.143	0.480	1.098
20.0	17324	12919	10411	7764	0.190	0.640	0.907
25.0	32837	24486	19813	14775	0.238	0.799	0.875
30.0	54567	40691	33526	25000	0.285	0.959	0.818
36.0	98864	73723	56743	42313	0.343	1.151	0.947
39.0	145315	108362	71493	53313	0.371	1.247	1.306
42.0	214949	160287	88552	66033	0.400	1.343	1.790

Table A13. JHSS BSS effective power in SS6 random waves, determined from model-scale added resistance measurements

JHSS DES Flap+BK in SS6 (PE from Rt input)

LAMBDA	SHIP		MODEL		FN	V-L	1000CR
	LWL	ft	28.660	ft			
S	109537	ft <sup>2</sup>	94.084	ft <sup>2</sup>			
WT	36491	LT	2000.6	lbs			
RHO	1.9905	(lbf*sec <sup>2</sup> )/ft <sup>4</sup>	1.9365	(lbf*sec <sup>2</sup> )/ft <sup>4</sup>			
NU	1.2817E-05	ft <sup>2</sup> /sec	1.0692E-05	ft <sup>2</sup> /sec			
Ca			0.0000				
Vs knots	EFFECTIVE POWER (PE)		FRICTIONAL POWER				
	HP	KW	HP	KW			
15.0	10517	7842	4544	3389	0.143	0.480	1.857
20.0	21919	16345	10411	7764	0.190	0.640	1.509
25.0	39923	29770	19813	14775	0.238	0.799	1.350
30.0	63842	47607	33526	25000	0.285	0.959	1.178
36.0	109655	81769	56743	42313	0.343	1.151	1.190
39.0	156508	116708	71493	53313	0.371	1.247	1.504
42.0	225188	167923	88552	66033	0.400	1.343	1.935

Table A14. JHSS BSS calm water powering at DES with stern flap

JHSS BSS Exp41 DES w/Flap Stock Props									
SHIP SPEED (KNOTS)		EFFECTIVE POWER (HP)		DELIVERED POWER (kW)		ETAD		ETAO	
15.0		7.72		5867.		1.2031.		0.654	
20.0		10.29		16866.		1.2578.		0.643	
25.0		12.86		23853.		1.9577.		0.691	
30.0		15.43		39639.		2.6253.		0.634	
36.0		18.52		96351.		50426.		0.692	
39.0		20.06		141664.		149593.		0.644	
42.0		21.61		209630.		1.11552.		0.698	
TOTAL (ALL FOUR SHAFTS COMBINED)									
LENGTH (LWL)		977.9 FT ( 298.1 M)		36490.4 TONS ( 37074.2 TONNES)		106844.9 SQ FT ( 9926.2 SQ M)		INBD & OTBD PROP DIA	
WETTED SURFACE		21.33 FT ( 6.50 M)		CORRELATION ALLOWANCE		0.000000		ITTC FRICTION USED	

Table A15. JHSS BSS calm water powering at DES with stem flap and bilge keels

BSS DES Flap+BK Stock Props (iProg=2)									
TOTAL (ALL FOUR SHAFTS COMBINED)									
SHIP SPEED (KNOTS)	EFFECTIVE POWER (HP)	DELIVERED POWER (HP)	ETAD	ETAQ	ETAB	1-t	CTS	CR	PROPELLER
15.0	7.72	6023.	12318.	9185.	0.6556	0.700	0.925	2.511	1.098
20.0	10.29	17324.	12919.	26895.	0.644	0.693	0.922	2.272	0.907
25.0	12.86	32837.	24487.	51611.	0.6346	0.695	0.693	2.205	0.875
30.0	15.43	54567.	40691.	85961.	0.635	0.694	0.691	2.121	0.818
36.0	18.52	98864.	73723.	153007.	0.646	0.701	0.687	2.224	0.947
39.0	20.06	145315.	108361.	222405.	0.653	0.713	0.696	2.571	1.306
42.0	21.61	214949.	160287.	324518.	0.662	0.720	0.720	0.893	3.044
									1.790

Table A16. JHSS BSS powering estimate in SS6 random waves, determined from effective power prediction in SS6 and calm water interaction coefficients

BSS DES Flap+BK ESTIMATED Sea State 6 StockProps (iProg=2)									
LENGTH (LWL)		977.9 FT ( 298.1 M)							
DISPLACEMENT		36490.4 TONS ( 37074.2 TONNES)							
WETTED SURFACE		109536.6 SQ FT ( 10176.3 SQ M)							
INBD & OTBD PROP DIA		21.33 FT ( 6.50 M)							
CORRELATION ALLOWANCE		0.00000 ITTC FRICTION USED							
TOTAL (ALL FOUR SHAFTS COMBINED)									
SHIP SPEED (KNOTS)	EFFECTIVE POWER (HP)	DELIVERED POWER (HP)	ETAD	ETAO	ETAB	1-t	CTS	CR	PROPELLER
15.0	7.72	10517.	7843.	15758.	11751.	0.667	0.718	0.723	0.925
20.0	10.29	21919.	16345.	33302.	24833.	0.658	0.714	0.703	0.922
25.0	12.86	39923.	29771.	61563.	45908.	0.648	0.712	0.709	0.894
30.0	15.43	63842.	47607.	98867.	73725.	0.646	0.709	0.705	0.888
36.0	18.52	109655.	81770.	167923.	125220.	0.653	0.709	0.695	0.902
39.0	20.06	156508.	116708.	238330.	177723.	0.657	0.717	0.700	0.901
42.0	21.61	225188.	167923.	339463.	253118.	0.663	0.722	0.721	0.893
									1.935
									157.8

Table A17. JHSS BSS powering in SS6 random waves, determined from model-scale added powering Exp 57&58

BSS DES Flap+BK Exp57&58 Sea State 6 StockProps (iProg=3)		TOTAL (ALL FOUR SHAFTS COMBINED)							
		LENGTH (LWL)	977.9 FT ( 298.1 M)	DELIVERED POWER	ETAB	1-t	CTS	CR	PROPELLER
		DISPLACEMENT	36490.4 TONS ( 37074.2 TONNES)	(kW)	ETAO				RPM
WETTED SURFACE		109536.6 SQ FT ( 10176.3 SQ M)							
INBD & OTBD PROP DIA		21.33 FT ( 6.50 M)							
CORRELATION ALLOWANCE		0.00000	ITTC FRICTION USED						

Table A18. Wind drag estimates, for JHSS BSS in sea state 6 with associated mean sustained wind speed

Calm Water				Calm Water with SAD			
VS (kts)	Calm Water PE (hP)	R (lbs)	SAD (lbs)	Calm w/SAD (lbs)	PE (hP)	SAD (lbs)	△ (%)
15	8077	175,540	4,710	180,251	8294	2.7	
20	17324	282,381	8,374	290,755	17838	3.0	
25	32837	428,194	13,084	441,279	33840	3.1	
30	54567	592,961	18,842	611,803	56301	3.2	
36	98864	895,268	27,132	922,400	101860	3.0	
39	145315	1,214,684	31,842	1,246,527	149124	2.6	
42	214949	1,668,414	36,929	1,705,343	219707	2.2	

SS6 Waves				SS6 Waves with SAD			
VS (kts)	SS6 Ship PE (hP)	SS6 Waves R (lbs)	SS6 Waves △ (%)	SS6 w/SAD (lbs)	PE (hP)	SS6 Waves w/SAD (lbs)	△ (%)
15	10,517	228,566	30.2	4,710	233,276	10,734	32.9
20	21,919	357,274	26.5	8,374	365,648	22,432	29.5
25	39,923	520,592	21.6	13,084	533,677	40,926	24.6
30	63,842	693,752	17.0	18,842	712,593	65,576	20.2
36	109,655	992,982	10.9	27,132	1,020,114	112,651	13.9
39	156,508	1,308,243	7.7	31,842	1,340,085	160,317	10.3
42	225,188	1,747,892	4.8	36,929	1,784,821	229,946	7.0

SS6 Waves with SAD and Ambient Wind			
VS (kts)	Wind (kts)	SAD+Wind (lbs)	RT+ SAD+Wind (lbs)
15	37.5	57,702	286,268
20	37.5	69,217	426,490
25	37.5	81,778	602,370
30	37.5	95,385	789,137
36	37.5	113,097	1,106,079
39	37.5	122,517	1,430,760
42	37.5	132,315	1,880,206

SS6 Waves	SS6 Waves with SAD	SS6 Waves with SAD+Wind	SS6 Waves with SAD+Wind+Wind
VS (kts)	Wind (kts)	Wind (hP)	Wind (hP)
15	37.5	13,172	2,655
20	37.5	26,165	4,246
25	37.5	46,194	6,271
30	37.5	72,620	8,778
36	37.5	122,144	12,489
39	37.5	171,165	14,657
42	37.5	242,235	17,047

Table A19. JHSS BSS effective power in SS6 random waves with estimated wind drag included

JHSS DES Flap+BK in SS6 with Wind Drag Added (PE input)						
LAMBDA	SHIP	MODEL				
LWL	977.9	ft	28.660	ft		
S	109537	ft <sup>2</sup>	94.084	ft <sup>2</sup>		
WT	36491	LT	199.9	lbs		
RHO	1.9905	(lb <sup>r</sup> sec <sup>2</sup> )/ft <sup>4</sup>	1.9358	(lb <sup>r</sup> sec <sup>2</sup> )/ft <sup>4</sup>		
NU	1.2817E-05	ft <sup>2</sup> /sec	1.0279E-05	ft <sup>2</sup> /sec		
Ca			0.0000			
Vs		EFFECTIVE POWER (PE)	FRICTIONAL POWER		FN	V-L
knots	HP	KW	HP	KW		1000CR
15.0	13172	9822	4544	3389	0.143	0.480
20.0	26165	19511	10411	7764	0.190	0.640
25.0	46194	34447	19813	14775	0.238	0.799
30.0	72620	54153	33526	25000	0.285	0.959
36.0	122144	91083	56743	42313	0.343	1.151
39.0	171165	127637	71493	53313	0.371	1.247
42.0	242235	180635	88552	66033	0.400	1.343
						2.177

Table A20. JHSS BSS powering in SS6 random waves with estimated wind drag included

Table A21. JHSS BSS with bilge keels, summary and comparison of effective and delivered powers in calm water

VS (kts)	Exp40	Exp40+BK	Bilge Keel Added Effective Power	
	Calm Water w/Flap PE (hP)	Calm Water Flap+BK PE (hP)	Δ PE (hP)	Δ PE (%)
15	7867	8077	210	2.66
20	16866	17324	458	2.71
25	31986	32837	851	2.66
30	53156	54567	1411	2.65
36	96351	98864	2514	2.61
39	141664	145315	3651	2.58
42	209630	214949	5319	2.54

VS (kts)	Exp41		Exp41+BK		Bilge Keel Added Delivered Power		Bilge Keel Added Propeller RPM	
	PD (hP)	RPM	PD (hP)	RPM	ΔPD (hP)	ΔPD (%)	ΔRPM	ΔRPM (%)
15	12031	55.0	12318	55.2	287	2.39	0.2	0.36
20	26253	71.7	26895	72.0	642	2.45	0.3	0.42
25	50426	89.3	51611	89.6	1185	2.35	0.3	0.34
30	83951	106.1	85961	106.5	2010	2.39	0.4	0.38
36	149593	126.7	153007	127.2	3414	2.28	0.5	0.39
39	217339	140.0	222405	140.5	5066	2.33	0.5	0.36
42	317161	155.9	324518	156.5	7357	2.32	0.6	0.38

Table A22. JHSS BSS, summary and comparison of effective and delivered powers in SS6 random waves

VS (kts)	Exp56 Added Resistance Test in SS6			Estimated from SS6 Added PE Test 56 and Calm Water Interactions from Test 41					
	SS6 Flap+BK PE (hP)	Sea State 6 Added Effective Power APE (hP)	ΔPE (%)	SS6 Flap+BK PD (hP)	Sea State 6 Added Delivered Power ΔPD (hP)	ΔPD (%)	SS6 Flap+BK RPM	Sea State 6 Added Propeller RPM ΔRPM	ΔRPM (%)
15	10517	2440	30.2	15758	3440	27.9	57.4	2.2	4.0
20	21919	4595	26.5	33302	6407	23.8	74.4	2.4	3.3
25	39923	7086	21.6	61563	9952	19.3	92.1	2.5	2.8
30	63842	9275	17.0	98867	12906	15.0	108.7	2.2	2.1
36	109655	10790	10.9	167923	14916	9.7	129.0	1.8	1.4
39	156508	11192	7.7	238330	15925	7.2	142.1	1.6	1.1
42	225188	10240	4.8	339463	14945	4.6	157.8	1.3	0.8

VS (kts)	Exp56 Added Resistance Test in SS6			Exp57&58 Added Powering Tests in SS6					
	SS6 Flap+BK PE (hP)	Sea State 6 Added Effective Power APE (hP)	ΔPE (%)	SS6 Flap+BK PD (hP)	Sea State 6 Added Delivered Power ΔPD (hP)	ΔPD (%)	SS6 Flap+BK RPM	Sea State 6 Added Propeller RPM ΔRPM	ΔRPM (%)
15	10517	2440	30.2	15604	3286	26.7	57.1	1.9	3.5
20	21919	4595	26.5	32841	5946	22.1	74.0	2.0	2.8
25	39923	7086	21.6	60664	9053	17.5	91.5	1.9	2.2
30	63842	9275	17.0	97112	11151	13.0	108.1	1.6	1.5
36	109655	10790	10.9	164467	11460	7.5	128.1	0.9	0.7
39	156508	11192	7.7	234382	11977	5.4	141.1	0.6	0.5
42	225188	10240	4.8	336048	11530	3.6	156.9	0.4	0.3

Table A23. JHSS BSS, summary and comparison of effective and delivered powers in SS6 random waves and associated wind

VS (kts)	Exps 40 & 41 Calm Water Flap+BK			Exps 56, 57 & 58 SS6 Random Waves Flap+BK			Exps 56, 57 & 58 SS6, with SAD + Ambient Wind Flap+BK		
	PE (hP)	PD (hP)	RPM	PE (hP)	PD (hP)	RPM	PE (hP)	PD (hP)	RPM
	15	8077	12318	55.2	10517	15604	57.1	13172	19553
20	17324	26895	72.0	21919	32841	74.0	26165	38946	76.2
25	32837	51611	89.6	39923	60664	91.5	46194	69692	93.7
30	54567	85961	106.5	63842	97112	108.1	72620	109495	110.2
36	98864	153007	127.2	109655	164467	128.1	122144	181587	130.2
39	145315	222405	140.5	156508	234382	141.1	171165	255518	143.2
42	214949	324518	156.5	225188	336048	156.9	242235	361504	159.0

VS (kts)	SS6 Random Waves Added Values to Calm Water Predictions			Ambient Wind Added Values to SS6 Predictions			SS6 Waves + Ambient Wind Added Values to Calm Water Predictions		
	ΔPE (%)	ΔPD (%)	ΔRPM	ΔPE (%)	ΔPD (%)	ΔRPM	ΔPE (%)	ΔPD (%)	ΔRPM
15	30.2	26.7	1.9	25.2	25.3	2.4	63.1	58.7	4.3
20	26.5	22.1	2.0	19.4	18.6	2.2	51.0	44.8	4.2
25	21.6	17.5	1.9	15.7	14.9	2.2	40.7	35.0	4.1
30	17.0	13.0	1.6	13.7	12.8	2.1	33.1	27.4	3.7
36	10.9	7.5	0.9	11.4	10.4	2.1	23.5	18.7	3.0
39	7.7	5.4	0.6	9.4	9.0	2.1	17.8	14.9	2.7
42	4.8	3.6	0.4	7.6	7.6	2.1	12.7	11.4	2.5

Table A24. Model 5653-3 Exp 59, regular waves, variations in wavelength and wave height targeting desired wave slope of 1/75, and calculation of added resistance operator (ARO)

Wavemaker Output: Regular Waves				Wave Encounter Characteristics				Model Resistance Characteristics In Regular Waves								
Wave Length $\lambda$ (ft)	Wave Height $\zeta$ (inches)	$\zeta/\lambda$	Amplitude (ft)	Wave Speed (ft/s)	Sample Time (sec)	Encounter Speed (ft/s)	Encounter Period (sec)	Wave Encounters	Encounter Frequency (wave/s)	VS (kts)	In Waves RTw (lbs)	Calm Water RT (lbs)	Added Drag	$\lambda/L$ OA	ARO	
23.17	3.33	0.0120	1/83	0.139	10.95	33	18.17	1.27	26	0.784	25	20.06	17.20	2.86	0.809	7.23
23.17	3.53	0.0127	1/79	0.147	10.95	60	21.35	1.09	55	0.922	36	37.83	35.24	2.59	0.809	5.82
23.17	3.45	0.0124	1/81	0.144	10.95	40	18.17	1.27	31	0.784	25	20.55	17.20	3.36	0.809	7.90
23.17	<b>3.70</b>	<b>0.0133</b>	<b>1/75</b>	<b>0.154</b>	10.95	<b>58</b>	<b>21.35</b>	<b>1.09</b>	<b>53</b>	<b>0.922</b>	<b>36</b>	<b>38.17</b>	<b>35.24</b>	<b>2.93</b>	<b>0.809</b>	<b>6.00</b>
23.17	<b>3.69</b>	<b>0.0133</b>	<b>1/75</b>	<b>0.154</b>	10.95	<b>42</b>	<b>18.17</b>	<b>1.27</b>	<b>33</b>	<b>0.784</b>	<b>25</b>	<b>20.47</b>	<b>17.20</b>	<b>3.27</b>	<b>0.809</b>	<b>6.73</b>
23.17	3.88	0.0140	1/72	0.162	10.95	58	21.35	1.09	53	0.922	36	38.97	35.24	3.73	0.809	6.94
25.27	3.75	0.0124	1/81	0.156	11.26	43	18.48	1.37	31	0.731	25	21.42	17.20	4.22	0.882	8.41
25.27	3.82	0.0126	1/79	0.159	11.26	57	21.66	1.17	49	0.857	36	39.74	35.24	4.50	0.882	8.64
25.27	<b>4.07</b>	<b>0.0134</b>	<b>1/75</b>	<b>0.170</b>	11.26	<b>40</b>	<b>18.48</b>	<b>1.37</b>	<b>29</b>	<b>0.731</b>	<b>25</b>	<b>22.04</b>	<b>17.20</b>	<b>4.85</b>	<b>0.882</b>	<b>8.19</b>
25.27	4.18	0.0138	1/73	0.174	11.26	56	21.66	1.17	48	0.857	36	40.96	35.24	5.72	0.882	9.18
25.27	<b>4.04</b>	<b>0.0133</b>	<b>1/75</b>	<b>0.168</b>	<b>11.26</b>	<b>56</b>	<b>21.66</b>	<b>1.17</b>	<b>48</b>	<b>0.857</b>	<b>36</b>	<b>40.49</b>	<b>35.24</b>	<b>5.25</b>	<b>0.882</b>	<b>9.01</b>
29.01	5.07	0.0146	1/69	0.211	12.26	40	19.49	1.49	27	0.672	25	24.17	17.20	6.98	1.013	7.60
29.01	5.13	0.0147	1/68	0.214	12.26	58	22.66	1.28	45	0.781	36	46.24	35.24	11.00	1.013	11.71
29.01	<b>4.65</b>	<b>0.0134</b>	<b>1/75</b>	<b>0.194</b>	<b>12.26</b>	<b>40</b>	<b>19.49</b>	<b>1.49</b>	<b>27</b>	<b>0.672</b>	<b>25</b>	<b>22.97</b>	<b>17.20</b>	<b>5.78</b>	<b>1.013</b>	<b>7.48</b>
29.01	4.82	0.0138	1/72	0.201	12.26	56	22.66	1.28	44	0.781	36	44.95	35.24	9.71	1.013	11.71
29.01	4.49	0.0129	1/78	0.187	12.26	40	19.49	1.49	27	0.672	25	22.46	17.20	5.26	1.013	7.30
29.01	<b>4.64</b>	<b>0.0133</b>	<b>1/75</b>	<b>0.193</b>	<b>12.26</b>	<b>48</b>	<b>22.66</b>	<b>1.28</b>	<b>37</b>	<b>0.781</b>	<b>36</b>	<b>44.21</b>	<b>35.24</b>	<b>8.97</b>	<b>1.013</b>	<b>11.67</b>
26.43	4.03	0.0127	1/79	0.168	11.62	40	18.84	1.40	29	0.713	25	22.23	17.20	5.03	0.923	8.68
26.43	4.03	0.0127	1/79	0.168	11.62	49	22.02	1.20	41	0.833	36	42.26	35.24	7.02	0.923	12.10
26.43	<b>4.26</b>	<b>0.0134</b>	<b>1/74</b>	<b>0.178</b>	<b>11.62</b>	<b>40</b>	<b>18.84</b>	<b>1.40</b>	<b>29</b>	<b>0.713</b>	<b>25</b>	<b>22.45</b>	<b>17.20</b>	<b>5.26</b>	<b>0.923</b>	<b>8.11</b>
26.43	<b>4.25</b>	<b>0.0134</b>	<b>1/75</b>	<b>0.177</b>	<b>11.62</b>	<b>53</b>	<b>22.02</b>	<b>1.20</b>	<b>44</b>	<b>0.833</b>	<b>36</b>	<b>42.38</b>	<b>35.24</b>	<b>7.14</b>	<b>0.923</b>	<b>11.07</b>
24.19	3.91	0.0135	1/74	0.163	11.09	40	18.31	1.32	30	0.757	25	21.96	17.20	4.76	0.844	8.72
24.19	3.96	0.0136	1/73	0.165	11.09	58	21.49	1.13	52	0.889	36	40.26	35.24	5.03	0.844	8.98
24.19	3.74	0.0129	1/78	0.156	11.09	45	18.31	1.32	34	0.757	25	21.38	17.20	4.18	0.844	8.37
24.19	3.82	0.0132	1/76	0.159	11.09	55	21.49	1.13	49	0.889	36	39.36	35.24	4.12	0.844	7.90
24.19	<b>3.89</b>	<b>0.0134</b>	<b>1/75</b>	<b>0.162</b>	<b>11.09</b>	<b>44</b>	<b>18.31</b>	<b>1.32</b>	<b>33</b>	<b>0.757</b>	<b>25</b>	<b>21.59</b>	<b>17.20</b>	<b>4.39</b>	<b>0.844</b>	<b>8.13</b>
24.19	3.95	0.0136	1/73	0.165	11.09	59	21.49	1.13	52	0.889	36	39.70	35.24	4.46	0.844	8.01
24.19	<b>3.85</b>	<b>0.0133</b>	<b>1/75</b>	<b>0.160</b>	<b>11.09</b>	<b>57</b>	<b>21.49</b>	<b>1.13</b>	<b>51</b>	<b>0.889</b>	<b>36</b>	<b>39.51</b>	<b>35.24</b>	<b>4.27</b>	<b>0.844</b>	<b>8.08</b>
31.99	<b>5.10</b>	<b>0.0133</b>	<b>1/75</b>	<b>0.160</b>	<b>11.09</b>	<b>57</b>	<b>21.49</b>	<b>1.13</b>	<b>51</b>	<b>0.889</b>	<b>36</b>	<b>39.51</b>	<b>35.24</b>	<b>4.27</b>	<b>0.844</b>	<b>8.08</b>
31.99	5.41	0.0144	1/71	0.225	12.89	35	20.11	1.59	22	0.629	25	23.72	17.20	6.52	1.116	6.24
31.99	5.47	0.0143	1/70	0.228	12.89	51	23.29	1.37	37	0.728	36	47.21	35.24	11.98	1.116	11.21
31.99	5.24	0.0137	1/73	0.218	12.89	40	20.11	1.59	25	0.629	25	23.57	17.20	6.38	1.116	6.50
31.99	<b>5.19</b>	<b>0.0135</b>	<b>1/74</b>	<b>0.216</b>	<b>12.89</b>	<b>59</b>	<b>23.29</b>	<b>1.37</b>	<b>43</b>	<b>0.728</b>	<b>36</b>	<b>45.61</b>	<b>35.24</b>	<b>10.37</b>	<b>1.116</b>	<b>10.79</b>
31.99	<b>5.19</b>	<b>0.0136</b>	<b>1/73</b>	<b>0.215</b>	<b>12.89</b>	<b>40</b>	<b>20.11</b>	<b>1.59</b>	<b>25</b>	<b>0.629</b>	<b>25</b>	<b>23.42</b>	<b>17.20</b>	<b>6.22</b>	<b>1.116</b>	<b>6.70</b>
31.99	<b>4.44</b>	<b>0.0134</b>	<b>1/75</b>	<b>0.185</b>	<b>12.00</b>	<b>58</b>	<b>22.40</b>	<b>1.24</b>	<b>47</b>	<b>0.809</b>	<b>36</b>	<b>44.01</b>	<b>35.24</b>	<b>8.77</b>	<b>0.966</b>	<b>12.46</b>
35.44	4.92	0.0116	1/86	0.205	13.47	40	20.69	1.71	23	0.584	25	21.99	17.20	4.79	1.237	5.54
35.44	4.52	0.0116	1/86	0.205	13.47	42	23.87	1.48	28	0.674	36	42.75	35.24	7.51	1.237	8.69
35.44	4.54	0.0137	1/73	0.189	12.00	57	22.40	1.24	46	0.809	36	43.30	23.30	0.584	25	1.237
35.44	5.34	0.0126	1/80	0.223	13.47	40	20.69	1.71	23	0.584	25	22.76	17.20	6.11	1.237	9.01
35.44	5.48	0.0129	1/78	0.228	13.47	48	23.87	1.48	32	0.674	36	45.17	35.24	9.94	1.237	9.27
35.44	<b>5.65</b>	<b>0.0133</b>	<b>1/75</b>	<b>0.235</b>	<b>13.47</b>	<b>40</b>	<b>20.69</b>	<b>1.71</b>	<b>23</b>	<b>0.584</b>	<b>25</b>	<b>24.27</b>	<b>17.20</b>	<b>7.07</b>	<b>1.237</b>	<b>6.21</b>
35.44	<b>5.65</b>	<b>0.0133</b>	<b>1/75</b>	<b>0.235</b>	<b>13.47</b>	<b>57</b>	<b>23.87</b>	<b>1.48</b>	<b>38</b>	<b>0.674</b>	<b>36</b>	<b>45.91</b>	<b>35.24</b>	<b>10.67</b>	<b>1.237</b>	<b>9.36</b>
21.31	3.44	0.0134	1/74	0.143	10.40	40	17.63	1.21	33	0.827	25	20.12	17.20	2.92	0.744	6.92
21.31	<b>3.38</b>	<b>0.0132</b>	<b>1/76</b>	<b>0.141</b>	<b>10.40</b>	<b>45</b>	<b>20.80</b>	<b>1.02</b>	<b>44</b>	<b>0.976</b>	<b>36</b>	<b>37.62</b>	<b>35.24</b>	<b>2.38</b>	<b>0.744</b>	<b>5.83</b>

Table A25. Model 5653-3 Exp 59, regular waves, determination of critical wavelengths (maximum ARO) at 25 and 36 knots,  
selected data at desired wave slope of 1/75

Wavemaker Output: Regular Waves				Wave Encounter Characteristics				Model Resistance Characteristics In Regular Waves								
Wave Length $\lambda$ (ft)	Wave Height $\zeta$ (inches)	$\zeta/\lambda$	Amplitude (ft)	Wave Speed (ft/s)	Sample Time (sec)	Encounter Period (ft/s)	Wave Encounters	Encounter Frequency (wave/s)	VS (kts)	In Waves RTw (lbs)	Water RT (lbs)	Added Drag	$\lambda/LOA$	ARO		
21.31	3.44	0.0134	1/74	0.143	10.40	40	17.63	1.21	33	0.827	25	20.12	2.92	0.744	6.92	
23.17	3.69	0.0133	1/75	0.154	10.95	42	18.17	1.27	33	0.784	25	20.47	17.20	3.27	6.73	
24.19	3.89	0.0134	1/75	0.162	11.09	44	18.31	1.32	33	0.757	25	21.59	17.20	4.39	8.13	
25.27	4.07	0.0134	1/75	0.170	11.26	40	18.48	1.37	29	0.731	25	22.04	17.20	4.85	8.19	
26.43	4.26	0.0134	1/74	0.178	11.62	40	18.84	1.40	29	0.713	25	22.45	17.20	5.26	8.11	
27.68	4.41	0.0133	1/75	0.184	12.00	40	19.23	1.44	28	0.695	25	22.76	17.20	5.56	8.01	
29.01	4.65	0.0134	1/75	0.194	12.26	40	19.49	1.49	27	0.672	25	22.97	17.20	5.78	7.48	
31.99	5.10	0.0133	1/75	0.213	12.89	40	20.11	1.59	25	0.629	25	23.42	17.20	6.22	6.70	
35.44	5.65	0.0133	1/75	0.235	13.47	40	20.69	1.71	23	0.584	25	24.27	17.20	7.07	6.21	
21.31	3.38	0.0132	1/76	0.141	10.40	45	20.80	1.02	44	0.976	36	37.62	35.24	2.38	0.744	5.83
23.17	3.70	0.0133	1/75	0.154	10.95	58	21.35	1.09	53	0.922	36	38.17	35.24	2.93	0.809	6.00
24.19	3.85	0.0133	1/75	0.160	11.09	57	21.49	1.13	51	0.889	36	39.51	35.24	4.27	0.844	8.08
25.27	4.04	0.0133	1/75	0.168	11.26	56	21.66	1.17	48	0.857	36	40.49	35.24	5.25	0.882	9.01
26.43	4.25	0.0134	1/75	0.177	11.62	53	22.02	1.20	44	0.833	36	42.38	35.24	7.14	0.923	11.07
27.68	4.44	0.0134	1/75	0.185	12.00	58	22.40	1.24	47	0.809	36	44.01	35.24	8.77	0.966	12.46
29.01	4.64	0.0133	1/75	0.193	12.26	48	22.66	1.28	37	0.781	36	44.21	35.24	8.97	1.013	11.67
31.99	5.19	0.0135	1/74	0.216	12.89	59	23.29	1.37	43	0.728	36	45.61	35.24	10.37	1.116	10.79
35.44	5.65	0.0133	1/75	0.235	13.47	57	23.87	1.48	38	0.674	36	45.91	35.24	10.67	1.237	9.36

Table A26. Model 5653-3 Exp 60, added resistance operator (ARO) at 25 knots, for variations of wave slope at critical wavelength  $\lambda/LOA = 0.882$

**25 Knots**

Wavemaker Output: Regular Waves				Wave Encounter Characteristics						Model Resistance Characteristics In Regular Waves						
Wave Length $\lambda$ (ft)	Wave Height $\zeta$ (inches)	$\zeta/\lambda$	Amplitude (ft)	Wave Speed (ft/s)	Sample Time (sec)	Encounter Speed (ft/s)	Encounter Period (sec)	Wave	Encounter	Encounter	Encounter	Encounter	Encounter	Encounter	Encounter	
25.27	5.21	0.0172	1/58	0.217	11.37	70	18.60	1.36	52	0.736	25	24.77	17.20	7.57	0.882	7.81
25.27	5.20	0.0171	1/58	0.217	11.37	75	18.60	1.36	55	0.736	25	24.91	17.20	7.72	0.882	7.99
25.27	4.14	0.0137	1/73	0.173	11.37	75	18.60	1.36	55	0.736	25	22.20	17.20	5.00	0.882	8.17
25.27	4.10	0.0135	1/74	0.171	11.37	70	18.60	1.36	52	0.736	25	21.91	17.20	4.71	0.882	7.86
25.27	4.07	0.0134	1/75	0.170	11.37	40	18.60	1.36	29	0.736	25	22.04	17.20	4.85	0.882	8.19
25.27	3.75	0.0124	1/81	0.156	11.37	43	18.60	1.36	32	0.736	25	21.42	17.20	4.22	0.882	8.41
25.27	3.01	0.0099	1/101	0.125	11.37	75	18.60	1.36	55	0.736	25	20.12	17.20	2.92	0.882	9.02
25.27	2.98	0.0098	1/102	0.124	11.37	70	18.60	1.36	52	0.736	25	20.14	17.20	2.94	0.882	9.27
25.27	2.50	0.0082	1/121	0.104	11.37	72	18.60	1.36	53	0.736	25	19.29	17.20	2.09	0.882	9.37
25.27	2.48	0.0082	1/122	0.103	11.37	70	18.60	1.36	52	0.736	25	19.34	17.20	2.14	0.882	9.73
25.27	2.04	0.0067	1/149	0.085	11.37	70	18.60	1.36	52	0.736	25	19.03	17.20	1.83	0.882	12.32
25.27	2.02	0.0067	1/150	0.084	11.37	75	18.60	1.36	55	0.736	25	18.93	17.20	1.74	0.882	11.92
25.27	1.90	0.0063	1/160	0.079	11.37	95	18.60	1.36	70	0.736	25	18.57	17.20	1.37	0.882	10.61
25.27	1.89	0.0062	1/160	0.079	11.37	50	18.60	1.36	37	0.736	25	18.70	17.20	1.51	0.882	11.81

**25 knot Fairied Data at Incremental Wave Slopes**

VS (kts)	$\zeta$ (inch)	$\lambda/LOA$	$\lambda/\zeta$	Rw (lb)	25kt ARO
25	2.02	0.882	150.0	1.78	12.21
25	2.53	0.882	120.0	2.24	9.85
25	3.03	0.882	100.0	2.80	8.54
25	4.04	0.882	75.0	4.84	8.29
25	5.05	0.882	60.0	7.23	7.93

Table A27. Model 5653-3 Exp 60, added resistance operator (ARO) at 36 knots, for variations of wave slope at critical wavelength  $\lambda/LOA = 0.966$

36 Knots				Wavemaker Output: Regular Waves				Wave Encounter Characteristics				Model Resistance Characteristics in Regular Waves				
Wave Length $\lambda$ (ft)	Wave Height $\zeta$ (inches)	$\zeta/\lambda$	Amplitude (ft)	Wave Speed (ft/s)	Sample Time (sec)	Encounter Speed (ft/s)	Encounter Period (sec)	Wave Encount-ers	Encounter Frequency (waves/s)	Encounter	VS (kts)	In Waves RTw (lbs)	Calm Water Rt (lbs)	Added Drag	$\lambda/LOA$	ARO
27.68	4.54	0.0137	1/73	0.189	11.90	57	22.30	1.24	46	0.806	36	43.30	35.24	8.07	0.966	10.96
27.68	4.49	0.0135	1/74	0.187	11.90	48	22.30	1.24	39	0.806	36	43.45	35.24	8.21	0.966	11.41
27.68	4.44	0.0134	1/75	0.185	11.90	58	22.30	1.24	47	0.806	36	44.01	35.24	8.77	0.966	12.46
27.68	4.34	0.0131	1/77	0.181	11.90	45	22.30	1.24	36	0.806	36	43.30	35.24	8.06	0.966	11.99
27.68	3.25	0.0098	1/102	0.135	11.90	49	22.30	1.24	39	0.806	36	40.45	35.24	5.21	0.966	13.82
27.68	3.20	0.0096	1/104	0.133	11.90	45	22.30	1.24	36	0.806	36	40.67	35.24	5.43	0.966	14.86
27.68	2.44	0.0073	1/136	0.102	11.90	25	22.30	1.24	20	0.806	36	37.92	35.24	2.68	0.966	12.62
27.68	2.44	0.0073	1/136	0.102	11.90	45	22.30	1.24	36	0.806	36	37.49	35.24	2.25	0.966	10.60
27.68	2.15	0.0065	1/154	0.090	11.90	46	22.30	1.24	37	0.806	36	37.94	35.24	2.70	0.966	16.37
27.68	2.12	0.0064	1/157	0.088	11.90	42	22.30	1.24	34	0.806	36	37.69	35.24	2.45	0.966	15.27
27.68	2.08	0.0063	1/160	0.087	11.90	45	22.30	1.24	36	0.806	36	37.30	35.24	2.06	0.966	13.33
27.68	2.06	0.0062	1/161	0.086	11.90	50	22.30	1.24	40	0.806	36	37.42	35.24	2.18	0.966	14.39
27.68	2.03	0.0061	1/164	0.085	11.90	50	22.30	1.24	40	0.806	36	37.41	35.24	2.17	0.966	14.78
27.68	2.00	0.0060	1/166	0.083	11.90	45	22.30	1.24	36	0.806	36	37.03	35.24	1.79	0.966	12.56

36 Knot Fairied Data at Incremental Wave Slopes				
VS (kts)	$\zeta$ (inch)	$\lambda/LOA$	$\lambda/\zeta$	Rw (lb)
36	2.21	0.966	150.0	2.25
36	2.77	0.966	120.0	3.77
36	3.32	0.966	100.0	5.53
36	4.43	0.966	75.0	8.24
36	5.54	0.966	60.0	9.98
				9.13

Table A28. Model 5653-3 Exp 60, resistance increase in regular waves, locked in surge, variations of wave slope at critical wavelengths, 25 and 36 knots

Regular Waves Exp 60, Locked (Fixed), Resistance Increase at 25 knots, $\lambda/L = 0.882$						
VS	Calm Water	Waves	Regular Waves			Added Resistance
			Exp53	Exp60	Increased Resistance (%)	
(kts)	Rt (lbs)	RTw (lbs)	Rw (lbs)	(%)	$\zeta/\lambda$	Wave Height $\zeta$ (in)
25	17.20	18.98	1.78	10.35	1/150	2.02
25	17.20	19.44	2.24	13.05	1/120	2.53
25	17.20	20.00	2.80	16.30	1/100	3.03
25	17.20	22.04	4.84	28.13	1/75	4.04
25	17.20	24.42	7.23	42.01	1/60	5.05
						7.93

Regular Waves Exp 60, Locked (Fixed), Resistance Increase at 36 knots, $\lambda/L = 0.966$						
VS	Calm Water	Waves	Regular Waves			Added Resistance
			Exp53	Exp60	Increased Resistance (%)	
(kts)	Rt (lbs)	RTw (lbs)	Rw (lbs)	(%)	$\zeta/\lambda$	Wave Height $\zeta$ (in)
36	35.24	37.49	2.25	6.38	1/150	2.21
36	35.24	39.01	3.77	10.70	1/120	2.77
36	35.24	40.77	5.53	15.70	1/100	3.32
36	35.24	43.48	8.24	23.37	1/75	4.43
36	35.24	45.22	9.98	28.32	1/60	5.54
						9.13

Table A29. Model 5653-3 Exp 62, powering increase in regular waves, locked in surge (ship propulsion point), variations of wave slope at critical wavelengths, 25 and 36 knots

Regular Waves Exp62, Locked in Surge (Fixed), Powering Increase at Ship Propulsion Point, 25 knots, $\lambda/L = 0.882$											
VS (kts)	RPM INBD	Total			Total			Power/Shaf Power/Shaf t OUTBD			Total Thrust (lbf)
		Torque INBD (in-lbf)	Thrust INBD (lbf)	RPM OUTBD	Torque OUTBD (in-lbf)	Thrust OUTBD (lbf)	(hP)	(hP)	(hP)		
25	529.20	16.87	8.02	527.17	13.04	5.73	0.07	0.05	0.25	528.18	
25	533.28	17.54	8.47	530.83	13.87	6.22	0.07	0.06	0.27	532.05	
25	535.56	17.76	8.55	533.07	14.23	6.45	0.08	0.06	0.27	534.31	
25	546.54	19.27	9.44	544.25	16.05	7.53	0.08	0.07	0.31	545.39	
25	561.14	21.47	10.83	559.11	18.56	8.98	0.10	0.08	0.36	560.12	
VS (kts)											
Wave Height $\zeta$ (in)											
25	1/150	2.02	0.030	13.77	10.2	1.98	16.79				
25	1/120	2.53	0.045	20.37	14.1	2.92	24.80				
25	1/100	3.03	0.051	23.07	16.4	3.23	27.49				
25	1/75	4.04	0.085	38.68	27.4	5.20	44.18				
25	1/60	5.05	0.135	61.43	42.2	8.04	68.29				
*PCT relative to measured model values at ship propulsion point											
VS (kts)											
Wave Height $\zeta$ (in)											
36	752.70	33.52	16.01	752.79	28.43	12.92	0.20	0.17	0.74	752.75	
36	754.06	33.87	16.22	754.15	29.49	13.30	0.20	0.18	0.76	754.11	
36	756.33	34.22	16.46	756.26	29.74	13.67	0.21	0.18	0.77	756.29	
36	770.93	36.68	17.88	770.65	33.29	15.79	0.22	0.20	0.86	770.79	
VS (kts)											
Wave Height $\zeta$ (in)											
36	1/150	2.21	0.078	11.73	10.2	3.26	12.68				
36	1/120	2.77	0.096	14.48	11.6	3.85	15.02				
36	1/100	3.32	0.105	15.89	13.8	4.46	17.39				
36	1/75	4.43	0.193	29.22	28.3	8.01	31.20				
Regular Waves Exp62, Locked in Surge (Fixed), Powering Increase at Ship Propulsion Point, 36 knots, $\lambda/L = 0.966$											
VS (kts)	RPM INBD	Total			Total			Power/Shaf Power/Shaf t OUTBD			Total Thrust (lbf)
		Torque INBD (in-lbf)	Thrust INBD (lbf)	RPM OUTBD	Torque OUTBD (in-lbf)	Thrust OUTBD (lbf)	(hP)	(hP)	(hP)		
36	752.70	33.52	16.01	752.79	28.43	12.92	0.20	0.17	0.74	752.75	
36	754.06	33.87	16.22	754.15	29.49	13.30	0.20	0.18	0.76	754.11	
36	756.33	34.22	16.46	756.26	29.74	13.67	0.21	0.18	0.77	756.29	
36	770.93	36.68	17.88	770.65	33.29	15.79	0.22	0.20	0.86	770.79	
VS (kts)											
Wave Height $\zeta$ (in)											
36	1/150	2.21	0.078	11.73	10.2	3.26	12.68				
36	1/120	2.77	0.096	14.48	11.6	3.85	15.02				
36	1/100	3.32	0.105	15.89	13.8	4.46	17.39				
36	1/75	4.43	0.193	29.22	28.3	8.01	31.20				
*PCT relative to measured model values at ship propulsion point											
VS (kts)											
Wave Height $\zeta$ (in)											
36	1/150	2.21	0.078	11.73	10.2	3.26	12.68				
36	1/120	2.77	0.096	14.48	11.6	3.85	15.02				
36	1/100	3.32	0.105	15.89	13.8	4.46	17.39				
36	1/75	4.43	0.193	29.22	28.3	8.01	31.20				

Table A30. Model 5653-3 Exp 61, powering increase in regular waves, free to surge (model self-propulsion), variations of wave slope at critical wavelengths, 25 and 36 knots

Regular Waves Exp61, Free to Surge, Powering Increase at Model Self-Propulsion, 25 knots, $\lambda/L = 0.882$									
VS	RPM INBD	Total		Total		Total		Total	
		Thrust INBD	Torque INBD (lbf)	RPM OUTBD	Torque OUTBD (in-lbf)	Thrust OUTBD	(lbf)	Power/Shaf t INBD	(hP)
25	566.11	21.96	11.32	566.33	18.57	9.05	0.10	0.08	566.22
25	570.49	22.71	11.97	569.79	19.09	9.32	0.10	0.09	570.14
25	573.29	23.07	12.11	576.49	20.32	10.06	0.10	0.09	574.89
25	584.34	24.70	13.03	589.06	22.46	11.41	0.11	0.10	586.70
25	598.26	26.87	14.43	598.49	23.89	12.34	0.13	0.11	598.38
*PCT relative to measured model values at ship propulsion point Free to Surge, Increased RPM									
VS	$\zeta/\lambda$	Wave Height $\zeta$ (in)		Increased Power, (hP)*		Increase		Thrust, Regular Waves (lbf)	
		1/150	2.02	0.016	7.18	5.5	1.25	10.60	
25	1/120	2.53	0.030	13.54	9.4	2.17	18.41		
25	1/100	3.03	0.047	21.52	14.2	3.05	25.95		
25	1/75	4.04	0.091	41.11	26.0	5.32	45.17		
25	1/60	5.05	0.134	60.63	37.7	7.65	64.96		

\*PCT relative to measured model values at ship propulsion point  
*Free to Surge, RPM Free to Surge, Increased  
 Increased Power.*

Regular Waves Exp61, Free to Surge, Powering Increase at Model Self-Propulsion, 36 knots, $\lambda/L = 0.966$											
VS	RPM INBD	Total Thrust		Total RPM OUTBD		Total Thrust		Power/Shaf Power/Shaf t OUTBD		Total Thrust (lbf)	
		Torque INBD (in-lbf)	INBD (lbf)	Torque OUTBD (in-lbf)	OUTBD (lbf)	Thrust OUTBD (lbf)	(hP)	Thrust OUTBD (lbf)	(hP)		
36	806.10	44.27	22.96	803.34	38.37	18.86	0.28	0.24	1.06	804.72	
36	809.49	44.96	23.45	806.58	39.39	19.43	0.29	0.25	1.08	808.04	
36	811.62	45.51	23.75	813.27	41.27	20.55	0.29	0.27	1.12	812.44	
36	827.85	48.72	25.68	828.99	44.97	22.85	0.32	0.30	1.23	828.42	
VS										*PCT relative to measured model values at ship propulsion point	
										Free to Surge, RPM Increase	
										Free to Surge, Increased Thrust, Regular Waves	
										(lbf) (%)*	
										(lbf) (%)*	
25	1/150	2.21	2.21	0.041	6.17	3.7	7.62	7.62	7.62	7.62	
25	1/120	2.77	0.067	10.14	7.0	3.03	11.79	11.79	11.79	11.79	
25	1/100	3.32	0.104	15.73	11.4	4.44	17.31	17.31	17.31	17.31	
25	1/75	4.43	0.217	32.77	27.4	8.67	33.77	33.77	33.77	33.77	

*PCT relative to measured model values at ship propulsion point				
Free to Surge, Increased Power, (hP)	RPM	Free to Surge, Increased Increase (%)	Thrust, Regular Waves (lbf)	(%)*
0.041	6.17	3.7	1.96	7.62
0.067	10.14	7.0	3.03	11.79
0.104	15.73	11.4	4.44	17.31
0.217	32.77	27.4	8.67	33.77

Table A31. Model 5653-3, summary of resistance and powering increases in regular waves

Summary of Model 5653-3 Tests In Regular Waves											
Model Attachment	Slope $C_d$	Model-Scale Measurements, 25 kts, $\lambda/LOA = 0.882$				Model-Scale Measurements, 36 kts, $\lambda/LOA = 0.966$				RPM	PD (hP)
		RT (lbs)	T (lb)	Q (in-lbs)	RPM	RT (lbs)	T (lb)	Q (in-lbs)	RPM		
Fixed	Calm	17.20	11.77	26.82	517.95	0.22	35.24	25.67	56.21	742.53	0.66
	1/150	18.98	13.74	29.91	528.18	0.25	37.49	28.92	61.95	752.75	0.74
	1/120	19.44	14.69	31.42	532.05	0.27	39.01	29.52	63.36	754.11	0.76
	1/100	20.00	15.00	31.99	534.31	0.27	40.77	30.13	63.95	756.29	0.77
	1/75	22.04	16.97	35.31	545.39	0.31	43.48	33.68	69.97	770.79	0.86
	1/60	24.42	19.81	40.03	560.12	0.36	45.22	-	-	-	-
Free to Surge	Calm	N/A	19.12	39.15	560.73	0.35	N/A	39.86	79.82	801.06	1.01
	1/150	"	20.37	40.53	566.22	0.36	"	41.82	82.64	804.72	1.06
	1/120	"	21.29	41.80	570.14	0.38	"	42.89	84.35	808.04	1.08
	1/100	"	22.17	43.39	574.89	0.40	"	44.30	86.78	812.44	1.12
	1/75	"	24.43	47.16	586.70	0.44	"	48.53	93.69	828.42	1.23
	1/60	"	26.76	50.76	598.38	0.48	"	-	-	-	-
Model Attachment	Increased Values in Waves, 25 kts										
	Slope $C_d$	Rw (lbs)	Tw (lbs)	Qw (in-lbs)	RPM	PDW (hP)	Rw (lbs)	Tw (lbs)	Qw (in-lbs)	RPM	PDW (hP)
	1/150	1.78	1.98	3.09	10.23	0.03	2.25	3.26	5.74	10.22	0.08
	1/120	2.24	2.92	4.60	14.10	0.04	3.77	3.85	7.15	11.58	0.10
	1/100	2.80	3.23	5.17	16.36	0.05	5.53	4.46	7.74	13.76	0.11
	1/75	4.84	5.20	8.49	27.44	0.09	8.24	8.01	13.76	28.26	0.19
Free to Surge	1/60	7.23	8.04	13.21	42.17	0.14	9.98	-	-	-	-
	1/150	N/A	1.25	1.38	5.49	0.02	N/A	1.96	2.82	3.66	0.04
	1/120	"	2.17	2.64	9.41	0.03	"	3.03	4.53	6.98	0.07
	1/100	"	3.05	4.24	14.17	0.05	"	4.44	6.96	11.38	0.10
	1/75	"	5.32	8.00	25.97	0.09	"	8.67	13.87	27.36	0.22
	1/60	"	7.65	11.61	37.65	0.13	"	-	-	-	-
Model Attachment	Increased Percentage* in Waves, 25 kts										
	Slope $C_d$	Rw (%)	Tw (%)	Qw (%)	RPMW (%)	PDW (%)	Rw (%)	Tw (%)	Qw (%)	RPMW (%)	PDW (%)
	1/150	10.4	16.8	11.5	2.0	13.8	6.4	12.7	10.2	1.4	11.7
	1/120	13.1	24.8	17.1	2.7	20.4	10.7	15.0	12.7	1.6	14.5
	1/100	16.3	27.5	19.3	3.2	23.1	15.7	17.4	13.8	1.9	15.9
	1/75	28.1	44.2	31.7	5.3	38.7	23.4	31.2	24.5	3.8	29.2
Free to Surge	1/60	42.0	68.3	49.3	8.1	61.4	28.3	-	-	-	-
	1/150	N/A	10.6	5.1	1.1	7.2	N/A	7.6	5.0	0.5	6.2
	1/120	"	18.4	9.9	1.8	13.5	"	11.8	8.1	0.9	10.1
	1/100	"	26.0	15.8	2.7	21.5	"	17.3	12.4	1.5	15.7
	1/75	"	45.2	29.8	5.0	41.1	"	33.8	24.7	3.7	32.8
	1/60	"	65.0	43.3	7.3	60.6	"	-	-	-	-

\*Percent relative to measured model values at ship propulsion point

Table A32. Model 5653-3, model measurement uncertainty, calm water

Calm Water 25 knot Ship Speed						
Measurement	Units	Nominal Mean	Bias Error	Precision Error	Uncertainty* (units)	Four Shafts (percent)
			±	±	±	±
Speed	ft/sec	7.25	0.002	0.002	0.003	0.04
Resistance	lbf	17.20	0.060	0.301	0.307	1.78
INbd Prop Shaft Rate	RPM	517.77	0.005	2.910	2.910	0.56
OUTbd Prop Shaft Rate	RPM	518.12	0.005	3.110	3.110	0.60
INbd Shaft Thrust - combined	lbf	6.91	0.056	0.150	0.160	2.32
OUTbd Shaft Thrust - combined	lbf	4.86	0.056	0.110	0.124	2.55
INbd Shaft Torque - combined	lbf-in	15.14	0.097	0.209	0.230	1.52
OUTbd Shaft Torque - combined	lbf-in	11.68	0.097	0.170	0.196	1.67
INbd Shaft Power - combined	hP	0.124	0.0008	0.0019	0.0020	1.62
OUTbd Shaft Power - combined	hP	0.096	0.0008	0.0015	0.0017	1.78
Calm Water 36 knot Ship Speed						
Measurement	Units	Nominal Mean	Bias Error	Precision Error	Uncertainty* (units)	Four Shafts (percent)
			±	±	±	±
Speed	ft/sec	10.43	0.003	0.007	0.008	0.07
Resistance	lbf	35.24	0.065	0.209	0.219	0.62
INbd Prop Shaft Rate	RPM	742.40	0.006	1.000	1.000	0.13
OUTbd Prop Shaft Rate	RPM	742.67	0.006	2.390	2.390	0.32
INbd Shaft Thrust - combined	lbf	14.59	0.059	0.090	0.108	0.74
OUTbd Shaft Thrust - combined	lbf	11.08	0.059	0.139	0.151	1.36
INbd Shaft Torque - combined	lbf-in	31.10	0.102	0.245	0.265	0.85
OUTbd Shaft Torque - combined	lbf-in	25.11	0.102	0.102	0.144	0.57
INbd Shaft Power - combined	hP	0.366	0.0012	0.0029	0.0032	0.86
OUTbd Shaft Power - combined	hP	0.296	0.0012	0.0015	0.0019	0.66

\*Overall Uncertainty has been determined by combining the bias and precision limits using the root-sum-square (RSS) method for a 95 percent confidence level.

Table A33. Model 5653-3, model measurement variability, SS6 random waves

SS6 Random Waves 25 knot Ship Speed, Fixed-in-Surge						
Measurement	Units	Nominal	Bias	Precision	Variability*	Four Shafts (percent)
		Mean	Error	Error	(units)	
			±	±	±	±
Speed	ft/sec	7.25	0.002	0.004	0.004	0.06
Resistance	lbf	19.88	0.060	0.990	0.992	4.99
INbd Prop Shaft Rate	RPM	529.90	0.006	7.510	7.510	1.42
OUTbd Prop Shaft Rate	RPM	530.55	0.006	7.640	7.640	1.44
INbd Shaft Thrust - combined	lbf	8.06	0.057	0.680	0.682	8.47
OUTbd Shaft Thrust - combined	lbf	6.31	0.057	0.560	0.563	8.92
INbd Shaft Torque - combined	lbf-in	16.77	0.097	1.040	1.045	6.23
OUTbd Shaft Torque - combined	lbf-in	14.14	0.097	0.960	0.965	6.82
INbd Shaft Power - combined	hP	0.141	0.0008	0.0090	0.0090	6.39
OUTbd Shaft Power - combined	hP	0.119	0.0008	0.0083	0.0083	6.68

SS6 Random Waves 36 knot Ship Speed, Fixed-in-Surge						
Measurement	Units	Nominal	Bias	Precision	Variability*	Four Shafts (percent)
		Mean	Error	Error	(units)	
			±	±	±	±
Speed	ft/sec	10.43	0.003	0.006	0.007	0.06
Resistance	lbf	38.29	0.066	1.390	1.392	3.63
INbd Prop Shaft Rate	RPM	748.50	0.006	1.560	1.560	0.21
OUTbd Prop Shaft Rate	RPM	748.33	0.006	3.040	3.040	0.41
INbd Shaft Thrust - combined	lbf	15.47	0.059	0.200	0.209	1.35
OUTbd Shaft Thrust - combined	lbf	12.41	0.059	0.420	0.424	3.42
INbd Shaft Torque - combined	lbf-in	32.55	0.102	0.310	0.326	1.00
OUTbd Shaft Torque - combined	lbf-in	27.35	0.102	0.640	0.648	2.37
INbd Shaft Power - combined	hP	0.387	0.0012	0.0038	0.0040	1.02
OUTbd Shaft Power - combined	hP	0.325	0.0012	0.0077	0.0078	2.40

SS6 Random Waves, Free to Surge, 25 knot Ship Speed						
Measurement	Units	Nominal	Bias	Precision	Variability*	Four Shafts (percent)
		Mean	Error	Error	(units)	
			±	±	±	±
Speed	ft/sec	7.25	0.002	0.005	0.006	0.08
INbd Prop Shaft Rate	RPM	569.00	0.006	6.98	6.980	1.23
OUTbd Prop Shaft Rate	RPM	572.39	0.006	4.29	4.290	0.75
INbd Shaft Thrust - combined	lbf	11.54	0.058	0.63	0.633	5.48
OUTbd Shaft Thrust - combined	lbf	9.80	0.058	0.330	0.335	3.42
INbd Shaft Torque - combined	lbf-in	22.71	0.099	0.970	0.975	4.29
OUTbd Shaft Torque - combined	lbf-in	19.92	0.099	0.570	0.579	2.90
INbd Shaft Power - combined	hP	0.205	0.0009	0.0091	0.0092	4.47
OUTbd Shaft Power - combined	hP	0.181	0.0009	0.0054	0.0054	3.73

SS6 Random Waves, Free to Surge, 36 knot Ship Speed						
Measurement	Units	Nominal	Bias	Precision	Variability*	Four Shafts (percent)
		Mean	Error	Error	(units)	
			±	±	±	±
Speed	ft/sec	10.43	0.003	0.006	0.007	0.06
INbd Prop Shaft Rate	RPM	806.02	0.006	5.350	5.350	0.66
OUTbd Prop Shaft Rate	RPM	805.31	0.006	6.590	6.590	0.82
INbd Shaft Thrust - combined	lbf	22.69	0.061	0.700	0.703	3.10
OUTbd Shaft Thrust - combined	lbf	19.18	0.061	0.830	0.832	4.34
INbd Shaft Torque - combined	lbf-in	44.56	0.106	1.130	1.135	2.55
OUTbd Shaft Torque - combined	lbf-in	38.72	0.106	1.450	1.454	3.72
INbd Shaft Power - combined	hP	0.570	0.0014	0.0149	0.0150	2.63
OUTbd Shaft Power - combined	hP	0.495	0.0014	0.0190	0.0190	3.24

\*Overall Variability has been determined by combining the bias and precision limits using the root-sum-square (RSS) method for a 95 percent confidence level.

## **APPENDIX B**

### **MODEL 5653-3 MOTIONS DATA & ANALYSIS**

**Bryson Metcalf  
Code 5800**

## FIGURES OF APPENDIX B

	Page
B1. Roll Decays Illustrating "With" and "Without" Bilge Keels .....	B6
B2. Motions and Acceleration SSA Data for the Unpropelled, Fixed-in-surge Resistance Test #56, 25 knots .....	B8
B3. Motions and Acceleration SSA Data for the Unpropelled, Fixed-in-surge Resistance Test #56, 36 knots .....	B8
B4. Spectral Analysis Plots for the Unpropelled, Fixed-in-surge Resistance Test #56, 36 knots ..	B9
B5. Spectral Analysis Plots for the Calm-Water, Fixed-in-surge Powering Test #54, 36 knots ....	B9
B6. Propulsion Influence on Motions @ 25 Knots .....	B11
B7. Surging Influence on Motions @ 25 Knots .....	B11
B8. Propulsion Influence on Motions @ 36 Knots .....	B12
B9. Surging Influence on Motions @ 36 Knots .....	B12
B10. Test #56 (Unpropelled, Fixed-in-Surge) Concatenated SS6 Time History Data, 25 Knots ....	B15
B11. Test #56 (Unpropelled, Fixed-in-Surge) Concatenated SS6 Time History Data, 36 Knots ....	B16
B12. Test #57 (Propelled, Fixed-in-Surge) Concatenated SS6 Time History Data, 25 Knots .....	B17
B13. Test #57 (Propelled, Fixed-in-Surge) Concatenated SS6 Time History Data, 36 Knots .....	B18
B14. Test #58 (Propelled, Free-to-Surge) Concatenated SS6 Time History Data, 25 Knots .....	B19
B15. Test #58 (Propelled, Free-to-Surge) Concatenated SS6 Time History Data, 36 Knots .....	B20

## TABLES OF APPENDIX B

	Page
B1. Desired & Achieved Mass Properties for Design Displacement .....	B5
B2. Influence of Surging Tow-Post Weight on Model Mass Properties .....	B5
B3. Averaged Least-Squares-Fit Ship-Scale Roll Decay Coefficients .....	B7
B4. Test #56 (Unpropelled, Fixed-in-Surge) Concatenated Data Results .....	B13
B5. Test #57 (Propelled, Fixed-in-Surge) Concatenated Data Results .....	B14
B6. Test #58 (Propelled, Free-to-Surge) Concatenated Data Results .....	B14

The objective of this appendix is to present the motions data collected during the added resistance and powering tests for Model 5653-3. The model was ballasted to the desired longitudinal and vertical mass distribution and instrumented to acquire properly sealed motions and accelerations due to advancement in waves from ahead. The resulting data is presented to highlight the influence of test procedures with regards to the use of an un-propelled or a self-propelled model and the model freedom-to-surge.

The tests conducted in this effort are summarized as;

- fixed-in-surge resistance tests (Test 56)
- fixed-in-surge powering tests at the ship self-propulsion-point (Test 57)
- free-to-surge powering tests at the model self-propulsion-point (Test 58)

Test No.	Test Type	Test Method	Sea State	Speed (kts)
56	ADDED Resistance (included additional wave sampling)	Fixed-in-Surge	SS6	25, 36
57	ADDED Power, Ship Propulsion Point	Fixed-in-Surge		25, 36
58	ADDED Power, Model Self-Propulsion Point	Free-to-Surge		25, 36

A model resistance test inherently requires a “towed” model configuration, described herein, as a model which is fixed-in-surge. Ideally, it is also fixed-in-sway, and -yaw while it is free-to-heave, -roll, and -pitch as configured throughout this testing.

Propulsion tests however, require a self-propelled model. The amount of propulsion applied to the model describes the type of propulsion test and directly impacts the accuracy of a full-scale powering prediction. Ideally, self-propulsion tests are conducted with the propulsor operating at the ship propulsion point where the model is slightly under-propelled. The additional force required to maintain the desired speed is applied to the model through the external tow force. This technique is used to ensure that the propulsion performance is sealed properly by maintaining the proper thrust loading on the propulsion system. This requirement is due to the larger coefficient of friction on the model due to the lower Reynolds number since speed is sealed by Froude number. During this series of work, tests were conducted in the former manner described herein as a “fixed-in-surge” powering test at the ship propulsion point.

Additionally, a propulsion test was conducted where the propulsor operated at the model self-propulsion point. At the model self-propulsion point the model is fully propelled without the assistance of an external tow force. This permits the model to be uncoupled from the tow carriage and freely progress into a wave system resulting in a surging motion (fluctuating speed). Within the context of this report, this model/test configuration is referred to as a “free-to-surge” powering test at the model self-propulsion point.

This series of tests provides sufficient information to illustrate the influence of propelling the restrained model and the freedom to surge on the measured motions and accelerations. However, the impact on ship motions and accelerations due to the additional thrust required at the model self-propulsion-point cannot be determined from these tests. It is expected that the small additional thrust wouldn't result in measurable differences in motions or accelerations.

## MODEL BALLASTING

The model without ballast was inclined and swung from a pivot to determine the center of gravity and mass moments of inertia of the empty hull. The desired center of gravity and mass moments of inertia were attained by calculation and precise placement of ballast weights in the empty hull. The total model weight came from scaling the provided ship displacement in the hydrostatic tables, compensating for the differences in salt and fresh water properties. The results and the coordinate/schematic of the forces are presented in Table - 1. The vertical- and longitudinal-center of gravity was matched within 1.4% while pitch- and yaw-gyradii were matched within 1.1%. These values were accepted as measured and used as an initial value of VCG. The model was subsequently inclined in water to measure the metacntric height, GM<sub>t</sub>. Inclining in water revealed that it was not necessary to readjust the ballast weights to match desired GM<sub>t</sub>. See Table - 1 for a comparison of desired and attained mass properties used during the testing.

Additional influence on the ballast condition is illustrated in Table - 2 for the free-to-surge model condition. The mass properties are affected during this test due to the model attachment technique. Since the influence of longitudinal motion was desired, the model was allowed to surge resulting in a varying location of the tow-gear weight. The tow gear was attached to the carriage while the model surged fore and aft, relative to the carriage in the oncoming wave field. Therefore the weight of the tow-gear supported by the model moved fore and aft relative to the model. Surging forward thus caused the LCG of the model to shift aft and vice versa. The resulting influence on the model mass properties is presented in Table - 2.

Table - 1. Desired & Achieved Mass Properties for Design Displacement

**Fully Rigged Model Hull @ Design Displ. - w/ attached tow posts**

Model Scale:	34.121	Full-Scale	MODEL	JHSS- Model 5653-3
Gravity, g	32.155 in. <sup>2</sup>			
P-SW,15C	64 lbs/in <sup>3</sup>			
P-FW,20C	62.4 lbs/in <sup>3</sup>			
Desired Parameters	(in)	Desired (in.)	Achieved (in.)	%Difference
Length (LOA)	97.75	94.93	-	-
Length (LBP)	960.5	334.3	-	-
Beam (BPX)	105	36.93	-	-
Beam (BWL)	105	36.93	-	-
Draft (avg)	28.02	10.14	-	-
Displacement (Lbs/in.)	36490.36	2006	2000	-0.30%
LCG, + aft of STN 0	476.22	167.48	168.48	0.60%
LCG, + fwd of STN 10	-0.97	-0.34	-1.34	-
TOG, port of CL	0	0	0.14	1.39%
VCG, above keel	47.11	16.57	16.80	3.59%
VCG, above waterline	18.23	6.43	6.66	3.59%
Pitch gyrodius (about cg)	232.45	81.75	82.38	0.77%
Roll gyrodius (about cg)	40.39	14.20	UNKNOWN	UNKNOWN
Yaw gyrodius (about cg)	232.34	81.71	82.57	1.05%
SECTION 11.5 (10' / 14 INCHES TWO DECK) (1000000000)				

Table - 2. Influence of Surging Tow-Post Weight on Model Mass Properties

FWD blockgauge stack = 66.46Lbs @ 37.375" FWD of LCG	
AFT blockgauge stack = 52.79Lbs @ 118.00" AFT of LCG	
MODEL DIRECTION	SURGE (IN)
STATIONARY	0.0
BACK	+8.20
FORWARD	-8.20
LCG FWD AP (IN)	%
168.48	—
167.99	-0.29%
168.97	0.29%
I <sub>xx</sub> (IN)	%
82.38	—
82.35	-0.04%
82.41	0.04%

## ROLL DECAY DATA-REDUCTION METHOD

The roll decay tests performed on the JHSS model 5653-3 with and without bilge keels appended were analyzed using a Levenberg-Marquardt algorithm to obtain the least-squares fit to the following equation.

$$(1) \quad \Theta = \Theta_0 * \exp^{-t/\tau} \sin(\omega t + \varphi) + b$$

Where:  
 $\Theta_0$  = initial maximum roll angle (normalized to 1)  
 $\tau$  = decay constant  
 $b$  = mean roll angle  
 $\omega$  = angular roll rate  
 $\varphi$  = initial roll phase angle

Resulting roll decay data in Table - 3 represents the average decay coefficients from multiple repeat tests for each test condition. The presented graphs in Figure - 1 are single selected tests to illustrate the effect of the “with” and “without” bilge keel conditions.

The effect of the bilge keels is visible in Figure - 1. The curve fits of the roll decay time history data are presented for both with and without bilge keels. The roll amplitudes have been normalized by the maximum initial amplitude. Additionally, curves of the exponential decay of the roll amplitudes are shown. It is obvious that with the bilge keels installed the roll amplitudes reduce much more rapidly.

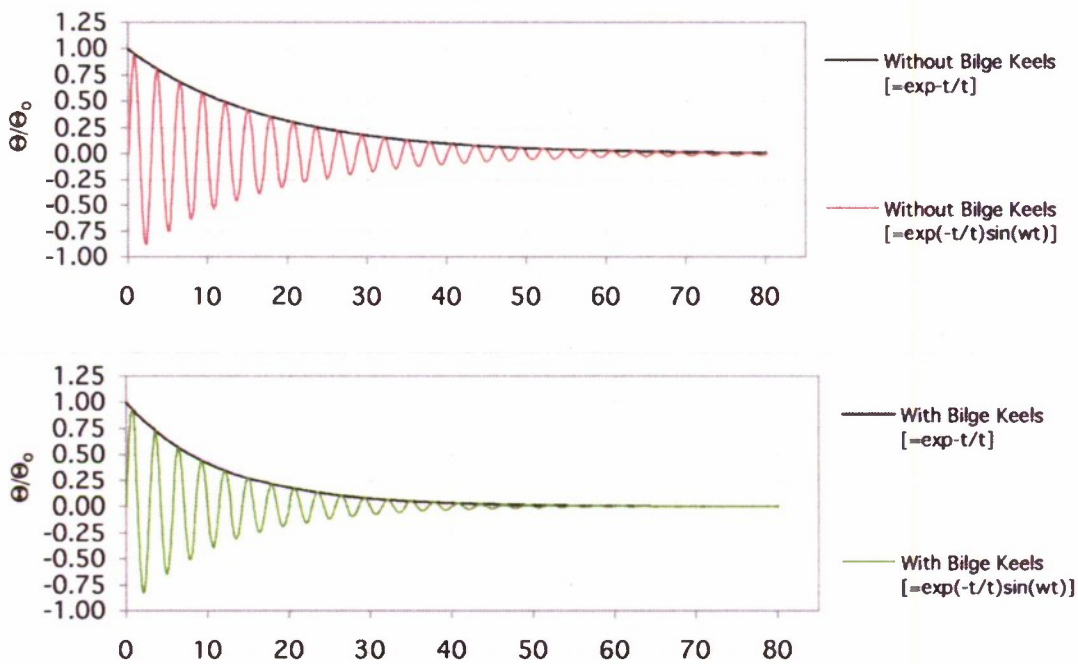


Figure - 1. Roll Decays Illustrating “With” and “Without” Bilge Keels

**Table - 3. Averaged Least-Squares-Fit Ship-Scale Roll Decay Coefficients**

Hull Appendage Condition	Roll Decay Constants				
	$\tau$ (RAD/SEC)	$\omega$ (RAD/SEC)	$\tau/\omega$	$T_{ROLL}$ (SEC)	$T_{ROLL<1\%}$ (SEC)
Without Bilge Keel	17.386	2.200	7.902	2.856	80.2
With Bilge Keel	11.574	2.220	5.213	2.830	53.4
% of "Without"	66.6%	100.9%	66.0%	99.1%	66.6%

In fact, Table -3 shows a reduced decay constant of 66.6% for the condition “with” bilge keels. This results in a 33.4% shorter duration of a roll event decaying to within 1% of the initial amplitude. The roll rate and period remain identical between the two tested conditions and are also presented in Table – 3.

#### **MOTIONS & ACCELERATION DATA-REDUCTION**

Test engineers converted the raw data to engineering units and concatenated all the runs for a given test speed. Atypical spikes and anomalous data were removed from the data files. Odd behavior near the beginning or end of any run was suspect and removed. It must be noted, however, that the removal of data is a somewhat subjective process.

Test engineers processed the edited files to find the basic statistics of the data; maximums, minimums, means, and standard deviations. Significant single amplitude responses (SSA) are also computed for the identification of seakeeping motion characteristics. This is taken to be the average of the 1/3 highest recorded maxima. Mathematically, for a *narrow-band* spectrum this is defined as 2.0 times the standard deviation of the variable.

The results of the Added Resistance test (#56) are presented as a baseline for the motions and acceleration data. The Significant single amplitudes are illustrated in Figure - 2 and Figure - 3 and the spectral analysis of the accelerations for 36 knots is presented in Figure – 4 as an example.

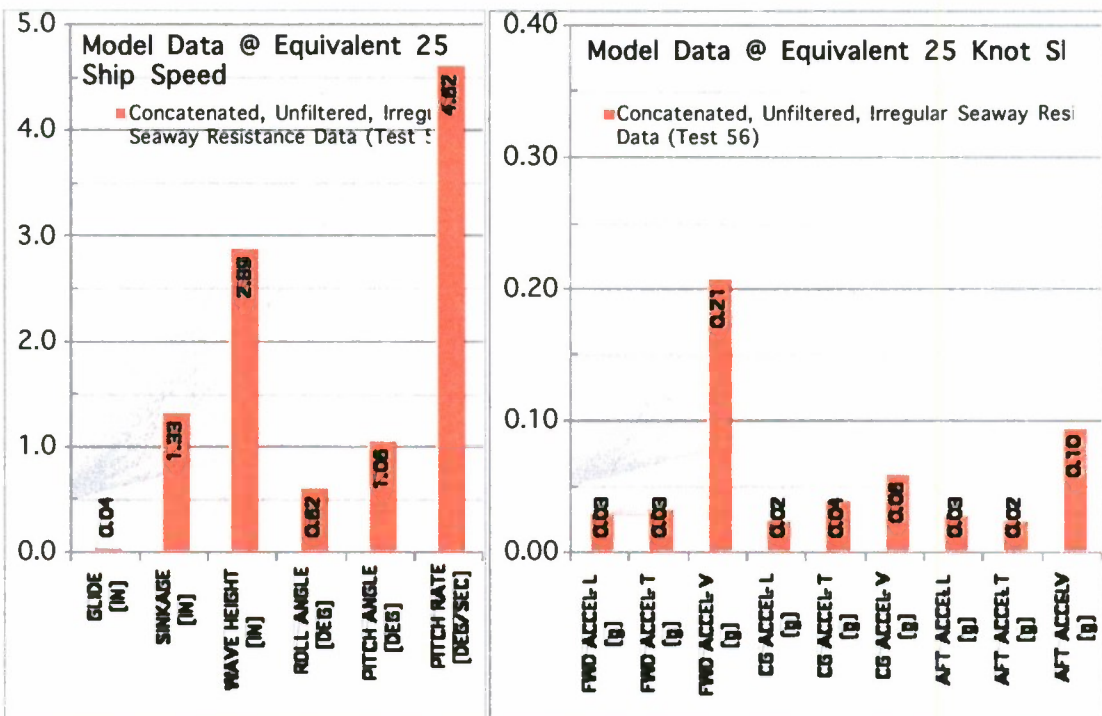


Figure - 2. Motions and Acceleration SSA Data for the Unpropelled, Fixed-in-surge Resistance Test #56, 25 knots

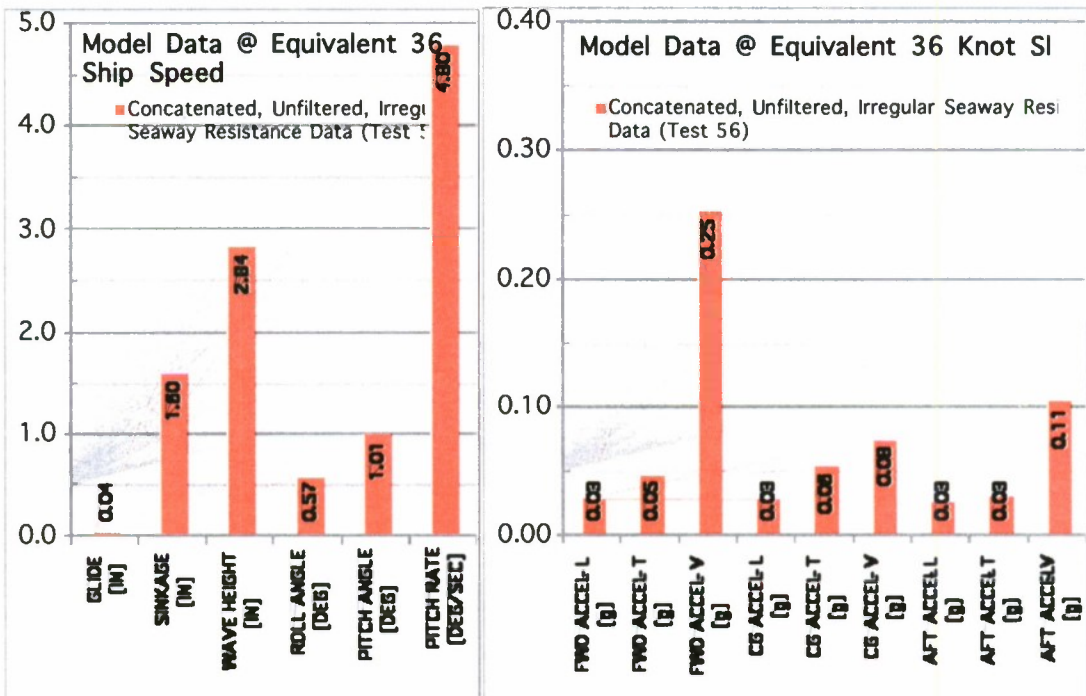
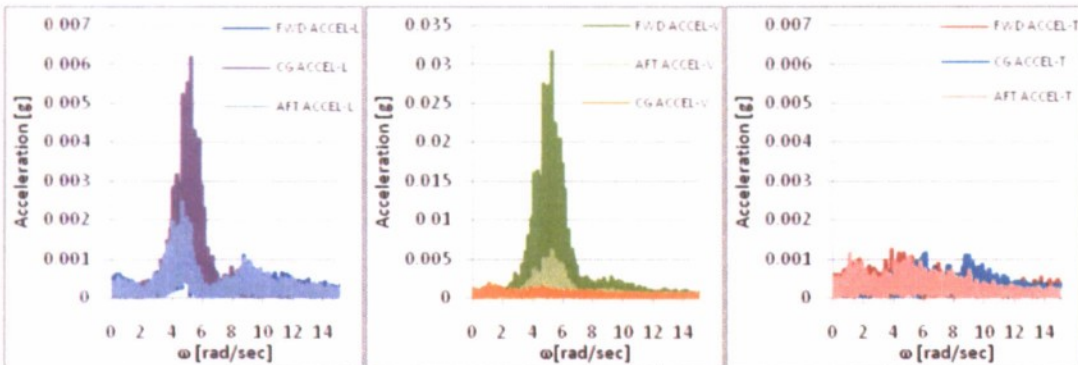


Figure - 3. Motions and Acceleration SSA Data for the Unpropelled, Fixed-in-surge Resistance Test #56, 36 knots



**Figure - 4. Spectral Analysis Plots for the Unpropelled, Fixed-in-surge Resistance Test #56, 36 knots**

The results of the spectral analysis show that most of the energy is contained within the frequency range of the sea state.

After analysis of the resulting acceleration data from the propulsion tests, it was found that the results were affected by electronic noise (later determined to be emanating from the drive motors). Spectral analysis revealed that broad-range noise existed throughout all of the acceleration data. The resulting influence can be seen in Figure - 5 from data collected during the calm-water powering test. To illustrate the magnitude of the broad range spectral energy caused by the propulsion motor, the axes were sealed the same as Figure - 4.

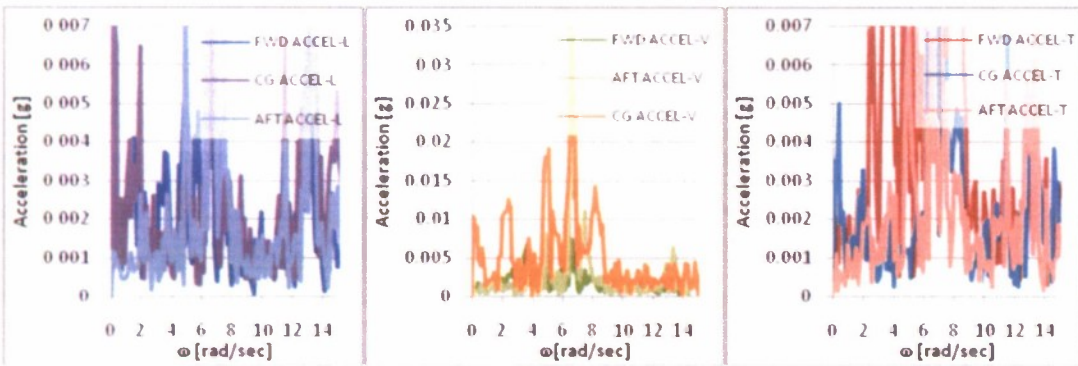


**Figure - 5. Spectral Analysis Plots for the Calm-Water, Fixed-in-surge Powering Test #54, 36 knots**

The resulting influence from the propulsion motor reveals values much larger in comparison to the results from the added resistance test in sea state six where the propulsion motor was not active. Further investigation revealed that the propulsion motor ground was disabled causing large amounts of electromotive force which interfered with the accelerometers. Unfortunately, even filtering the accelerometer data could not recover any valuable results. With great disappointment, we must say that it is not possible to make valid conclusions about the accelerations during any propulsion tests.

The resulting statistical data for the motions are however, valid data sets and are compared for the propelled and unpropelled test data and the fixed- and free-to-surge towing configurations at both speeds. The comparisons are illustrated in Figure - 6 through Figure - 15 with quantitative data presented in Table - 4 through Table - 6. The two different speeds, 25 and 36 knots are presented side-by-side.

Figure - 6 and Figure - 7 illustrate, for a model that is fixed-in-surge, the comparison between an unpropelled condition and one that is propelled for speeds 25 Knots and 36 Knots, respectively. It is apparent that the motions are damped by the addition of propulsion thrust. However, the wave heights during the propelled test are also slightly lower. These results indicate that there is no appreciable influence by the addition of propulsion thrust.

Figure - 8 and Figure - 9 illustrate, for a propelled model, the effect that the free-to-surge condition has on the measured motions as compared to those taken from a model that is fixed-in-surge. Again, the motions are not appreciably affected. The pitch rate does however, increase in the 36 knot condition when the model is free-to-surge even though the wave height is slightly lower.

The presented data illustrates that the motions of a model are not significantly influenced by propulsion thrust or the ability to surge longitudinally. Even though the data reveals that the motions are not appreciably affected, it is expected that the acceleration data would be influenced, most noticeably in the longitudinal accelerations.

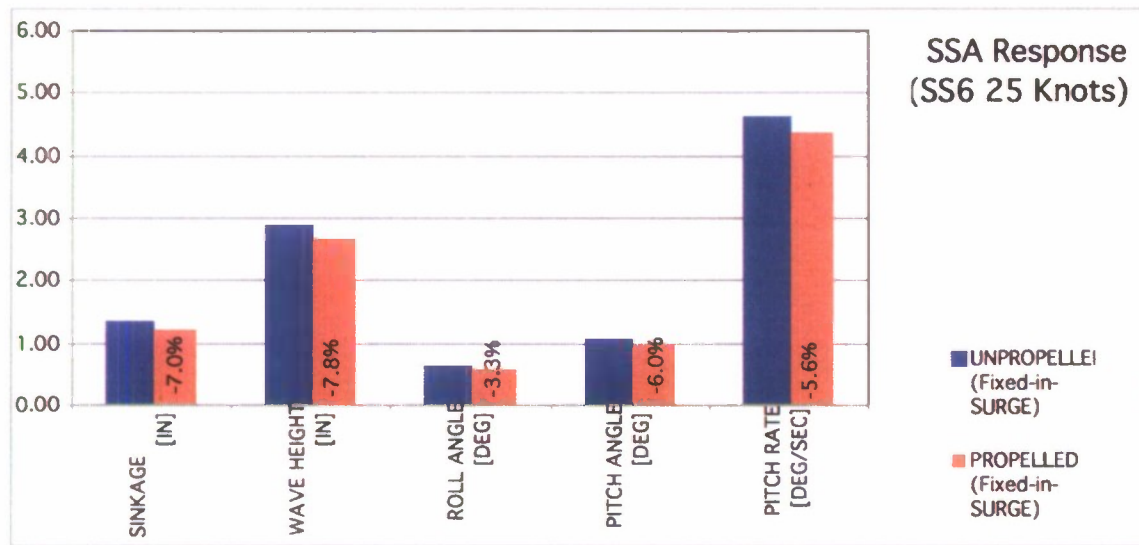


Figure - 6. Propulsion Influence on Motions @ 25 Knots

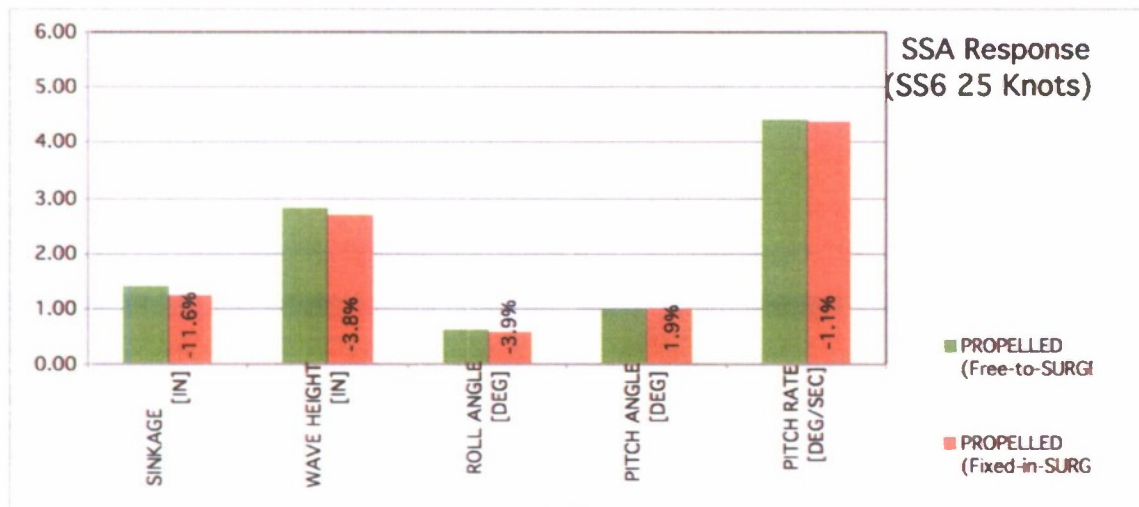


Figure - 7. Surging Influence on Motions @ 25 Knots

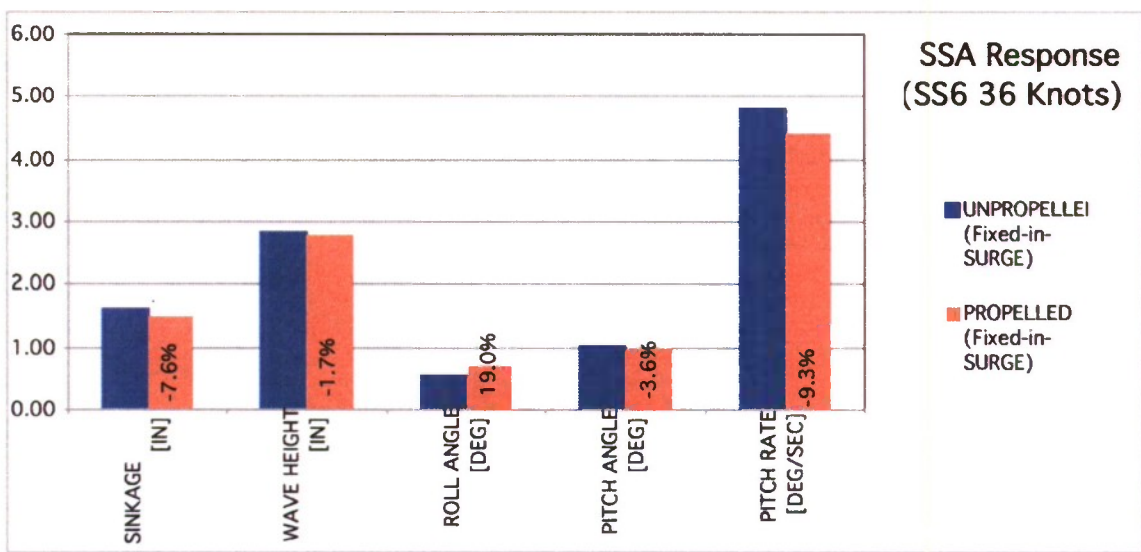


Figure - 8. Propulsion Influence on Motions @ 36 Knots

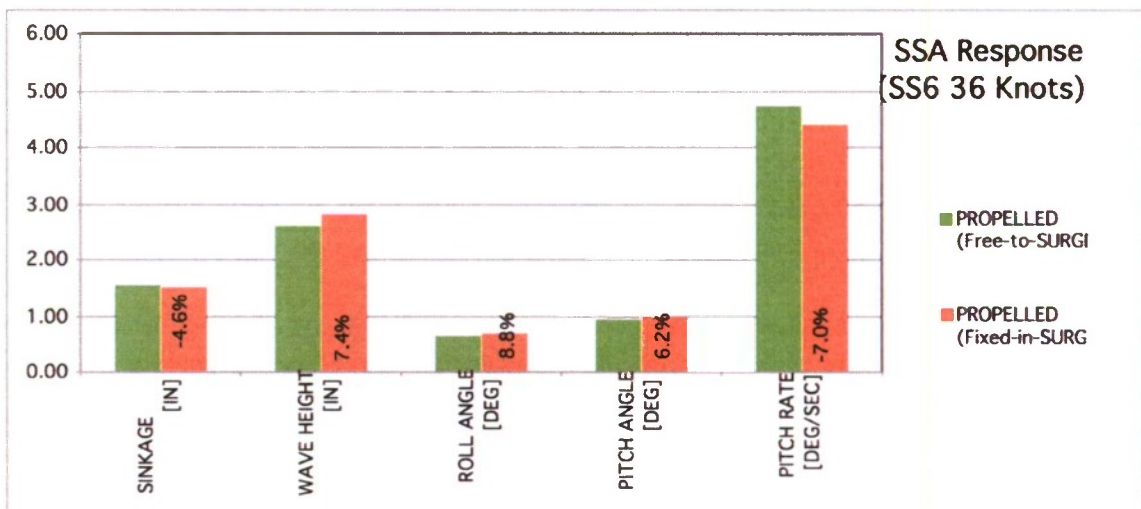


Figure - 9. Surging Influence on Motions @ 36 Knots

Table - 4. Test #56 (Unpropelled, Fixed-in-Surge) Concatenated Data Results

VARIABLE	25 KNOTS				36 KNOTS				SIG. SINGLE AMPL.	SIG. SINGLE AMPL.
	AVERAGE	STANDARD DEV	MAXIMUM	MINIMUM	AVERAGE	STANDARD DEV	MAXIMUM	MINIMUM		
MODEL SPEED	4.29	0.00	4.30	4.16	0.01	6.17	0.04	6.19	4.94	0.09
SURGE	0.000	0.000	0.000	0.000	0.000	0.000	0.000	0.000	0.000	0.000
SINKAGE	0.350	0.635	2.546	-1.748	1.270	0.774	0.806	3.264	-1.726	1.612
WAVE HEIGHT	0.011	1.410	4.834	-5.943	2.819	0.011	1.454	5.191	-5.845	2.908
ROLL ANGLE	0.09	0.31	1.28	-1.15	0.62	0.15	0.29	1.10	-0.88	0.57
PITCH ANGLE	-0.28	0.51	1.56	-2.16	1.02	-0.57	0.51	1.14	-2.30	1.01
PITCH RATE	0.0221	2.1916	8.1767	-7.4401	4.3831	0.0330	2.4132	7.3664	-8.3240	4.8264
FWD ACCEL-L	-0.003	0.015	0.049	-0.067	0.029	-0.008	0.015	0.068	-0.081	0.030
CG ACCEL-L	-0.005	0.012	0.063	-0.074	0.025	-0.007	0.015	0.172	-0.280	0.029
AFT ACCEL-L	-0.003	0.014	0.048	-0.070	0.028	-0.006	0.014	0.054	-0.090	0.028
FWD ACCEL-T	0.003	0.016	0.181	-0.149	0.032	0.005	0.023	0.593	-0.573	0.047
CG ACCEL-T	0.000	0.020	0.091	-0.086	0.039	0.000	0.028	0.181	-0.184	0.056
AFT ACCEL-T	0.003	0.012	0.081	-0.077	0.024	0.005	0.016	0.290	-0.236	0.032
FWD ACCEL-V	-0.999	0.098	-0.613	-1.322	0.197	-1.000	0.127	-0.549	-1.380	0.255
CG ACCEL-V	-1.011	0.030	-0.800	-1.219	0.060	-1.010	0.038	-0.275	-1.571	0.076
AFT ACCEL-V	-1.001	0.045	-0.820	-1.193	0.091	-1.000	0.053	-0.809	-1.190	0.106

Table - 5. Test #57 (Propelled, Fixed-in-Surge) Concatenated Data Results

VARIABLE	25 KNOTS						36 KNOTS					
	AVERAGE	STANDA RD DEV	MAXIMU M	MINIMU M	SIG. SINGLE AMPL.	AVERAG E	STANDA RD DEV	MAXIMU M	MINIMU M	SIG. SINGLE AMPL.		
MODEL SPEED	4.30	0.00	4.31	4.28	0.01	6.18	0.02	6.19	5.67	0.04		
SURGE	0.000	0.000	0.000	0.000	0.000	0.000	0.000	0.000	0.000	0.000		
SINKAGE	0.289	0.621	2.448	-1.944	1.243	0.728	0.749	3.048	-1.908	1.498		
WAVE HEIGHT	-0.050	1.374	4.774	-5.559	2.748	-0.048	1.410	5.502	-5.747	2.820		
ROLL ANGLE	0.18	0.30	1.45	-1.14	0.60	0.22	0.35	1.41	-1.08	0.71		
PITCH ANGLE	-0.32	0.50	1.49	-2.22	1.00	-0.70	0.49	1.12	-2.28	0.98		
PITCH RATE	0.1002	2.1873	9.1343	-8.4714	4.3746	0.1285	2.2088	7.5874	-7.6611	4.4175		

Table - 6. Test #58 (Propelled, Free-to-Surge) Concatenated Data Results

VARIABLE	25 KNOTS						36 KNOTS					
	AVERAGE	STANDA RD DEV	MAXIMU M	MINIMU M	SIG. SINGLE AMPL.	AVERAG E	STANDA RD DEV	MAXIMU M	MINIMU M	SIG. SINGLE AMPL.		
MODEL SPEED	4.29	0.01	4.31	4.17	0.01	6.18	0.01	6.20	5.86	0.02		
SURGE	2.558	4.057	12.408	-8.356	8.114	-0.523	4.109	8.694	-11.132	8.218		
SINKAGE	0.517	0.703	3.280	-1.866	1.406	0.938	0.785	3.584	-1.930	1.570		
WAVE HEIGHT	-0.012	1.413	5.163	-5.783	2.827	-0.023	1.414	5.586	-5.259	2.828		
ROLL ANGLE	0.19	0.31	1.27	-1.09	0.62	0.46	0.32	1.52	-0.62	0.65		
PITCH ANGLE	-0.07	0.49	1.56	-1.76	0.98	-0.08	0.46	1.70	-1.79	0.92		
PITCH RATE	0.0089	2.2110	7.6611	-6.7034	4.4219	0.0347	2.3747	9.1343	-9.2817	4.7493		

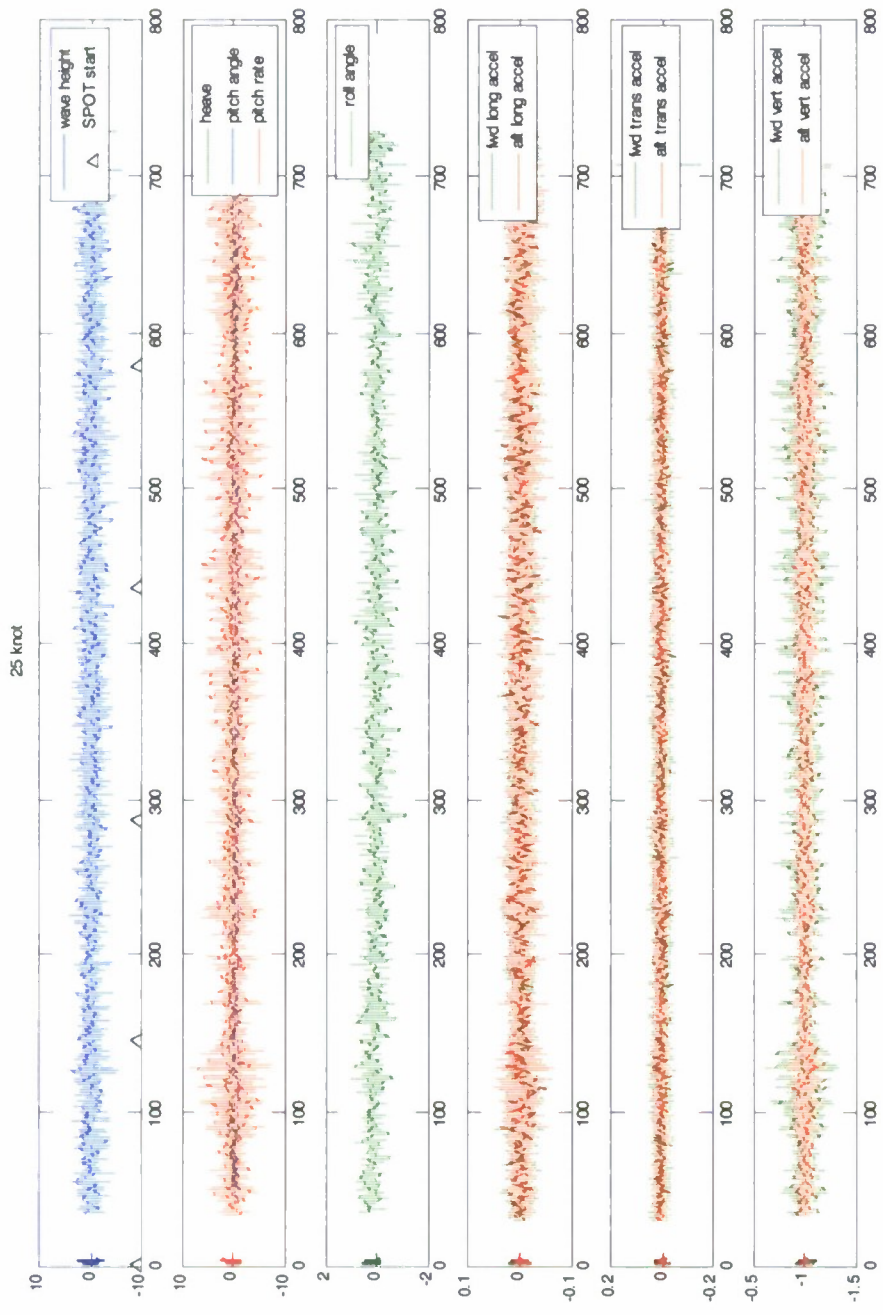


Figure – 10. Test #56 (Unpropelled, Fixed-in-Surge) Concatenated SS6 Time History Data, 25 Knots

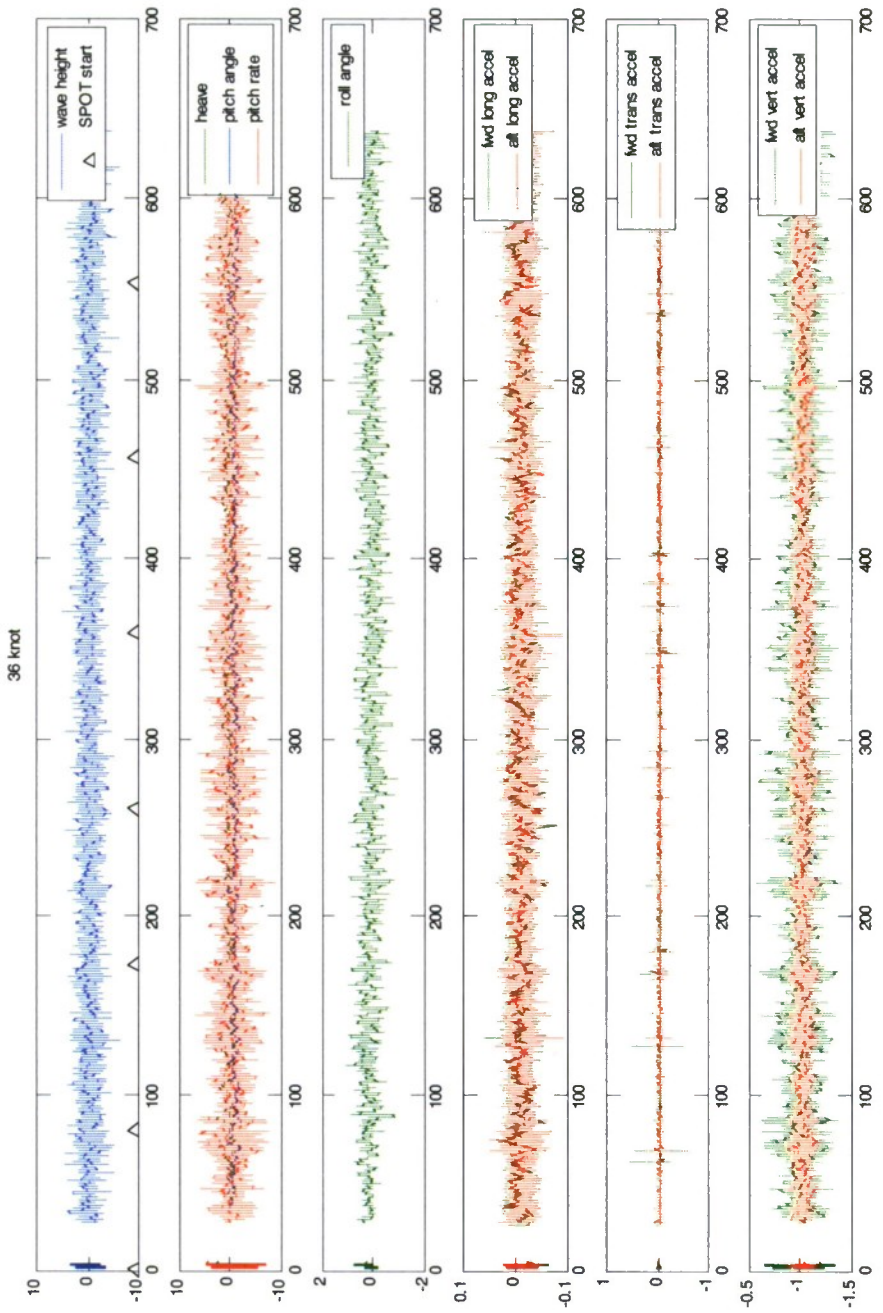


Figure - 11. Test #56 (Unpropelled, Fixed-in-Surge) Concatenated SS6 Time History Data, 36 Knots

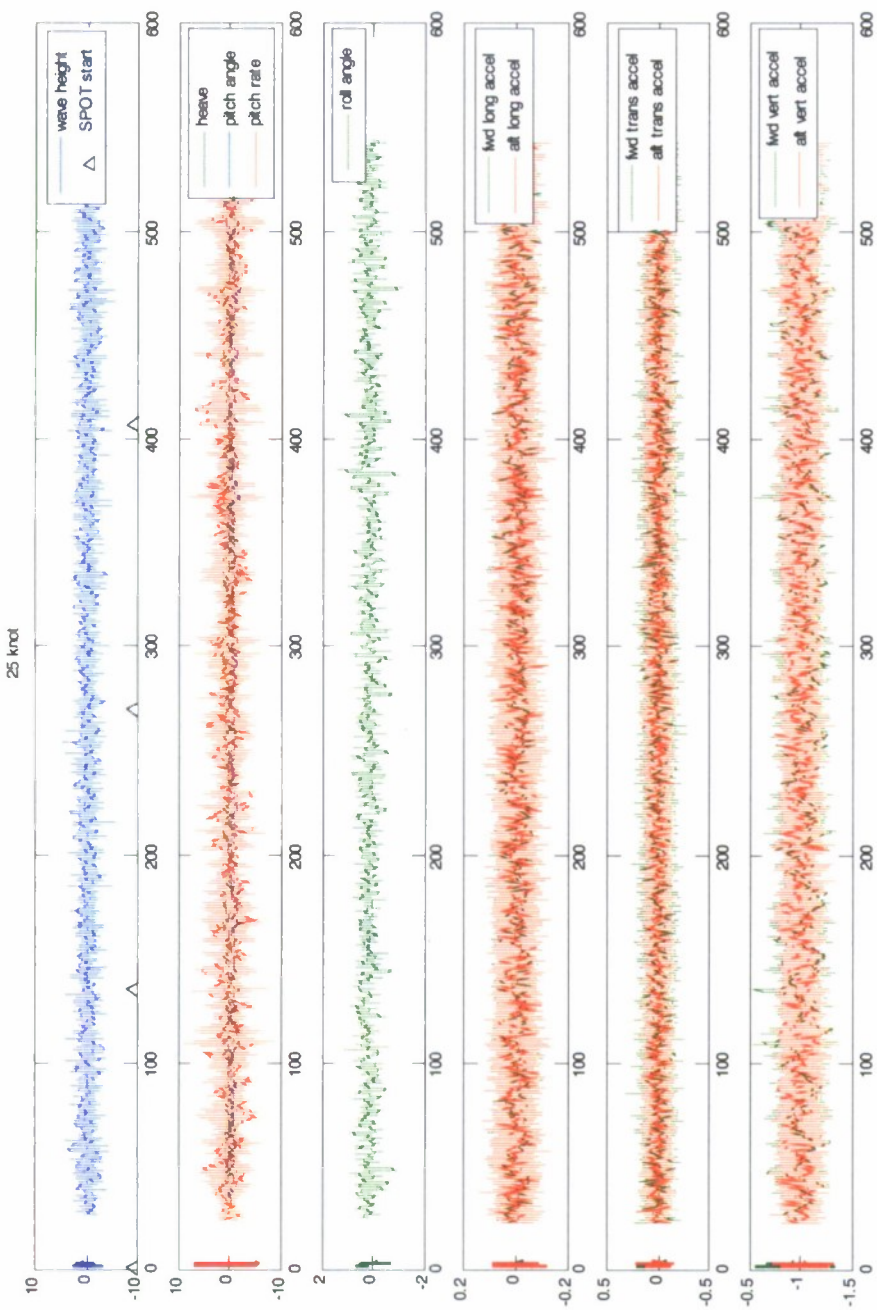


Figure - 12. Test #57 (Propelled, Fixed-in-Surge) Concatenated SS6 Time History Data, 25 Knots

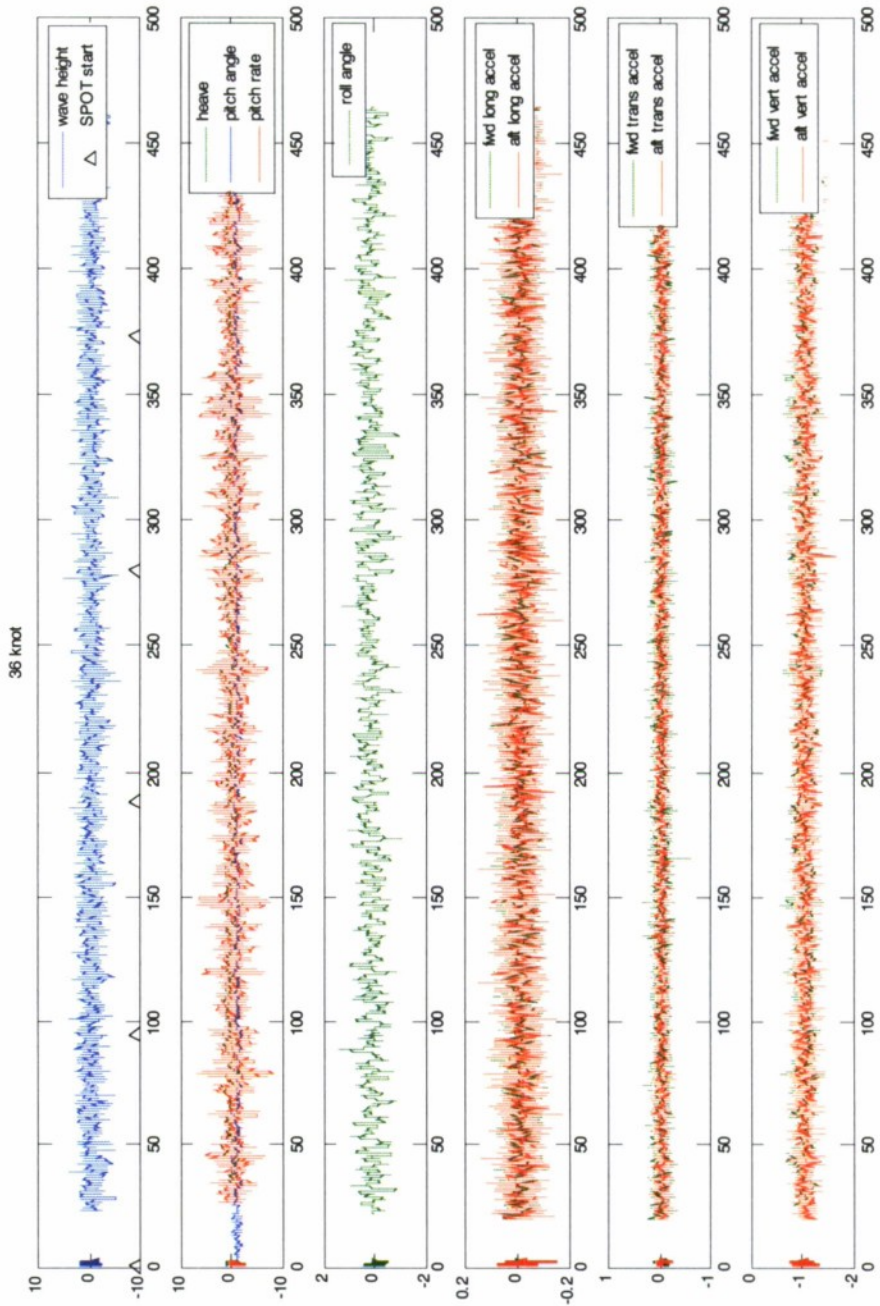


Figure - 13. Test #57 (Propelled, Fixed-in-Surge) Concatenated SS6 Time History Data, 36 Knots

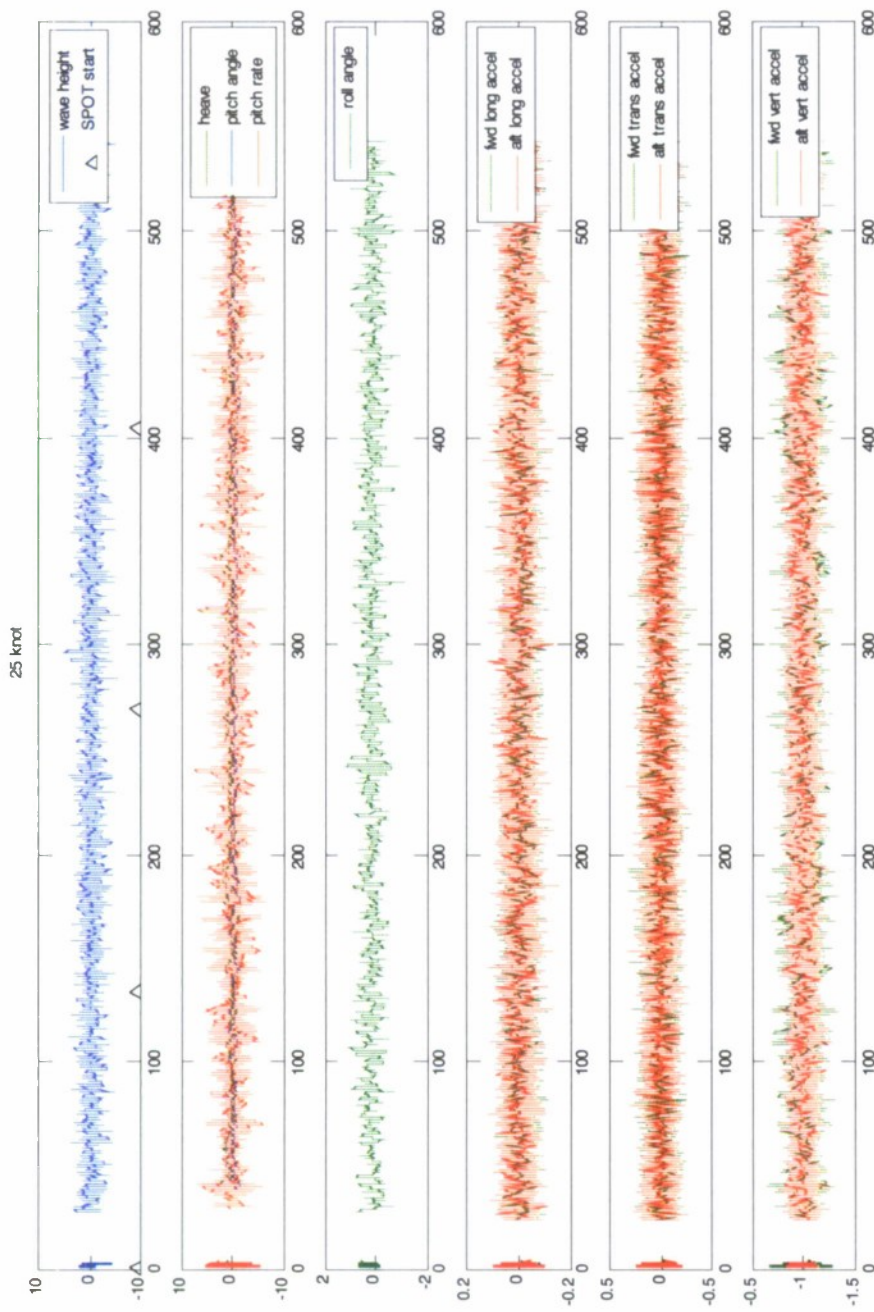


Figure - 14. Test #58 (Propelled, Free-to-Surge) Concatenated SS6 Time History Data, 25 Knots

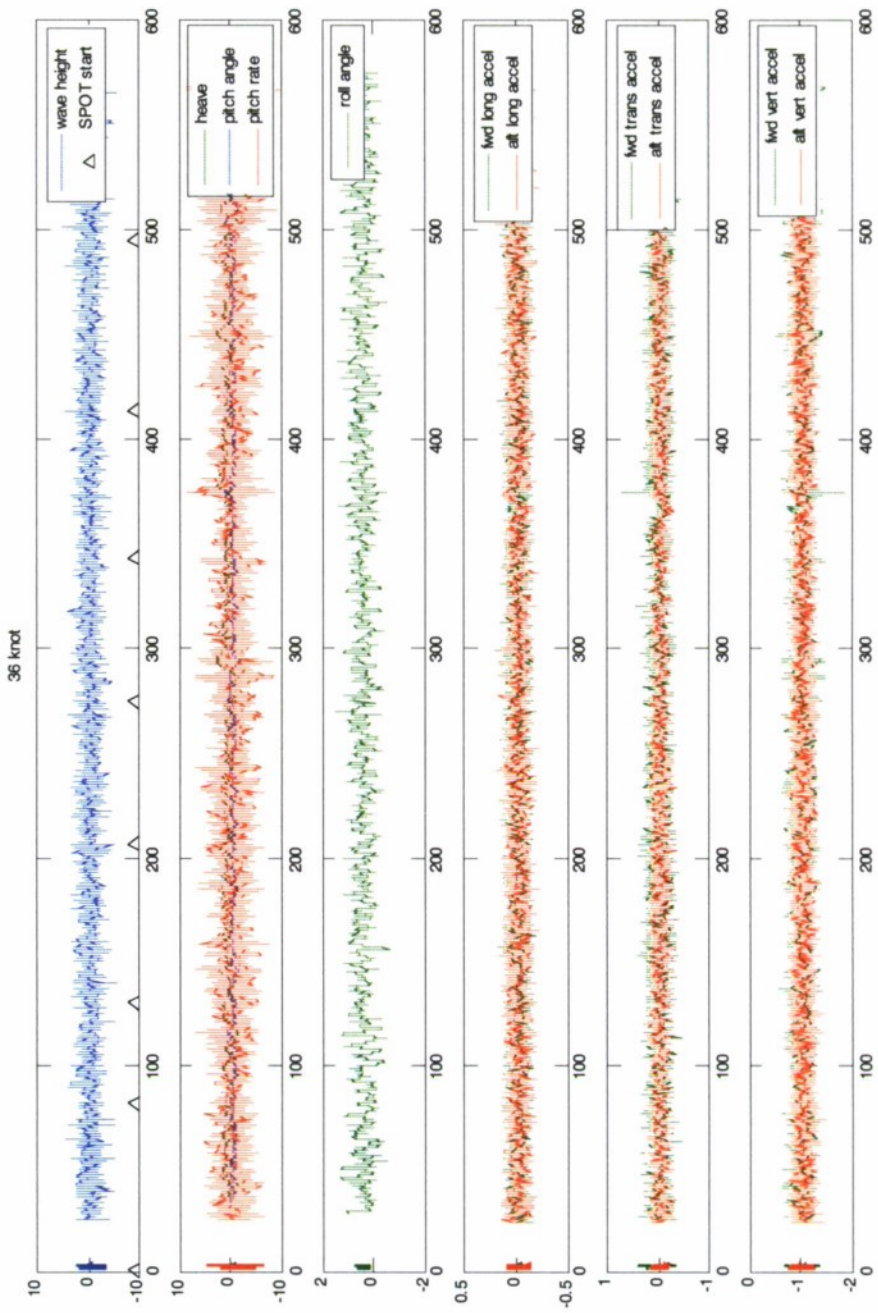


Figure - 15. Test #58 (Propelled, Free-to-Surge) Concatenated SS6 Time History Data, 36 Knots

**APPENDIX C**

**Measurement Report For Model 5653**

Ann Marie Powers  
Code 653

## Contents

<b>Overview .....</b>	<b>C3</b>
<i>Model 5653 Design Specifications</i>	
<i>Laser Tracker and Measurement</i>	
<i>Coordinate System</i>	
<b>Hull Surface Analysis .....</b>	<b>C5</b>
<i>Below the Waterline: Areas out of tolerance</i>	
<i>Entire Model: Areas out of tolerance</i>	
<i>General Color Plots</i>	
<i>Removable Bow Dome</i>	
<i>Transom</i>	
<i>Positive and Negative Regions</i>	
<b>Propeller Shaft Alignment .....</b>	<b>C12</b>
<i>Shaft Vectors</i>	
<i>Shaft Position</i>	
<b>Dropped Stool Angle .....</b>	<b>C17</b>
<b>Laser Tracker Calibration Certificate .....</b>	<b>C20</b>

## Overview

### **Model 5653 Design Specifications**

Station Spacing: 16.714 in

LBP = 334.280 in

Scale = 34.122

### **Laser Tracker and Measurement**

Ray Lerner and Ann Marie Powers used the Faro Xi Laser Tracker to measure Model 5653 for Dominic Cusanelli (227-7008) on Feb 20 – Feb 21, 2007. In order for the model to pass the construction criteria, 75% or more of the model surfaces must be within  $\pm 2$  mm of the design CAD file.

For Model 5653, Dominic requested that the best fit to CAD file be done using only the surfaces below the waterline. The following report contains color plots for these surfaces as well as color plots for the entire model in this same best fit position.

The Laser Tracker is calibrated yearly by the manufacturer and is traceable to NIST standards. The current calibration is valid through October 18, 2007. A copy of this certificate is provided in the Appendix.

The measurement data for Model 5653 is located in Insight file: Model5653 20Feb2007pm.SMX, and is available from Code 653. The data was compared to its CAD file (jhss 34.122 4 screw hull with gooseneck bulb and appendages.igs).

Figure C1 illustrates the 553,635 data points which are spread over the hull, rudders and skeg. The points on the hull and skeg are spaced every 0.5 in, while the points on the rudders are spaced every 0.01 in.

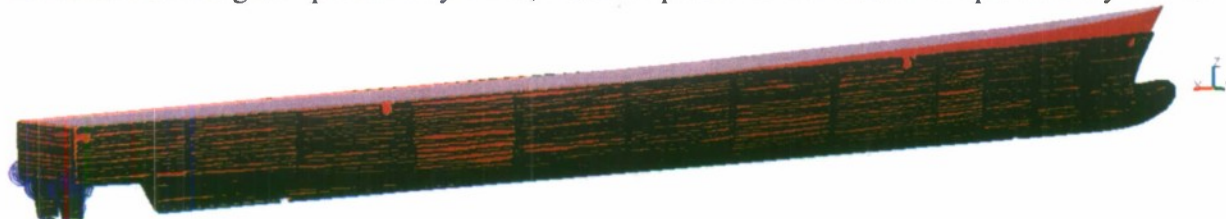


Figure C1. Model 5653 point cloud data superimposed on CAD surface.

Table C1 displays the summary statistics for the deviations from the measured point cloud data to the CAD surfaces. These maximum and average distances are measured along the normal vectors of the CAD surfaces. The absolute values of these distances are presented in the table.

Table C1. Data summary statistics.

	Absolute Value of Maximum (in)	Absolute Value of Average (in)	Standard Deviation (in)
Entire Hull	0.177	0.030	0.022
Under Waterline	0.177	0.029	0.022

### *Coordinate System*

The origin is located at the point where the forward perpendicular (FP) meets the waterline (Figure C2). The positive X-axis extends toward the stern of the model, and the positive y-axis extends toward the starboard side of the model. Therefore, the positive z-axis points aloft.



**Figure C2. Coordinate System on Model 5653**

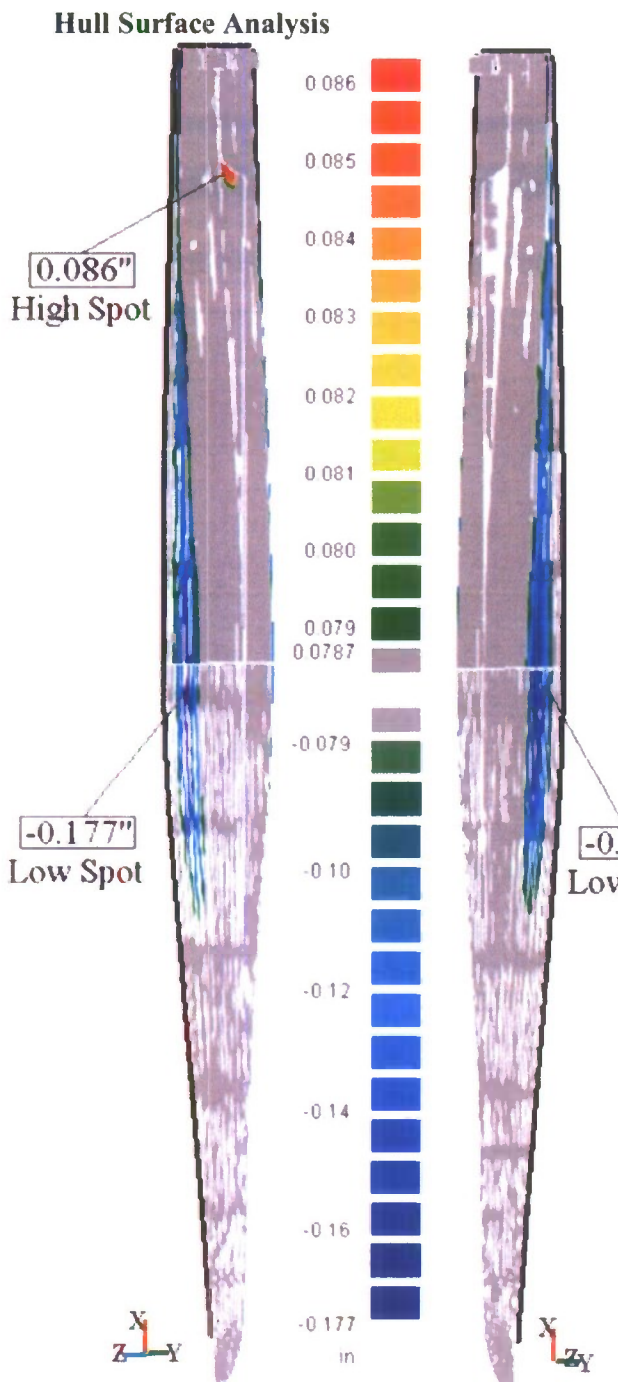


Figure C3. Oblique view of Port and Starboard regions out of 2mm tolerance

***Below the Waterline: Areas out of tolerance***

96.529% of the measured points below the waterline fall within  $\pm 2\text{mm}$  (0.0787 in) of the CAD file. The maximum positive deviation from the measured points to the CAD file is 0.086 in, while the maximum negative deviation is -0.177 in. The maximum deviation (-0.177 in) occurs in the outboard mid-ship region to the stern. This deviation, (shown as blue in Figure C3), indicates that this region of the model is too far amidships (in or toward the center of the boat). In other words, the blue regions are low spots. The maximum positive deviation (0.086 in) occurs on the port side of the skeg, in the aft region (shown in red). This means that the aft end of the skeg is skewed towards the port side of the model.

The gray regions are within the  $\pm 2\text{ mm}$  (0.0787 in) tolerance.

***Entire Model: Areas out of tolerance***

96.092% of all of the measured points ( $\sim 190,000$  points) on the model fall within  $\pm 2\text{mm}$  (0.0787 in) of the CAD file. Figure C4 shows that the maximum positive deviation (red) is 0.142 in, and occurs in two regions. One region is on the starboard hull above the waterline, near the bow. The other is on the aft port sidewall. This indicates that the model has too much material in these regions. The maximum negative deviation is -0.177 in, occurring amidships just under the waterline. This indicates that there is not enough material in those regions.

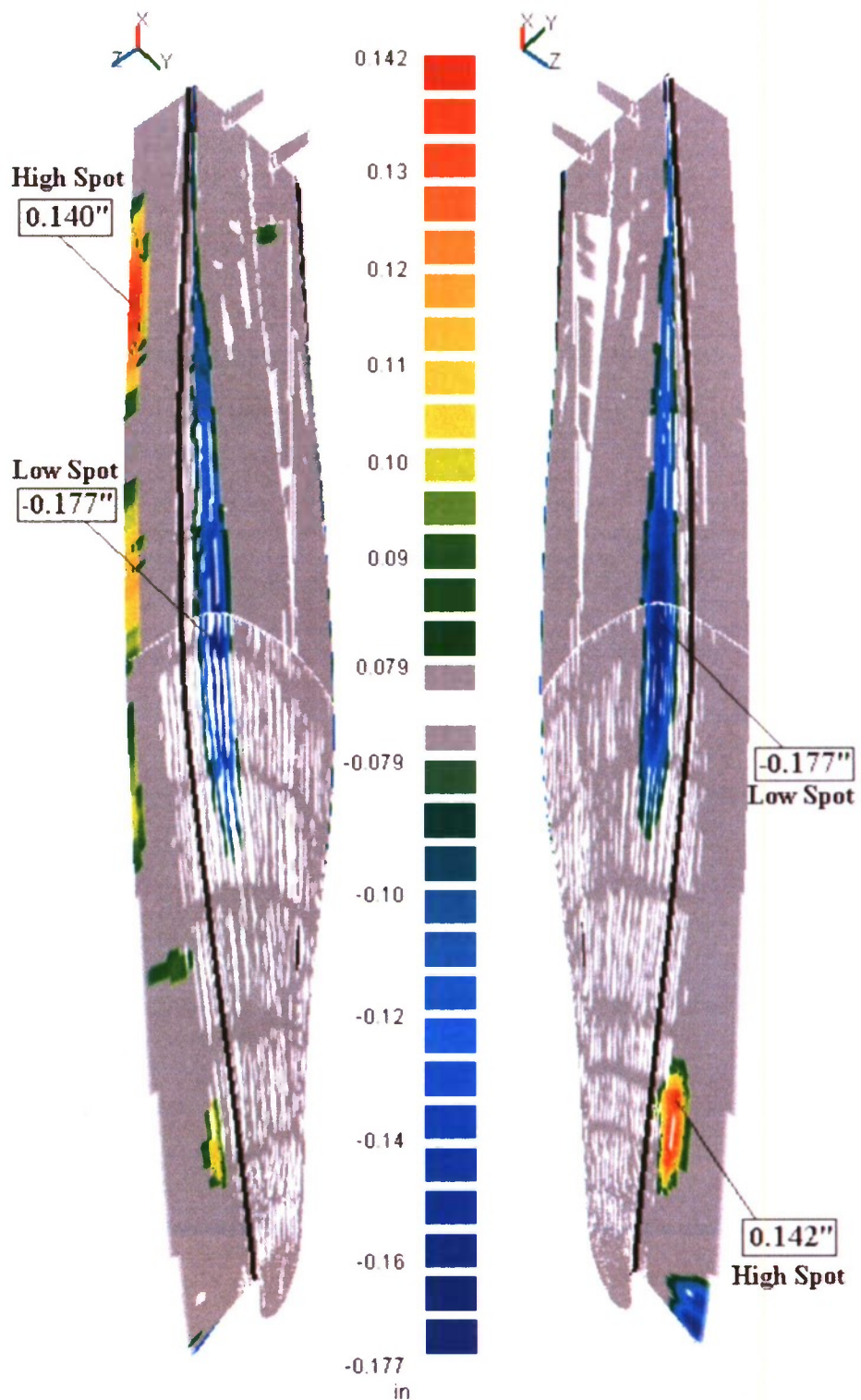


Figure C4. Oblique view of Port and Starboard regions out of 2mm tolerance

### General Color Plots

Figure C5 and Figure C6 illustrate the positive and negative deviations from the CAD file. Note that the positive values (red, yellow, and green) indicate the areas where the model has high spots, while the negative values (different shades of blues) indicate where the model has low spots.

Figure C6 has a zoomed in scale so that the localized deviations below the waterline can be seen more clearly.

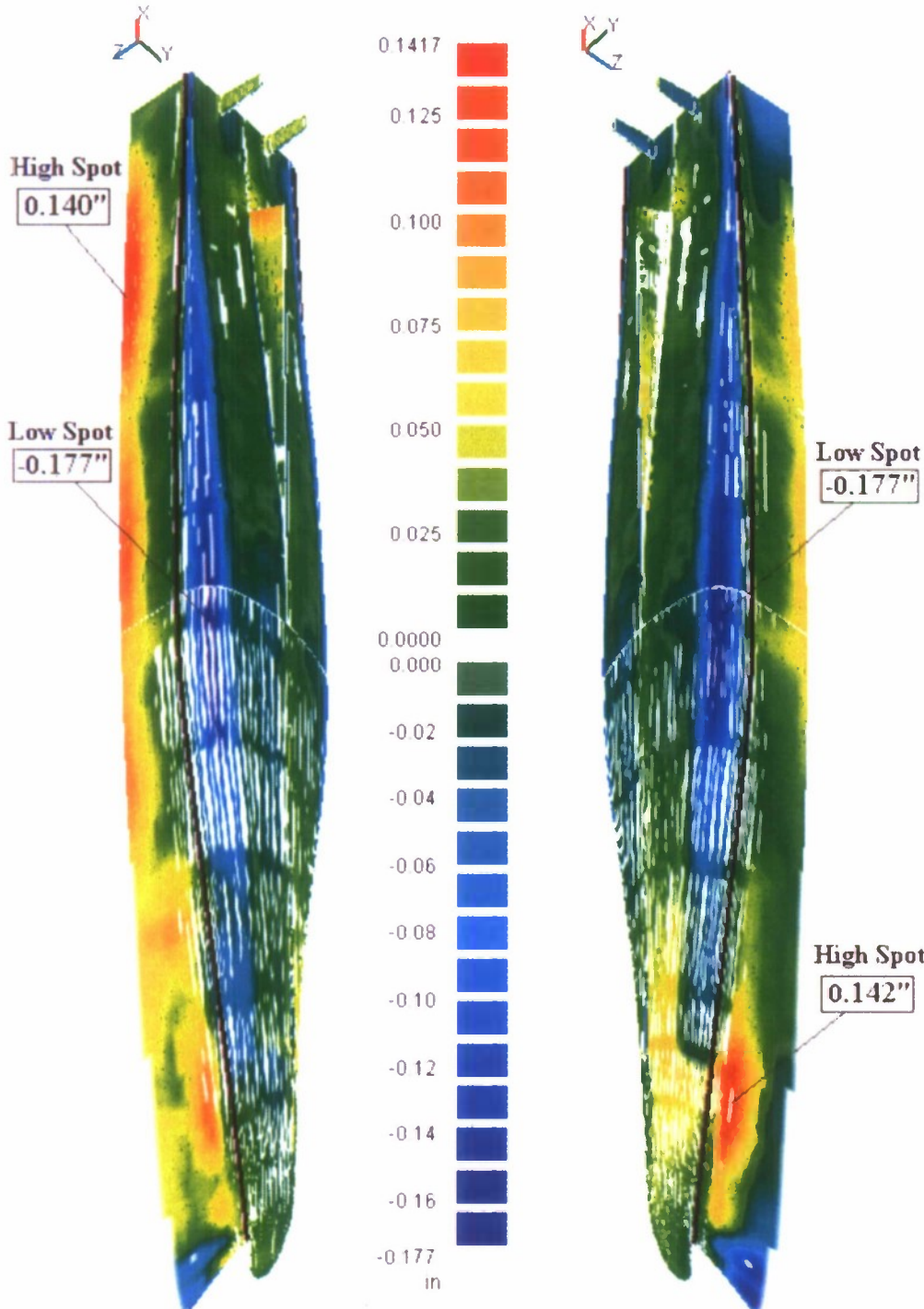


Figure C5. Oblique view Color Plots of Port and Starboard. Black line marks the waterline

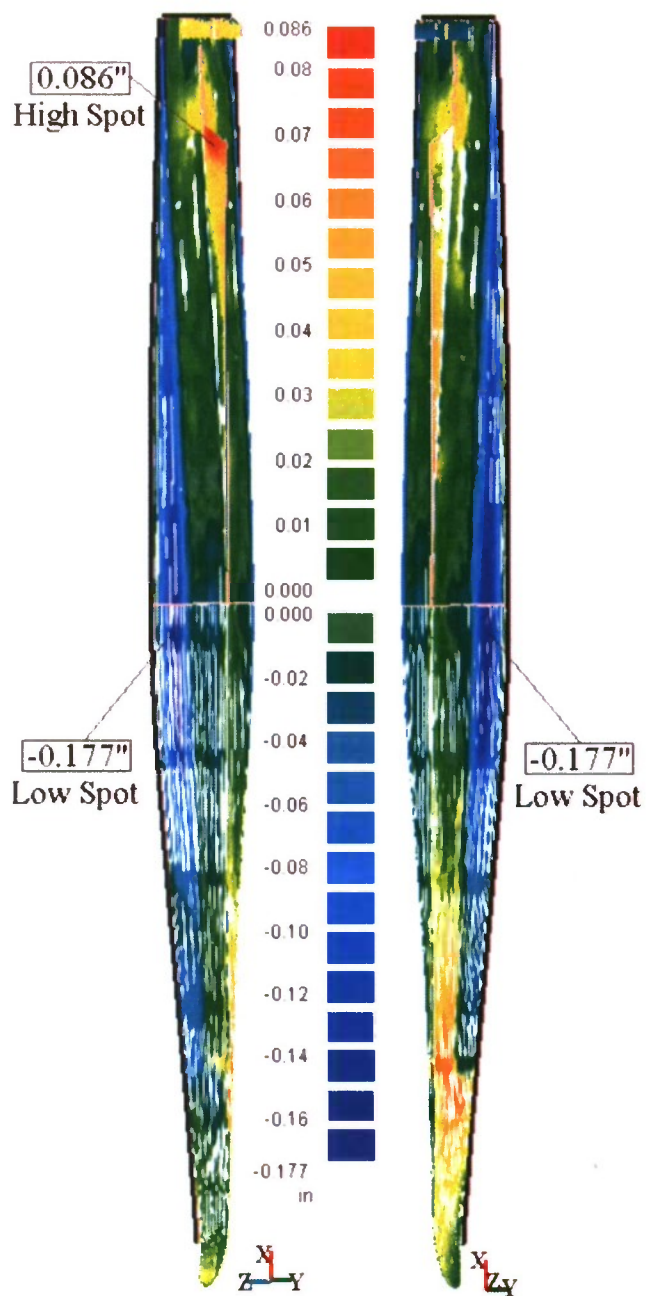


Figure C6. Oblique view Color Plot of Model below the waterline.

Note:

The measured data was translated and rotated into this “best fit” position so that the negative blue areas on each side of the hull would be symmetric. Based on this color plot, the rudders are placed about 0.030” too far to port.

Similarly, the skeg is skewed to port. It is important to realize that these offsets are a function of the “best fit” location. In other words, a fit could have been chosen which would position the rudders and the skeg in the correct location, however, there would no longer be symmetry on the sides of the hull.

### Removable Bow Dome

Of minor interest is the bow attachment illustrated in Figure C7. After the “best fit” position was chosen so that there would be symmetry along the sides of the hull, it is apparent that there is a slight shift to starboard in the position of the bow attachment. The fit-up of the removable bow dome contributes to the noticeable red and orange on the starboard side. Also, it is interesting to note the high spot (yellow) and low spot (green) pattern on the bow dome.

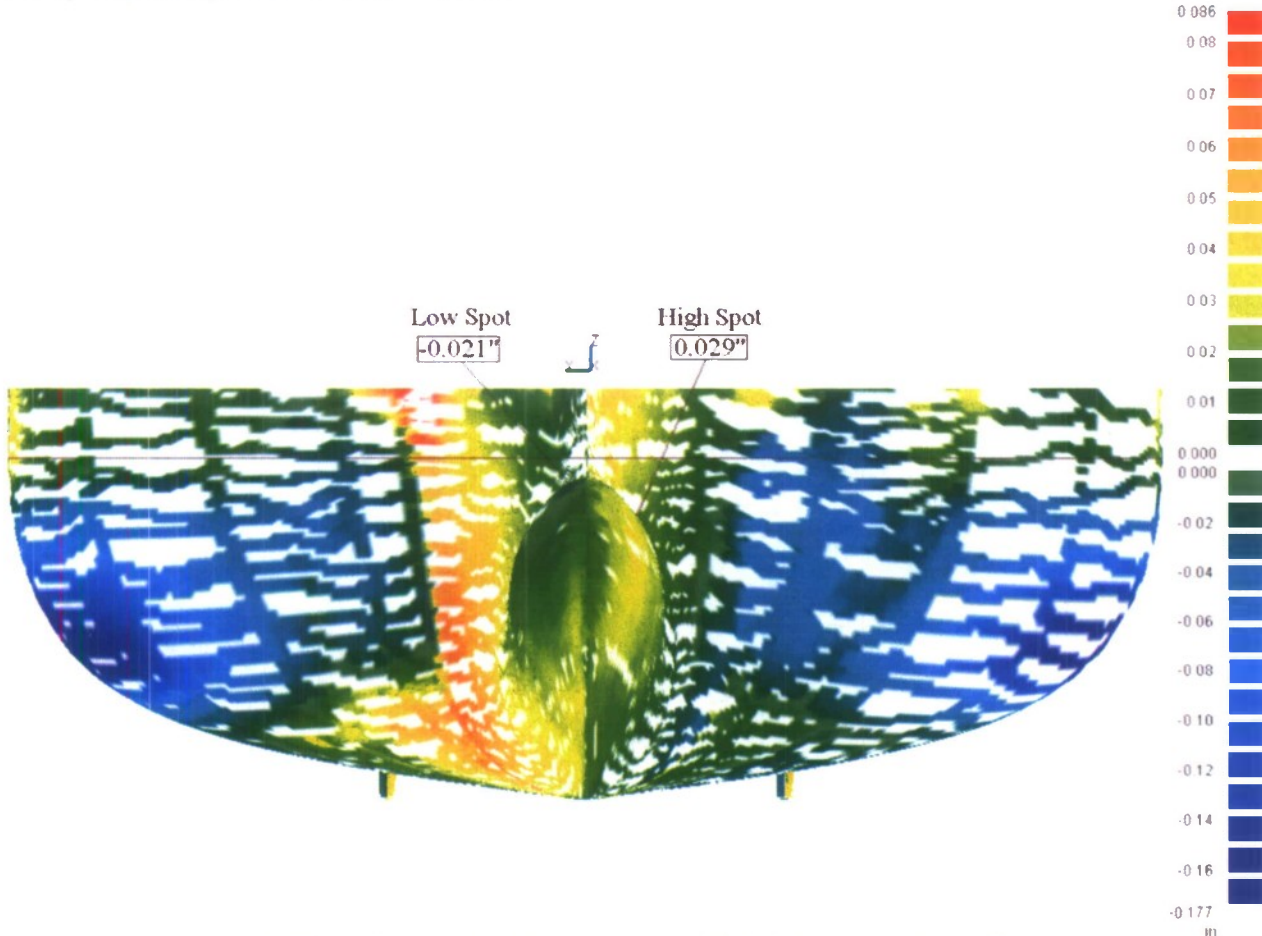


Figure C7. Head on view of the bow dome. Black line marks the waterline.

### Transom

Figure C8 illustrates the fit on the transom. The dark green corner on the port side represents a low spot (-0.011 in from the CAD surface), and the rest of the surface (light green and yellow) shows the high spots. Only one region on the Starboard side is out of the 2mm (0.0787 in) tolerance. This high spot region, shown in Figure C9, is 0.084 in from the CAD surface.

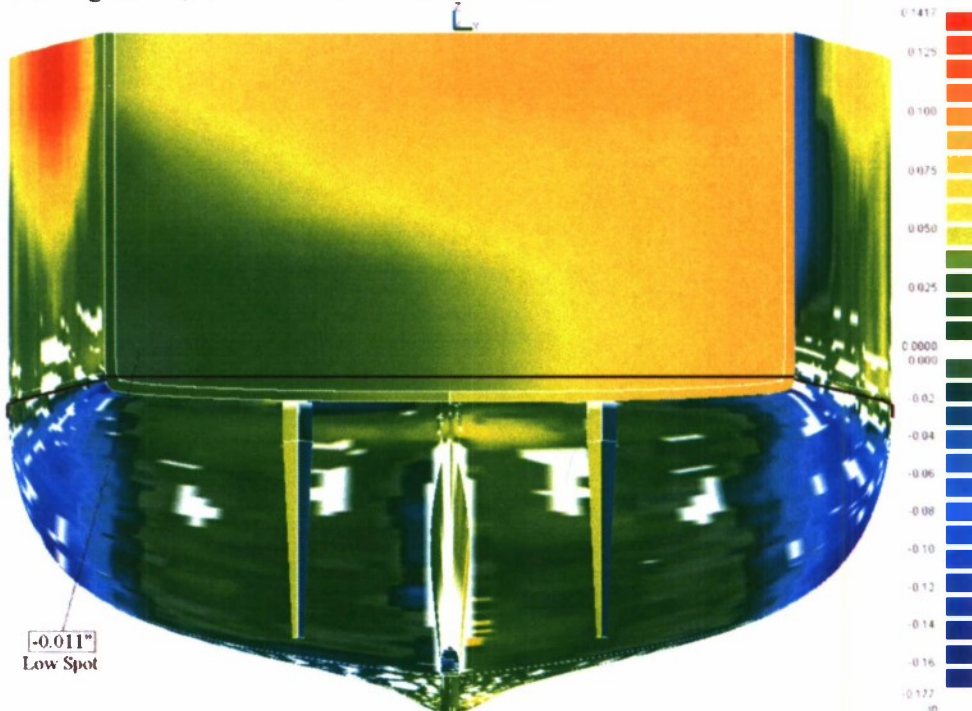


Figure C8. Transom view of Model 5653. The black line represents the waterline.

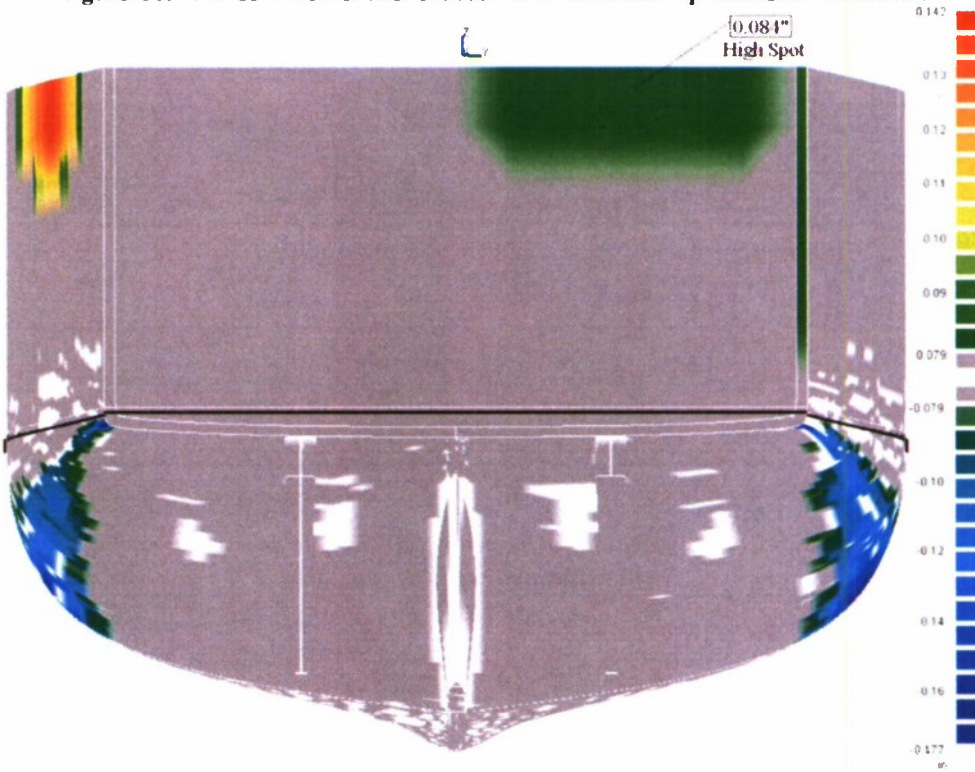


Figure C9. Transom view of Model 5653. The black line represents the waterline.

### Positive and Negative Regions

Figure C10 and Figure C11 illustrate the negative regions and positive regions respectively on the area below the waterline. The negative regions illustrate the low spots on the model. The positive regions show the high spots on the model.

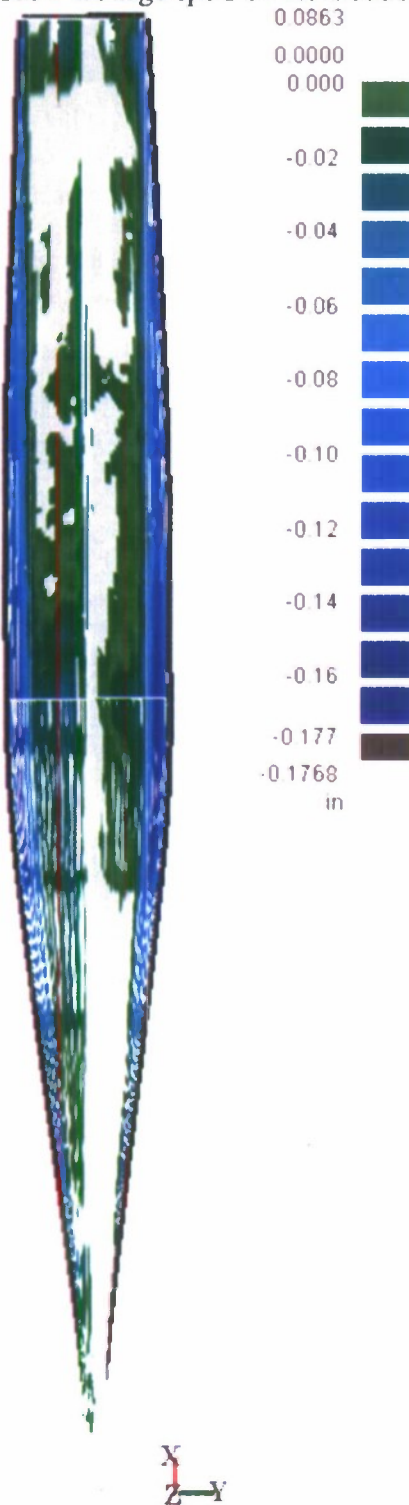


Figure C10. Bottom view of negative regions below the water line, these areas are low spots on the model

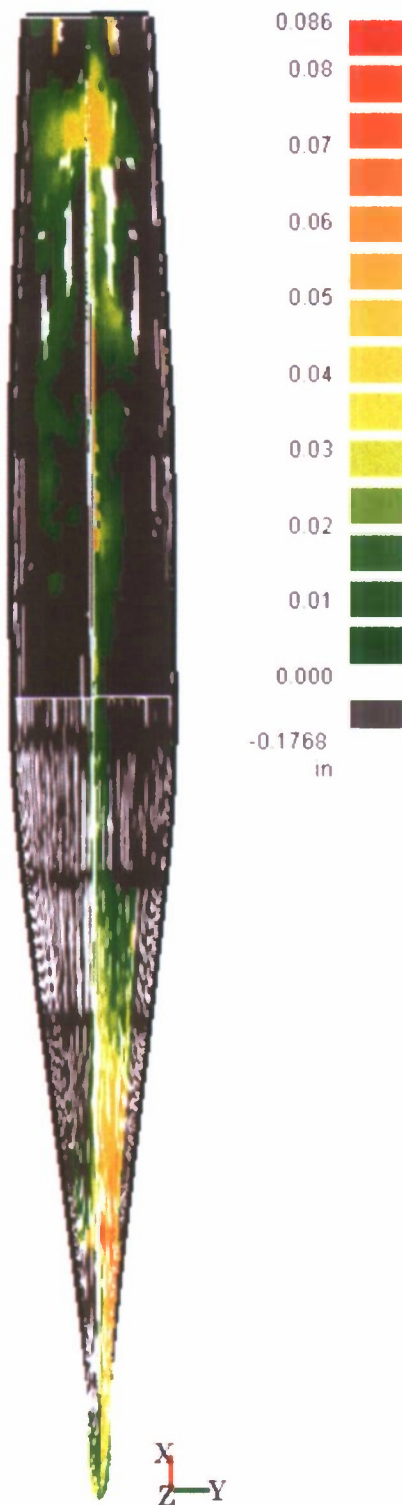


Figure C11. Bottom view of positive regions below the waterline, these areas are high spots on the model

## Propeller Shaft Alignment

The model shaft vectors and positions are compared to the design CAD shaft vectors and positions. However, the model shaft vectors and positions are dependent on the model best fit below the waterline. Any shift to the data to obtain a better fit will affect these values.

### Shaft Vectors

Figure C12 shows the design shaft vectors along with the measured shaft vectors. Table C2 shows the angles from each designed shaft to its respective measured shaft. Table C3 documents the angles from each shaft vector to each axis, for both the design and measured models. The differences between these angles are shown in Figure C12 (in red) and in Table C3. The vectors are based off of two measured circles around each shaft housing. Each of these circles was used to obtain a calculated center point on each model shaft. It is assumed that the shafts and shaft housings are concentric and linear. In hindsight, additional circle measurement should have been measured.

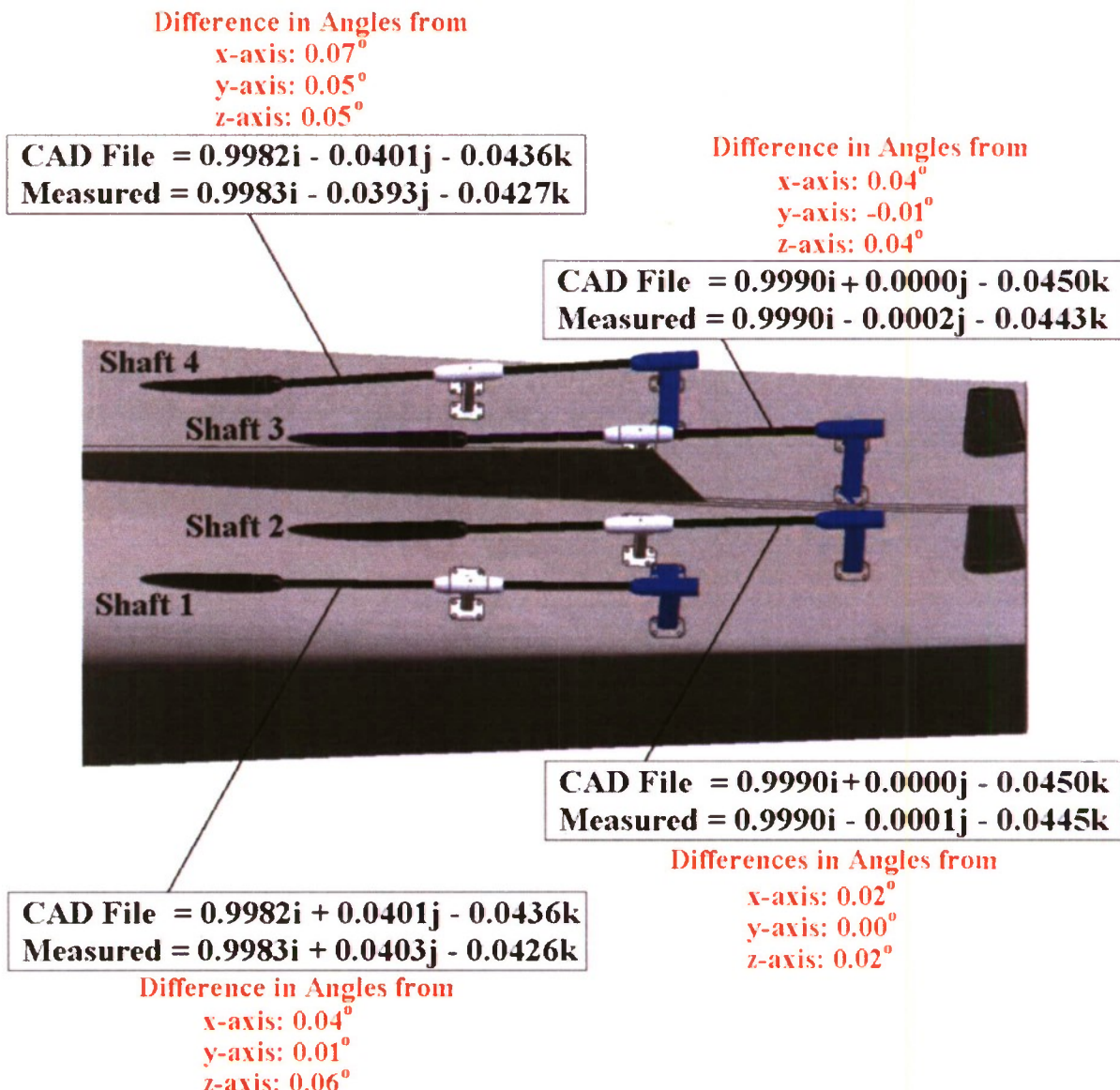


Figure C12. Design and Measured shaft vectors with their corresponding angle difference from the axis

**Table C2. Angles between design shafts and measured shafts**

	Angle (Deg)
Shaft 4	0.069
Shaft 3	0.041
Shaft 2	0.025
Shaft 1	0.061

**Table C3. Design and Measured angles from shafts to axis (and the corresponding difference)**

Shaft to x-axis Angle (Deg)			
	CAD	Model	CAD Angle - Measured Angle
Shaft 4	3.40	3.33	0.07
Shaft 3	2.58	2.54	0.04
Shaft 2	2.58	2.55	0.02
Shaft 1	3.40	3.36	0.04

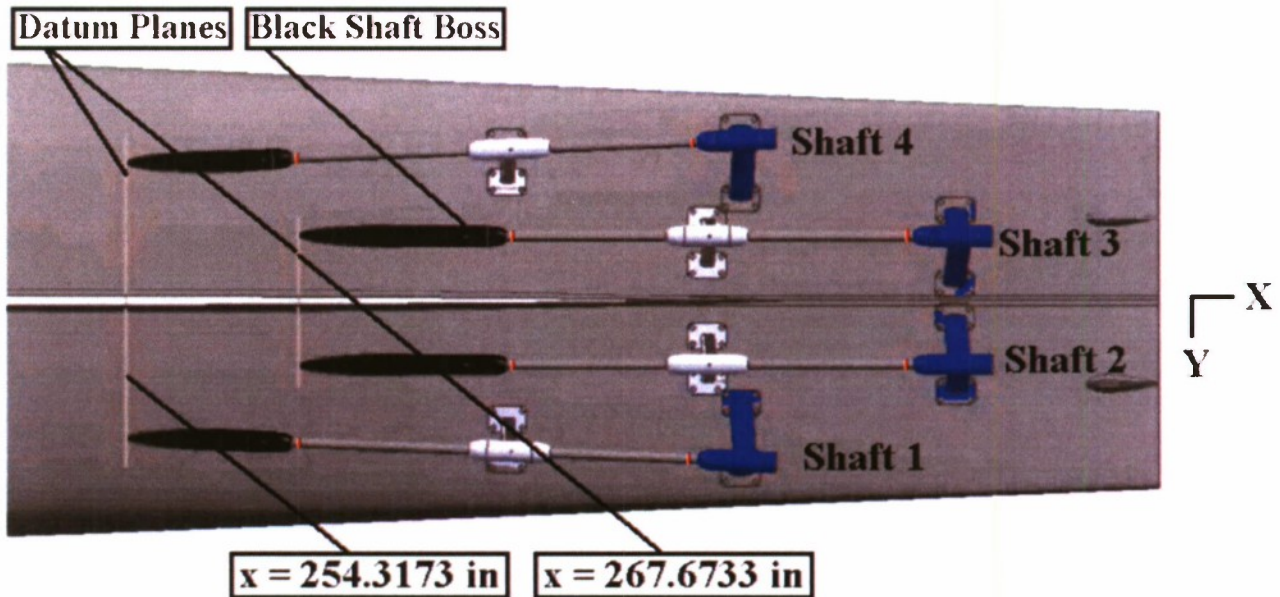
Shaft to y-axis Angle (Deg)			
	CAD	Model	CAD Angle - Measured Angle
Shaft 4	92.30	92.25	0.05
Shaft 3	90.00	90.01	-0.01
Shaft 2	90.00	90.00	0.00
Shaft 1	87.70	87.69	0.01

Shaft to z-axis Angle (Deg)			
	CAD	Model	CAD Angle - Measured Angle
Shaft 4	92.50	92.45	0.05
Shaft 3	92.58	92.54	0.04
Shaft 2	92.58	92.55	0.02
Shaft 1	92.50	92.44	0.06

### **Shaft Position**

A circle was measured around two points on each shaft housing. Figure C13 indicates these locations with two red rings around each shaft. The center point of this circle is assumed to lie on the center line of the shaft inside the housing. In order to determine how closely the model shafts are positioned to the design CAD file, a point on the fwd portion of each shaft will be compared to its corresponding location in the CAD file. This fwd point is located at the fwd end of the black shaft boss (Figure C13). The same comparison will be made with the aft most point on each shaft, at the V-Strut (shown as blue in Figure C13 - Figure C15). Since the fwd most and aft most points were not directly measured on the model, a line was drawn through each measured point. Then a datum plane (shown as pink in Figure C13 - Figure C15) slices through the line at the desired comparison location (Figure C13 specifies the x location where the datum planes sliced the line). The intersection of the line and the datum plane defines the fwd shaft point which will be used for comparison. Note that the fwd and aft points used for comparison were not directly measured, their location is interpolated, assuming that the housing and shaft are perfectly linear. Also, keep in mind that these values are strongly dependent on the best fit position which was chosen, and the accuracy of selecting the shaft housing as a substitute for the shaft itself.



Origin is located at intersection of FP and waterline

Figure C13. Bottom View of the location of the Shaft Datum Planes

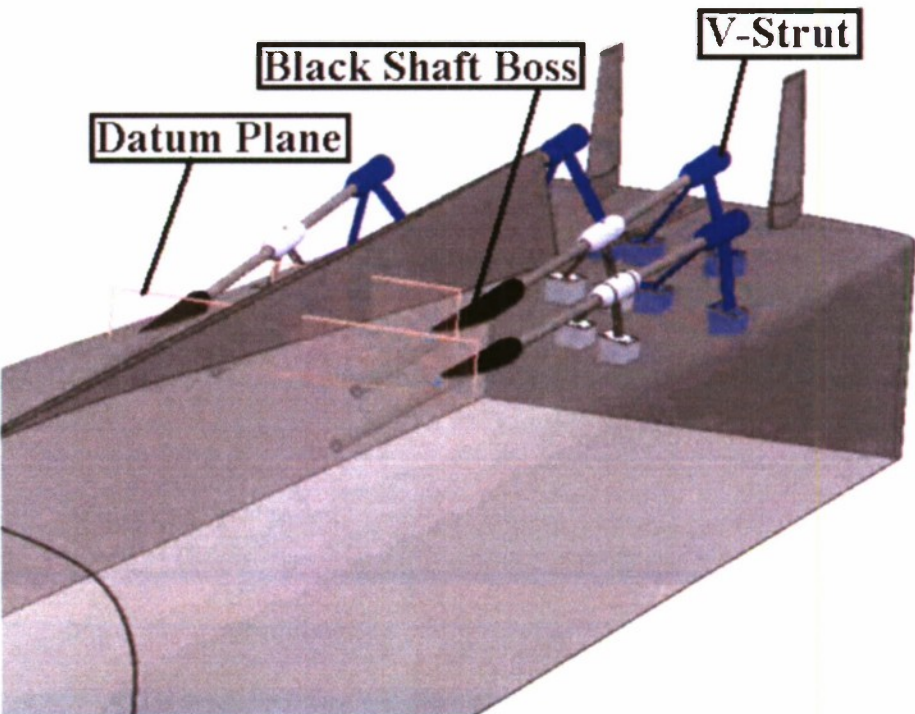


Figure C14. Oblique translucent view of the location of the shaft datum planes (shown in pink)

The datum plane slices through the model at the fwd base of each of the black shaft bosses. So, the fwd shaft point is actually positioned inside the model. Figure C15 highlights the location of the fwd shaft point with a red dot.

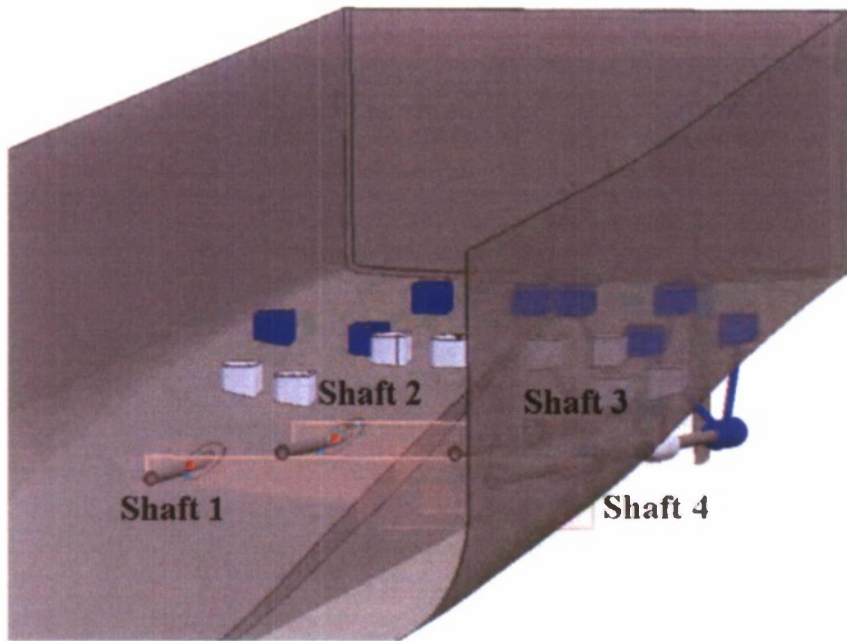


Figure C15. Oblique translucent view of the fwd shaft comparison locations (red dots) inside the model.

Figure C16 indicates the difference of positions between the design CAD file shaft fwd point and the interpolated model fwd point. This cartoon drawing is an inside view of the shafts, looking toward the stern. The blue dots indicate the design CAD location of the shaft center point, and the red dot indicates the interpolated location of each model shaft center point.

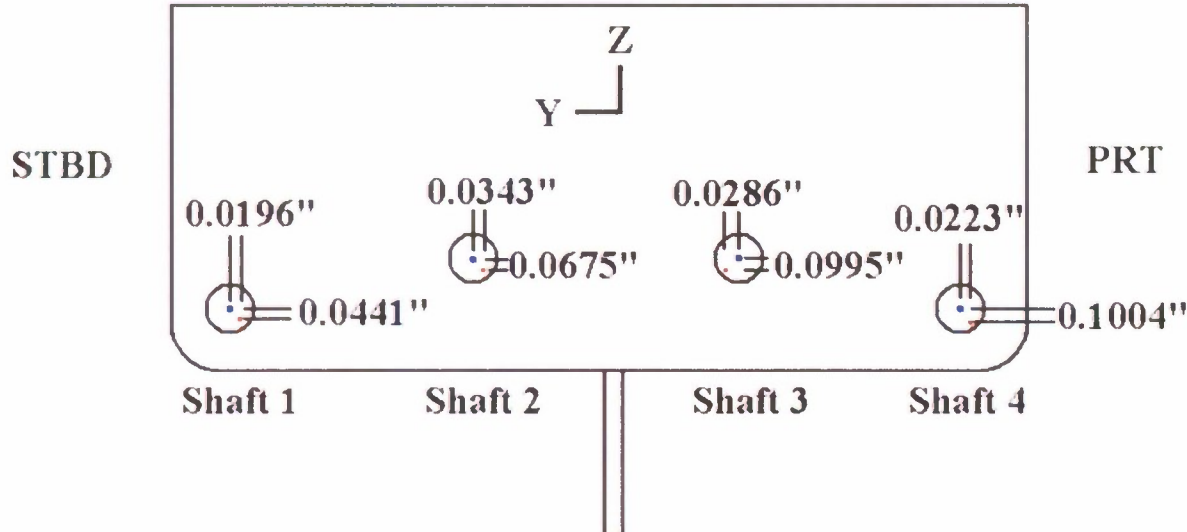


Figure C16. Cartoon drawing comparing fwd shaft point positions to respective design CAD file fwd shaft point positions. This view is similar to the view in Figure C15.

Figure C17 illustrates the position of the interpolated aft V-Strut with respect to the designed aft V-Strut. In the figure, the designed centers of the V-Struts are marked with blue points. The red points indicate where the interpolated model V-Struts are positioned.

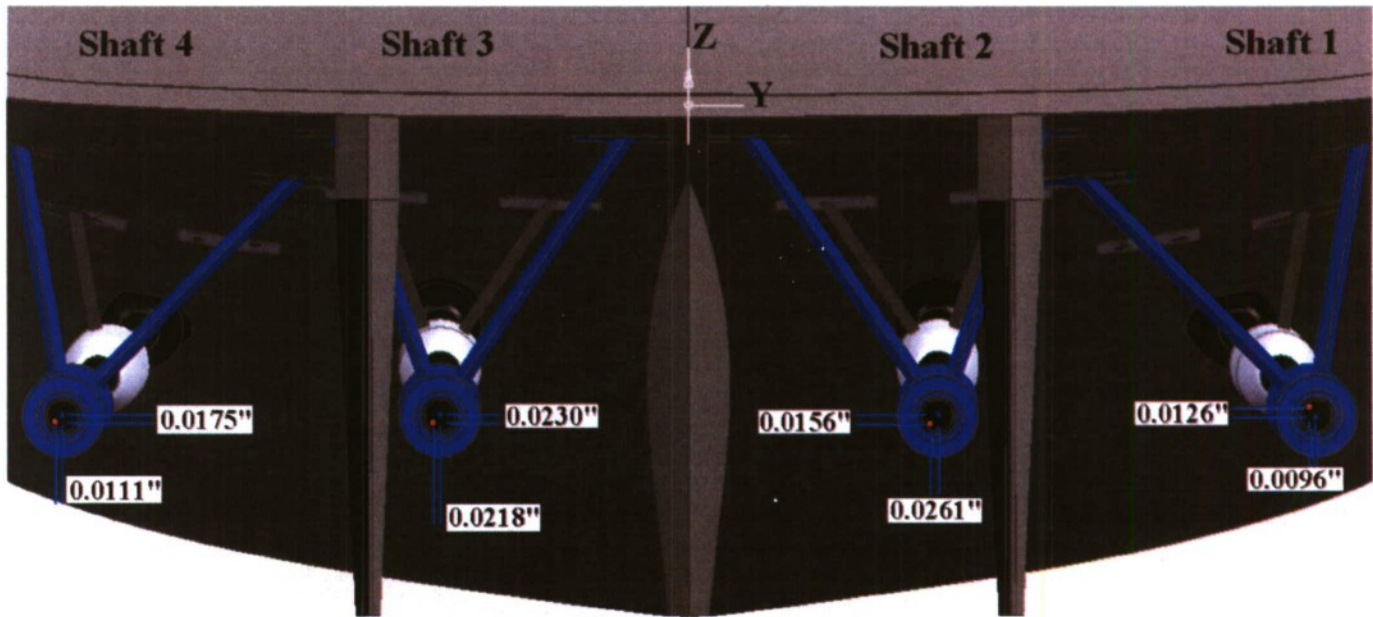


Figure C17. Interpolated aft V-strut position relative to design position

Figure C18 is a mirror image of Figure C16. Now, Figure C18 can be directly compared to Figure C17.

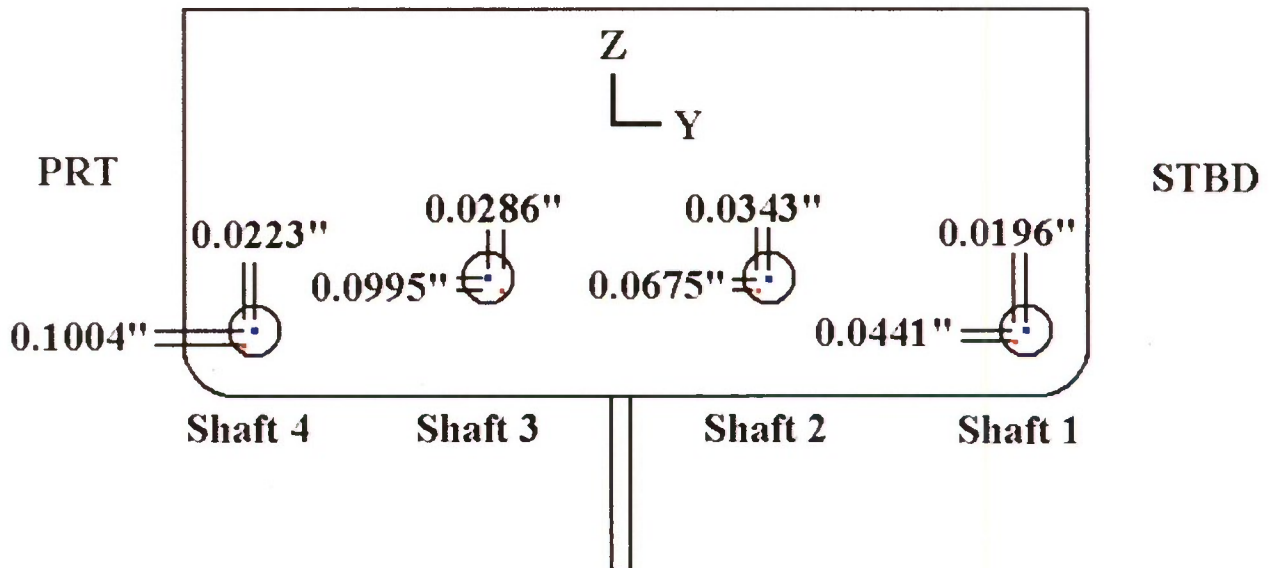


Figure C18. View of fwd shaft center points compared to the designed CAD locations, looking from the stern towards the bow

## Dropped Stool Angle

To determine the angle of the dropped stool, first the measured points on the dropped stool are isolated from the rest of the point cloud data. Figure C19 illustrates the dropped stool data points in red.

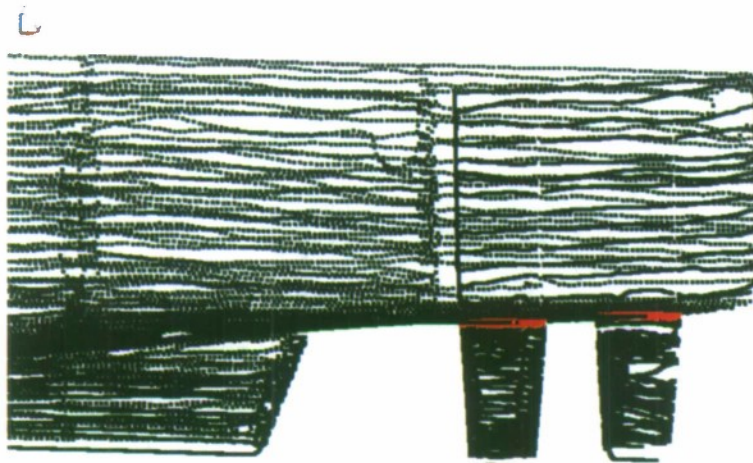


Figure C19. Laser Tracker point cloud data with dropped stool data points highlighted in red.

Then, these points are projected onto the z-plane. This results in a uniform curve, shown in Figure C20. Two circles can be used to locate the centerline of each dropped stool. Before fitting the two circles, the forward and aft regions of each curve must be isolated, so that the best fit circle is not influenced by points which do not lay on the circle. The points used to create the best fit circle are shown in red in Figure C20. Figure C21 illustrates the dropped stool curve with the best fit circles.

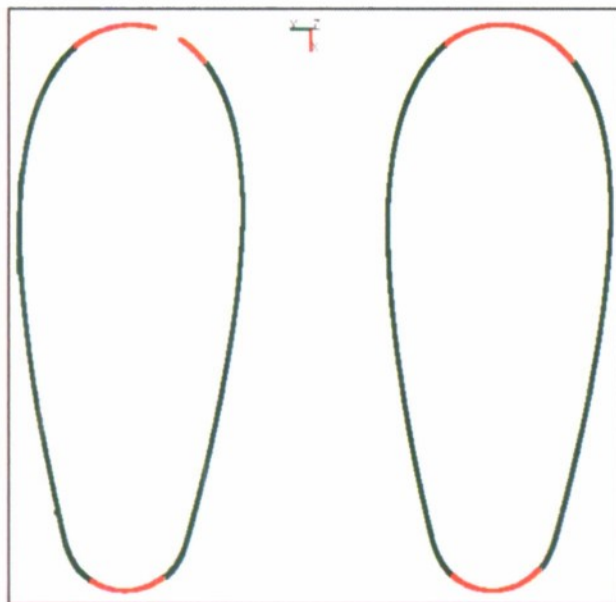


Figure C20. Projection of dropped stool data points onto the z-plane, with the points used to calculate best fit circles highlighted in red.

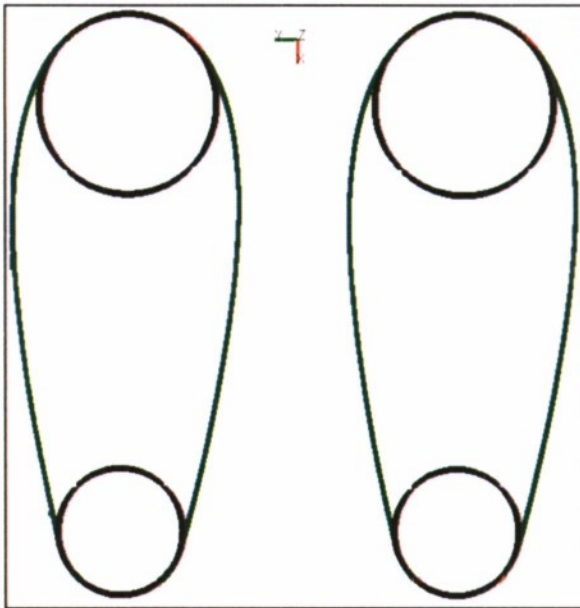


Figure C21. Projection of dropped stool data points onto the z-plane, with the calculated best fit circles.

Using each of the four center locations from Imageware's best fit circle algorithm outputs, each data point on the circles was used to calculate the radius of their respective best fit circle. Table C4 displays the standard deviations of these calculated radii. The standard deviations are quite small, so this gives us confidence that the best fit circles are accurate.

Table C4. Standard Deviations for each best fit circle on the dropped stool data.

Circle Location	No. of red pts on circle	Standard Deviation
STBD FWD	621	0.0010
STBD AFT	440	0.0010
PRT FWD	865	0.0010
PRT AFT	335	0.0008

A rudder centerline vector was created using the coordinates for the center of each circle, and then the angle to the x-axis was calculated. Based on these calculations and the best fit position of the model, the starboard rudder centerline is  $0.109^\circ$  from the x-axis, and the port rudder centerline is  $0.014^\circ$  from the x-axis. This results in a  $0.011''$  (for the starboard rudder) and a  $0.014''$  (for the port rudder) difference in the y direction from the fwd end to the aft end of each rudder. Figure C22 illustrates the model dropped stool (shown in green) in relation to the design CAD rudder (shown in white).

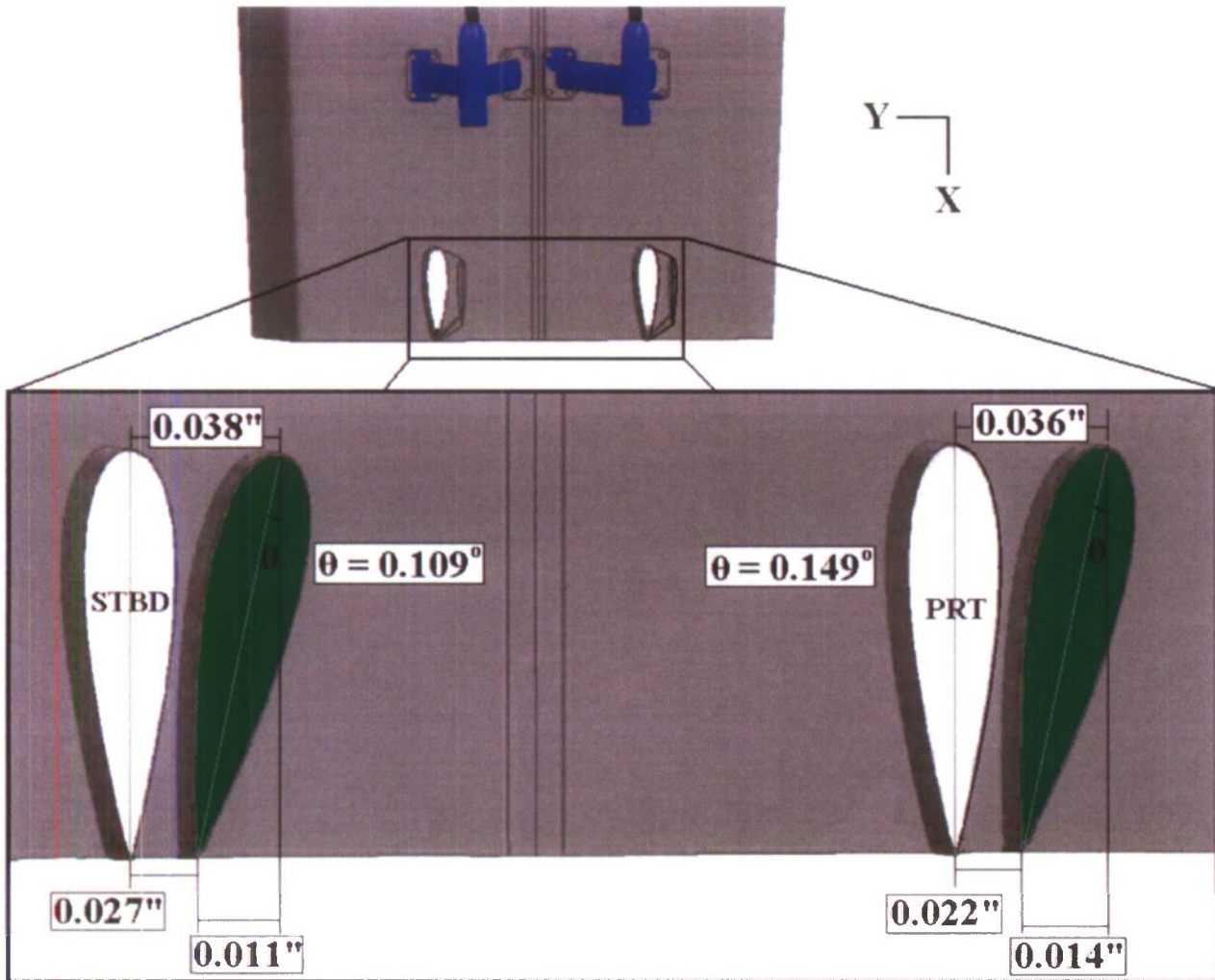


Figure C22. Location of Model rudders (green) in relation to Design CAD rudders (white).

It is important to note that these dropped stool angles are depended on the best fit position of the model. The data was translated and rotated as one set, as one area of the model comes into tolerance, another area of the model may go out of tolerance.

Laser Tracker Calibration Certificate



FARO Technologies  
222 Gale Lane  
Kennett Square, PA 19348

Voice: (610) 444-2300  
Fax 1: (610) 444-2323  
Fax 2: (610) 444-2321

## CALIBRATION CERTIFICATE LASER TRACKER MODEL Xi

Date	October 18, 2006
Certification Number	4651
Tracker Serial Number	L03000301102
Customer	Naval Surface Weapons Center 9500 MacArthur Blvd West Bethesda, MD 28017
Date Calibrated	October 18, 2006
Date Due	October 18, 2007
Certified By	 Marie A. Sigmund Lead Field Service Engineer
Condition Found	In Tolerance
Condition Left	In Tolerance

The instrument listed above has been tested, inspected and compensated against FARO working standards that have been calibrated using National Institute of Standards and Technology (NIST) or other appropriate nationally or internationally recognized standards.

*Calibrations conform to procedures developed in accordance with ISO-10012 and MIL-STD-45662A. Calibration results relate only to the items specified. This report shall not be reproduced except in full without the written consent of the FARO Technologies Laser Measurement Division.*



Date **October 18, 2006**  
Certification Number **4651**  
Tracker Serial Number **L03000301102**

### Calibration Standards Traceability Data

#### HUMIDITY STANDARD

Honeywell Opto. RH Sensor Model IH 3602A  
Serial Number: 02080816 - 237  
Calibrated by Honeywell, Hycal Sensing Products

#### TEMPERATURE STANDARD

Cornerstone Sensors Inc. Model TA1041  
Calibration Date: 15 March 2005  
Calibrated by FARO Technologies  
Calibration Standard: Hart Scientific Model 1521, Serial Number: A5C403  
Last Calibration: 12/8/05 Next Calibration: 12/8/06  
Trace Number: A5C09014

Allowable Deviation:  $\pm 0.4^{\circ}\text{C}$  as compared to Standard.

As Received ( $^{\circ}\text{C}$ )			Post Calibration ( $^{\circ}\text{C}$ )		
Standard	Actual	Deviation	Standard	Actual	Deviation
20.48	20.47	0.01	19.36	19.32	0.04

#### PRESSURE STANDARD

Vaisala Model PMB 100 Pressure Module  
Serial Number: X2010020  
Calibration Date: 15 March 2005  
Calibrated by FARO Technologies  
Calibration Standard: Druck Model 740, Serial Number: 695/99-11  
Last Calibration: 3/9/06 Next Calibration: 3/9/07  
Trace Number: TN-261146

Allowable Deviation:  $\pm 1.4 \text{ mmHg}$  as compared to Standard.

As Received (mmHg)			Post Calibration (mmHg)		
Standard	Actual	Deviation	Standard	Actual	Deviation
759.44	759.43	0.01	748.61	748.49	0.12

*Calibrations conform to procedures developed in accordance with ISO-10012 and MIL-STD-45662A.  
Calibration results relate only to the items specified. This report shall not be reproduced except in full  
without the written consent of the FARO Technologies Laser Measurement Division*

## INITIAL REPORT DISTRIBUTION

<b>No. of Copies</b>			
<b>Print</b>	<b>PDF</b>	<b>Office</b>	<b>Individual</b>
-	2	PMS 385	M. Fink, D. Licsc
-	1	SEA 05D1	S. Wynn
-	1	SEA 05H	J. Schumann
-	1	Consultant	J. Offutt
-	1	CSC	O. Clark
1	-	DTIC	
		<b>NSWCCD Code</b>	<b>Individual</b>
-	1	2000	C. Dicks
-	1	2240	C. Kennell
1	1	2410	R. Anderson
-	1	3452 (Library)	
1	-	5060	D. Walden
-	1	5500	A. Silver
2	-	5800	5200 Office Files
2	6	5800	D. Cusancelli (2 print, 1 PDF), B. Metcalf, A. Powers, M. Donnelly, G. Karafiath, R. Hurwitz
-	1	6530	A. Powers
<b>Total No. of Copies</b>			
<b>Print</b>	<b>PDF</b>		
7	18		